Open research issues on Nonlinear Dynamics, Dynamical Systems and Processes

A.V. Doroshin [1], F. Neri [2]
[1] Department of Space Engineering (Division of Flight Dynamics and Control Systems), Samara State Aerospace University (National Research University), RUSSIAN FEDERATION[2] Department of Computer Science, University of Naples "Federico II", Naples, ITALY
doran@inbox.ru, nerifil@gmail.com

Abstract - Nonlinear Dynamics is the well-known area of the modern science which studies numerous aspects of nonlinear evolutions and processes in natural and artificial (technical) systems. We will then present a number of research results into mathematical modeling, theoretical analysis, synthesis and numerical simulation of nonlinear phenomena in dynamical systems and corresponding applications.

Keywords - Nonlinear differential equations, Nonlinear effects in dynamical systems, Control of dynamical systems, stability analysis, bifurcation analysis, Lyapunov analysis.

Introduction

The format of special issues is well proved and continues to develop at this time [1-15]. The main aim of this special issue "Nonlinear Dynamics, Dynamical Systems and Processes" is the thematic integration of the research results into mathematical modeling, theoretical analysis, synthesis and numerical simulation of nonlinear phenomena in dynamical systems and corresponding applications [e.g. 16-28].

So, this special issue includes the following works with corresponding description of the aspects of the nonlinear dynamics:

1). A Linear Temperature Measurement System Based on Cu100 [29].

In this work a temperature measurement device is designed for the temperature measurement and control of industrial processes with high accuracy by using Cu_{100} thermal resistor. It consists of AD590M, resistors, amplifier, A/D converter, data sampling and processing system, digital display, alarming unit, serial output ports, etc. The single comparing method is used to find the thermal resistor value which is mapped to the corresponding temperature by looking into indexing table. Therefore, linearity is implemented, which greatly reduces the impact of temperature-drift and non-linearity in amplifier.

2). LMI based bounded output feedback control for uncertain systems [30].

This paper provides conditions for constrained dynamic output feedback controller to be cost guaranteeing and assuring asymptotic stability for both continuous and discrete-time systems with quadratically constrained nonlinear/uncertain elements. The conditions are formulated in the form of matrix inequalities, which can be rendered to be linear fixing one of the scalar parameters. An abstract multiplier method is applied. Numerical examples illustrate the application of the proposed method.

3). Fault Detection and Diagnosis in Non-Linear Process using Multi Model Adaptive H∞ Filter [31].

Here the Kalman Filter (KF) is described, which is widely used in process industries as state estimator to diagnose the faults either in the sensor, actuator or in the plant because of its recursive nature. But, due to increase in non-linearity and exogenous perturbations in the monitored plant, it is often difficult to use a simple KF as state estimator for nonlinear process monitoring purposes. Thus, the first objective of this paper is to design an Adaptive Linear H_∞ Filter ($ALH_\infty F$) using gain scheduling algorithm to estimate nonlinear process states in the presence of unknown noise statistics and unmodeled dynamics. Next the designed $ALH_\infty F$ is used to detect sensor and actuator faults which may occur either sequentially or simultaneously using Multi Model $ALH_\infty F$ ($MMALH_\infty F$). The proposed estimator is demonstrated on Continuously Stirred Tank Reactor (CSTR) process to show the efficacy. And the performance of $MMALH_\infty F$ is compared with MMALKF. The proposed $MMALH_\infty F$ is detecting and isolating the faults exactly in the presence of unknown noise statistics and unmodeled dynamics.

4). Permanence and Asymptotically Periodic Solution for A Cyclic Predator-PreyModelWith Sigmoidal Type Functional Response [32].
This paper is concerned with a cyclic predator-prey system with Sigmoidal type functional response. By using the differential inequality theory, some sufficient conditions are derived for the permanence of the system. By constructing a suitable Liapunov function, it is obtained that the system has a unique asymptotically periodic solution which is globally asymptotically stable. Some numerical simulations that illustrate our analytical predictions are carried out.
5). Dynamical Analysis and Synthesis of Inertia-Mass Configurations of a Spacecraft with Variable Volumes of Liquids in Jet Engine Tanks [33].
In this article the attitude motion of a spacecraft with variable mass/structure is considered at the variability of the volume of liquids (the fuel and the oxidizer) in tanks of the jet engines. The variability of the liquid's volume is occurred under the action of systems of the extrusion of liquids by the pressure creation and, as a result, by the diaphragm (a thin soft foil) deformation inside the fuel/oxidizer tank. The synthesis of the attitude dynamics is fulfilled by the change of directions of the extrusion of the liquids in tanks – this modifies the inertia-mass parameters (their corresponding time-dependencies) and affects the final motion dynamics. Here it is showed that the extrusion in the lateral radial―outside direction is most preferable in comparison with the longitudinal extrusion (in the direction of jet-vector). It means that the precession cone of the longitudinal axis of the spacecraft (the axis of the jet-engine reactive thrust) is ―twisted up to the precalculated necessary direction of jet-impulse, and it has not ―untwisted‖ phases. This scheme of the liquid extrusion is dynamically optimal, because it allows to improve the active inter-orbital manoeuvre by the natural/uncontrolled/passive way.

So, in this special issue the dynamical aspects are quite broadly presented and the main aim of the issue is locally reached.

Conclusions

Finally before diving into the collected research works [29-33], let us remember the reader that WSEAS Transactions on Systems has broad spectr of Special Issues, e.g. [1-15]. This is has the objective of creating an active and contributing research community around the journal and to present their latest efforts which have achieved wide interest among its members. As a reader of the journal you are invited to take inspiration by the presented papers and to consider to submit your future works to the journal itself.
Enjoy your reading!

References

[1] Ciufudean, C., Neri, F. (2014) Open research issues on Multi-Models for Complex Technological Systems. WSEAS Transactions on Systems, 13, in press.
[2] Neri, F. (2014) Open research issues on Computational Techniques for Financial Applications. WSEAS Transactions on Systems, 13, in press.
[3] Karthikeyan, P., Neri, F. (2014) Open research issues on Deregulated Electricity Market: Investigation and Solution Methodologies. WSEAS Transactions on Systems, 13, in press.
[4] Panoiu, M., Neri, F. (2014) Open research issues on Modeling, Simulation and Optimization in Electrical Systems. WSEAS Transactions on Systems, 13, in press.
[5] Neri, F. (2014) Open research issues on Advanced Control Methods: Theory and Application. WSEAS Transactions on Systems, 13, in press.
[6] Hájek, P., Neri, F. (2013) An introduction to the special issue on computational techniques for trading systems, time series forecasting, stock market modeling, financial assets modeling WSEAS Transactions on Business and Economics, 10 (4), pp. 201-292.
[7] Azzouzi, M., Neri, F. (2013) An introduction to the special issue on advanced control of energy systems (2013) WSEAS Transactions on Power Systems, 8 (3), p. 103.
[8] Bojkovic, Z., Neri, F.(2013) An introduction to the special issue on advances on interactive multimedia systems. WSEAS Transactions on Systems, 12 (7), pp. 337-338.
[10] Pekař, L., Neri, F. (2013) An introduction to the special issue on advanced control methods: Theory and application (2013) WSEAS Transactions on Systems, 12 (6), pp. 301-303.
[11] Guarnaccia, C., Neri, F. (2013) An introduction to the special issue on recent methods on physical polluting agents and environment modeling and simulation

WSEAS Transactions on Systems, 12 (2), pp. 53-54.

[12] Neri, F. (2012) An introduction to the special issue on computational techniques for trading systems, time series forecasting, stock market modeling, and financial assets modeling WSEAS Transactions on Systems, 11 (12), pp. 659-660.

[13] Muntean, M., Neri, F. (2012) Foreword to the special issue on collaborative systems WSEAS Transactions on Systems, 11 (11), p. 617.

[14] Pekař, L., Neri, F. (2012) An introduction to the special issue on time delay systems: Modelling, identification, stability, control and
applications WSEAS Transactions on Systems, 11 (10), pp. 539-540.

[15] Volos, C., Neri, F. (2012) An introduction to the special issue: Recent advances in defense systems: Applications, methodology, technology WSEAS Transactions on Systems, 11 (9), pp. 477-478.

[16] Doroshin, A.V. (2013) Exact solutions in attitude dynamics of a magnetic dual-spin spacecraft and a generalization of the lagrange top. WSEAS Transactions on Systems, Volume 12, Issue 10, October 2013, Pages 471-482.

[17] A.V. Doroshin, Synthesis of attitude motion of variable mass coaxial bodies, WSEAS Transactions on Systems and Control, Issue 1, Volume 3 (2008) 50-61.

[18] A.V. Doroshin, Analysis of attitude motion evolutions of variable mass gyrostats and coaxial rigid bodies system, International Journal of Non-Linear Mechanics, Volume 45, Issue 2 (2010) 193–205.

[19] A.V. Doroshin, Modeling of chaotic motion of gyrostats in resistant environment on the base of dynamical systems with strange attractors. Communications in Nonlinear Science and Numerical Simulation, Volume 16, Issue 8 (2011) 3188–3202.

[20] A.V. Doroshin, Heteroclinic dynamics and attitude motion chaotization of coaxial bodies and dual-spin spacecraft, Communications in Nonlinear Science and Numerical Simulation, Volume 17, Issue 3 (2012) 1460–1474.

[21] A.V. Doroshin, Evolution of the precessional motion of unbalanced gyrostats of variable structure. Journal of Applied Mathematics and Mechanics, Volume 72, Issue 3, October 2008, Pages 259-269.

[22] A.V. Doroshin, Chaos and its avoidance in spinup dynamics of an axial dual-spin spacecraft. Acta Astronautica, Volume 94, Issue 2, February 2014, Pages 563-576.

[23] A.V. Doroshin, M.M. Krikunov, Attitude Dynamics of a Spacecraft with Variable Structure at Presence of Harmonic Perturbations, Appl. Math. Modelling (2013).

[24] Neri F., Traffic packet based intrusion detection: decision trees and generic based learning evaluation. WSEAS Transactions on Computers, WSEAS Press (Wisconsin, USA), issue 9, vol. 4, 2005, pp. 1017-1024.

[25] Neri F., Software agents as a versatile simulation tool to model complex systems. WSEAS Transactions on Information Science and Applications, WSEAS Press (Wisconsin, USA), issue 5, vol. 7, 2010, pp. 609-618.

[26] L. Nechak, S. Berger, E. Aubry, Robust Analysis of Uncertain Dynamic Systems: Combination of the Centre Manifold and Polynomial Chaos theories, WSEAS TRANSACTIONS on SYSTEMS, Issue 4, Volume 9, April 2010, pp.386-395.

[27] N. Jabli, H. Khammari, M. F. Mimouni, R. Dhifaoui, Bifurcation and chaos phenomena appearing in induction motor under variation of PI controller parameters, WSEAS TRANSACTIONS on SYSTEMS, Issue 7, Volume 9, July 2010, pp.784-793.

[28] Thanh Dung Nguyen, Thi Thanh Dieu Phan, Roman Jasek, Parameter Estimation in Five Dimensions Chaotic Synchronization Systems by Self-Organizing Migrating Algorithm, WSEAS TRANSACTIONS on SYSTEMS, Issue 4, Volume 11, April 2012, pp.117-128.

[29] Jiu-Qiang Zhao, Zhi Cheng, Guang Chen (2014). A Linear Temperature Measurement System Based on Cu100. WSEAS Transactions on Systems, 13. Special Issue on Nonlinear Dynamics, Dynamical Systems and Processes (in press).

[30] Eva Gyurkovics, Tibor Takacs Kih. LMI based bounded output feedback control for uncertain systems. WSEAS Transactions on Systems, 13. Special Issue on Nonlinear Dynamics, Dynamical Systems and Processes (in press).

[31] M. Manimozhi, R. Saravanakumar. Fault Detection and Diagnosis in Non-Linear Process using Multi Model Adaptive H∞ Filter. WSEAS Transactions on Systems, 13.

Special Issue on Nonlinear Dynamics, Dynamical Systems and Processes (in press).

[32] Changjin Xu, Qiming Zhang. Permanence and Asymptotically Periodic Solution for A Cyclic Predator-Prey Model With Sigmoidal Type Functional Response. WSEAS Transactions on Systems, 13. Special Issue on Nonlinear Dynamics, Dynamical Systems and Processes (in press).

[33] A.V. Doroshin, M.M. Krikunov. Dynamical Analysis and Synthesis of Inertia-Mass Configurations of a Spacecraft with Variable Volumes of Liquids in Jet Engine Tanks. WSEAS Transactions on Systems, 13. Special Issue on Nonlinear Dynamics, Dynamical Systems and Processes (in press).

A Linear Temperature Measurement System Based on Cu_{100}

JIU-QIANG ZHAO, XIAO-FEN LI, ZHI CHENG, GUANG CHEN
College of Computer Science and Technology
Zhejiang University of Technology
Hangzhou, 310023, China
P.R.China
zjq890227@163.com

Abstract: - A temperature measurement device is designed for the temperature measurement and control of industrial processes with high accuracy by using Cu_{100} thermal resistor. It consists of AD590M constant current source, resistors, amplifier, A/D converter, data sampling and processing system, digital display, alarming unit, serial output ports, etc. The single comparing method is used to find the thermal resistor value which is mapped to the corresponding temperature by looking into indexing table. Therefore, linearity is implemented, which greatly reduces the impact of temperature-drift and non-linearity in amplifier. Besides, the device implements the measuring of full temperature range of the reference table. The theoretical error of the device is less than 0.1 ℃ and meets the requirements in most of industrial processes.

Key-Words: - linear temperature measurement, Cu_{100} copper resistor, MCU, linear indexing table

1 Introduction

Temperature is one of the seven basic physical units in the international system of units (SI), which occupies an important position in all of relevant disciplines [1-6]. At present, there are many methods of measuring temperature in the world, as well as the classification methods of classifying those measuring methods. In general, it is difficult to find an ideal temperature measuring method because of the numerous measuring principles [7-9]. It can be roughly divided into contact measurement and non-contact temperature measurement according to different measurement ways. Contact temperature measurement device which is characterized by a higher measurement precision, simple design, high reliability, wide application range, is carried out according to the principle of heat exchange, such as double metal thermometer, glass thermometer, thermocouple thermometer, hot resistor thermometer and pressure thermometer, etc[10-12]. In order to make the measurement precise, contact temperature measurement method must ensure the device well contacting with the object being measured, and after sufficient heat exchange to get the actual temperature. But contact temperature measurement method can't be used for too high temperature measurement due to the hysteretic response and the chemical reaction with the object being measured. At present non-contact temperature measurement is mainly the radiant temperature measurement in industry, which keeps a certain distance with the measured object. But it is vulnerable to the object emissivity, and the distance of the object being measured, as well as the media such as steam and smoke. The accuracy of the non-contact temperature measurement can't be guaranteed, which is typically used for high temperature measurement [13-17].

The traditional thermal resistor and thermocouple temperature measurement technology are characterized by simple structure, mature technology and convenient use, etc, which can be widely used in the future [17-19]. With the full development of electronic technology, a small temperature measuring instrument which includes temperature sensing device and the corresponding integrated electronic circuit can be designed, with which we can see voltage, frequency, or directly temperature display. It is not only convenient but also easy to carry.

Micro Controller Unit (MCU) [1-4,20-24] is usually applied to real-time measurement and control, especially to the development of electromechanical integration of intelligent systems and products which is characterized by small volume, low power consumption, cheap and strong control ability, etc. It has very extensive application in the field of measuring temperature because of high automation, intelligence in a system. In this paper, we design a copper resistor (Cu_{100}) linear

temperature measurement system based on MCU which can meet general industrial temperature measurement occasions [1-4,20,24].

This paper is organized as follows. In Sec.2, we give the theoretical analysis of the thermal resistor temperature measurement. In Sec.3, we provide the hardware design of the system. In Sec.4, we provide the software design of the system. In Sec.5, the error analysis is given. In Sec.6, the conclusion is given.

2 The theoretical analysis of the thermal resistor temperature measurement

Thermal resistor temperature measurement device is based on the principle that the value of the metal conductor resistor has linear relation with the measuring temperature[12-17]. The relationship between the metal conductor resistor value and temperature can be expressed as

$$R_t = R_{t_0}[1+\alpha(t-t_0)] \qquad (1)$$

Where R_t and R_{t_0} represent the value of the metal conductor resistance at t (℃) and t_0 (℃) respectively; α represents the temperature coefficient of resistor, namely the relative variation of the resistor as the temperature rise per 1 ℃.

Although the general metal material and temperature are not completely linear relationship, it can be approximate to linear relationship in a certain range, the commonly used thermal resistor characteristic curve is shown in figure 1.

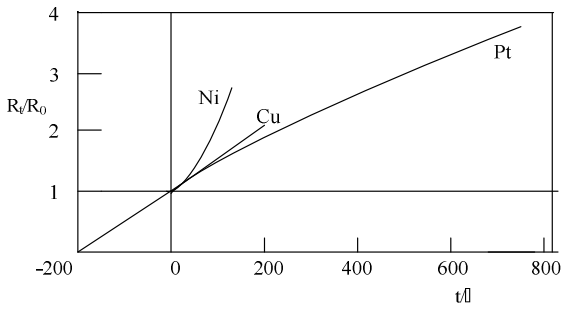

Fig.1 The commonly used thermal resistor characteristic curve

The temperature coefficient of resistor α is defined as

$$\alpha = \frac{R_t - R_{t_0}}{R_{t_0}(t-t_0)} = \frac{1}{R_{t_0}} \cdot \frac{\Delta R}{\Delta t} \qquad (2)$$

It represents the relative variation of the resistor as the temperature rise per 1 ℃, where R_t and R_{t_0} are the same as (1). In fact α is the average in the temperature range of $t_0 \sim t$, for any α

$$\alpha = \lim_{\Delta t \to 0} \frac{1}{R_{t_0}} \times \frac{\Delta R}{\Delta t} = \frac{1}{R} \cdot \frac{dR}{dt} \qquad (3)$$

Formula (3) is the general expression which has a broader significance, but it should be linearized.

Experiments show that the resistor of most metal conductor with a positive temperature coefficient increases 0.36% ~ 0.68% when the temperature raises 1℃. The purer a metal material is, the bigger α is, and vice versa. So the α of alloy is usually smaller than the pure metal. Copper resistor is commonly used in temperature measurement ranged from -50℃ to 150℃, whose resistor is linear with temperature. Its temperature coefficient is relatively big, and its price is cheap, as well as the material is easy purified. But it has low resistivity, and is easily oxidized, so it is reasonable to use copper resistor thermometer if the temperature is not too high and there is no special limit about the size of the temperature measuring element. In this paper, we choose Cu_{100} as the thermal resistor sensor. The relation between the copper thermal resistor and temperature can be expressed as

$$R_t = R_0(1 + At + Bt^2 + Ct^3) \qquad (4)$$

Where R_t and R_0 represent the value of the copper thermal resistor at t (℃) and 0 (℃) respectively; $A=4.28899\times10^{-3}$/℃, B= -2.133×10^{-7}/℃^{2}, C=1.233×10^{-9}/℃^{3}. Within a certain range formula (4) can be approximated as formula (5) ignoring B and C.

$$R_t = R_0(1+\alpha t) \qquad (5)$$

Where α =4.28×10^{-3}/℃, to simplified the calculation, we can set α =4.25×10^{-3}/℃, because the temperature coefficient of copper thermal resistor is very small and the purity of copper resistor material is not high. After determining the linear relation of copper thermal resistor and temperature, we can measure the value of thermal

copper resistor and check the linear indexing table to get temperature.

2.1 The current method model for measuring thermal resistor

With the control of the MCU, the thermal resistor adjusting circuit (Fig. 2) completes the signal data acquisition according to logic control table (Table 1).The circuit uses AD590M as constant current source to realize the resistor measurement, which is called "current method".

As shown in table 1 and Fig. 2, the IN0 channel of M_1 and M_2 multi-channel is open at step 1, and the output current I of AD590M pass through R_0 and R_1 in calibration circuit forming voltage signal U_1 as formula (6)

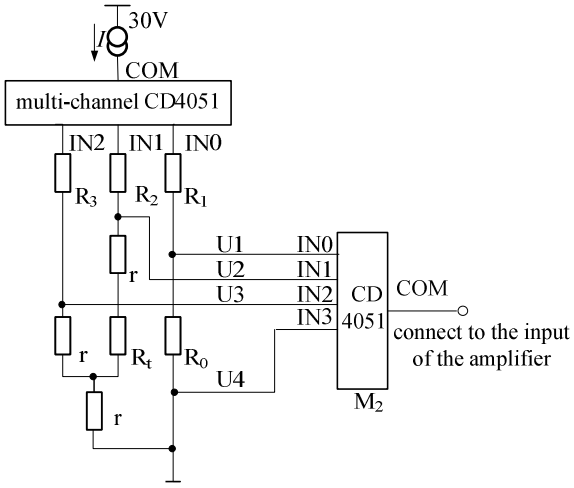

Fig. 2 The signal disposal module of thermal resistor

$$U_1 = I \cdot R_0 \qquad (6)$$

Table 1 Logic control function table

steps	U1	U2	P1.0	P1.1	P1.2	P1.3	collection the signal of
1	IN0 open	IN0 open	0	0	0	0	standard calibration signal U_1
2	IN1 open	IN1 open	1	0	1	0	the measured signal U_2
3	IN2 open	IN2 open	0	1	0	1	the line resistor signal U_3
4	IN1 open	IN3 open	1	0	1	1	zero calibration signal U_4

To simplify the calculation process, we can assume the zero calibration signal $U_4 = 0$. The calibrating signal sampling value S_1 is available after the amplifier, A/D conversion and zero calibration, which can be got as

$$S_1 = K \cdot U_1 = K \cdot I \cdot R_0 \qquad (7)$$

The IN1 channel of M_1 multi-channel and the IN2 channel of M_2 multi-channel are open at step 2, and the output current I of AD590M pass through R_t and R_2, as well as the line resistor 2r forms voltage signal U_2 as formula (8)

$$U_2 = I \cdot (R_t + 2r) \qquad (8)$$

The thermal resistor signal sampling value S_2 is available after the amplifier, A/D conversion and zero calibration, which can be expressed as follows

$$S_2 = K \cdot U_2 = K \cdot I \cdot (R_t + 2r) \qquad (9)$$

The IN2 channel of M_1 and M_2 multi-channel are open at step 3, and the output current I of AD590M pass through R_3 and the line resistor 2r in correcting circuit forms line correcting voltage signal U_3 as formula (10)

$$U_3 = 2r \cdot I \qquad (10)$$

The line resistor signal sampling value S_3 is available after the amplifier, A/D conversion and zero calibration, which can be expressed as follows

$$S_3 = K \cdot U_3 = K \cdot I \cdot 2r \qquad (11)$$

The IN1 channel of M_1 multi-channel and the IN3 channel of M_2 multi-channel is open at step 4 forming voltage signal U_4 and the zero calibrating signal sampling value S_4' is available after the amplifier, A/D conversion and zero calibration

$$S_4' = K \cdot U_4 \qquad (12)$$

The value of U_4 and S_4' is too small to converge to zero and the formula (12) is used to the zero calibration of S_1、S_2、S_3. We can get formula (13) based on formula (9)

$$R_t = \frac{S_2}{K \cdot I} - 2r \qquad (13)$$

Formula (14) can be get based on formula (11)

$$2r = \frac{S_3}{K \cdot I} \qquad (14)$$

Besides, Formula (15) which is not influenced by the line resistor can be get based on formula (13) and formula (14)

$$R_t = \frac{S_2}{K \cdot I} - \frac{S_3}{K \cdot I} \qquad (15)$$

Formula (16) can be get based on formula (7)

$$K \cdot I = \frac{S_1}{R_0} \qquad (16)$$

Finally, formula (17) can be get based on formula (15) and formula (16)

$$R_t = \frac{S_2 - S_3}{S_1} \cdot R_0 \qquad (17)$$

Formula (17) is the theoretical calculation model of the current method model for measuring thermal resistor. The measurement accuracy error caused by the line resistor can be completely eliminated, which makes the device is not affected by environmental temperature. From formula (17), we can see that R_t is related to R_0, S_1, S_2 and S_3 rather than the output current I of AD590M and the amplification factor K of the Amplifier, so this design can ignore the zero drift and nonlinear effects.

3. The hardware design of the system

The hardware of the system is designed as the block diagram Fig. 3 shows.

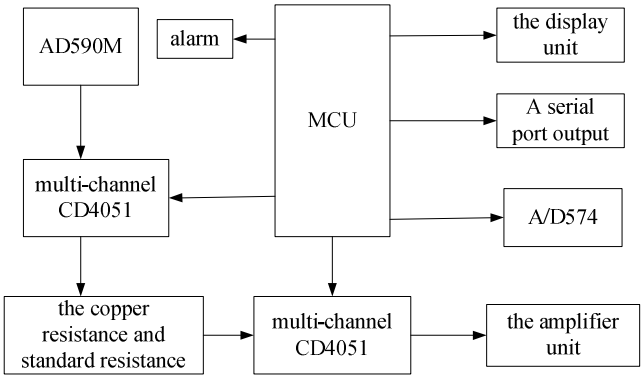

Fig. 3 The hardware block diagram of the system

3.1 The temperature signal processing unit

The signal measurement circuit is made up of the copper thermal resistor R_t, standard resistor R_0(in this paper R_0=164.27 Ω), resistor R_1~R_3, the multi-channel switch M_1 and M_2, etc. In addition, R_1, R_2 and R_3 can be calculated according to the standard that the total resistor of each line is nearly equal. In this paper, R_1=835.73Ω, R_2=868.62Ω, R_3=990Ω, r=5 Ω. The main functions of this unit are signal acquisition, the calibration of measuring range, zero calibration, the correction line resistor, etc. The hardware parts of the signal measurement circuit are shown as Fig. 4.

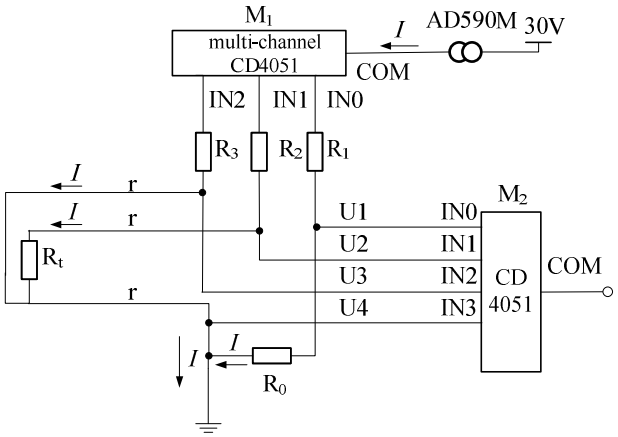

Fig.4 The hardware parts of the signal measurement circuit

3.2 The Signal amplification unit

The amplifier unit adopts three-stage amplifier, which is composed of operational amplifiers IC0 ~ IC2, etc. The amplifier unit is designed as Fig.5. Because the input signal is transformed by the current I from AD590M, the input impedance of the amplifier must be designed to be relatively high. The maximum value of Cu_{100} thermal resistor is

164.27 Ω , and the line equivalent resistor 2r is approximate to 10 Ω . The AD converter AD574 adopts 10V input method. The output current of AD590M is 323.2uA when the environment temperature is 50℃. We can get the magnification of the total amplifiers K=10V/[(164.27Ω+10Ω)×323.2 uA]=177.54. The magnification K_1、K_2、K_3 of each amplifier can be calculated as follows

$$K_1 = 1 \tag{18}$$

$$K_2 = \frac{R_6}{R_4} \tag{19}$$

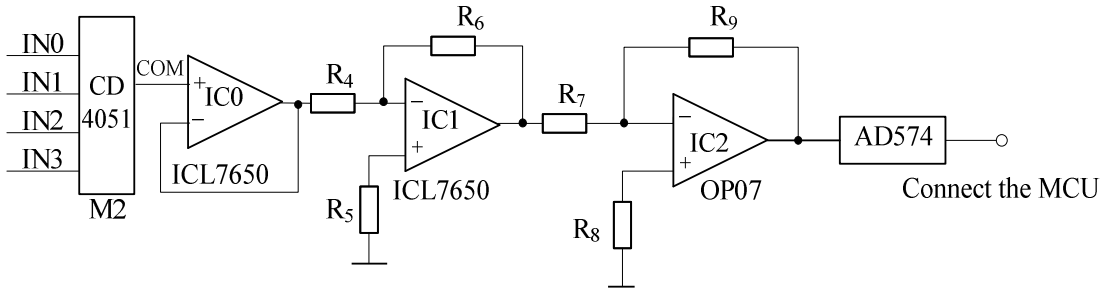

Fig.5 The signal amplification unit

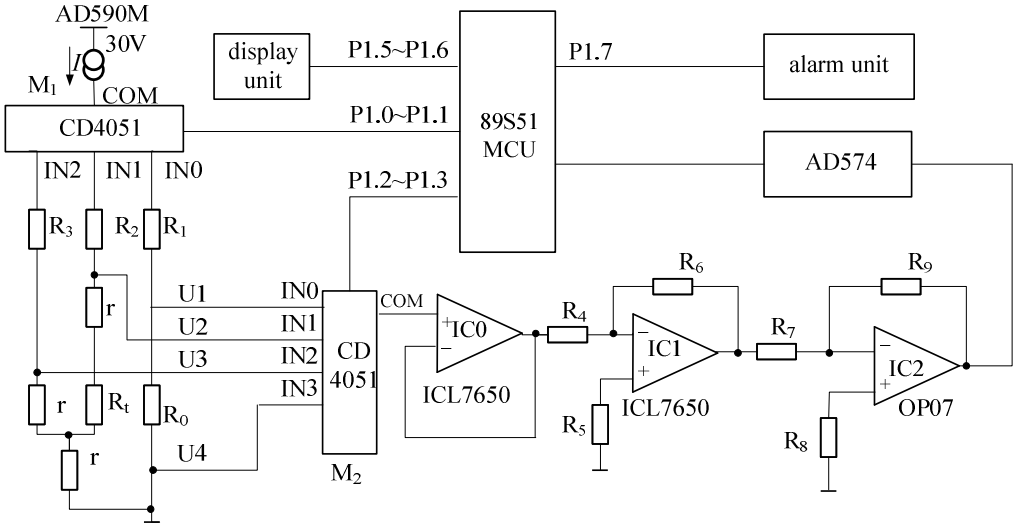

Fig.6 The data acquisition and processing unit

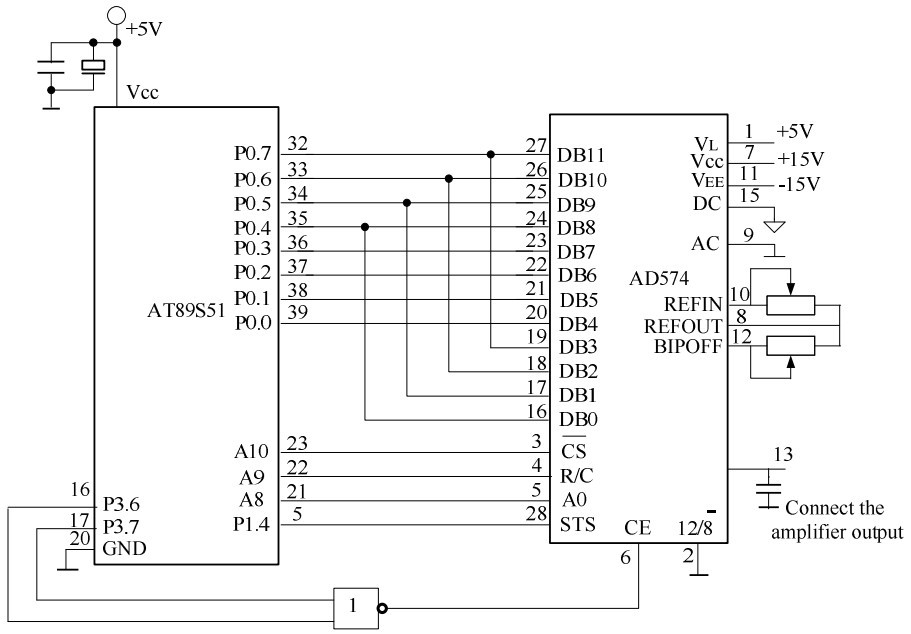

Fig.7 The interface circuit of the MCU and AD574

$$K_3 = \frac{R_9}{R_7} \tag{20}$$

Where R_4=2K Ω , R_6=51K Ω , R_7=1 K Ω , R_9=6.8K Ω , R_5=R_4//R_6 , R_8=R_7//R_9, the total magnification is

$$K = K_1 \cdot K_2 \cdot K_3 = \frac{R_6}{R_4} \cdot \frac{R_9}{R_7} = 173.4 \tag{21}$$

The actual magnification is slightly less than the calculated value of 177.54, but as a result of using the real-time calibration, the calculation model does not contain the magnification. So the magnification does not affect the accuracy of the results.

3.3 Sampling and Data Processing

The data sampling process has been introduced in the current method of measuring thermal resistor model [1-2,24-25]. The MCU samples according to table 1 and Fig. 6. We define the sampling value of U_1、U_2、U_3 and U_4 to be S_1'、S_2'、S_3' and S_4' respectively. After digital filter, bad data value processing and zero calibration (namely excluding the zero calibration signal S_4'), we can get the sampling data S_1、S_2 and S_3.

$$S_1 = S_1' - S_4' \tag{22}$$

$$S_2 = S_2' - S_4' \tag{23}$$

$$S_3 = S_3' - S_4' \tag{24}$$

3.4 The design of A/D conversion part

This part adopts conversion chip AD574 with single polarity input method [1-4,25], which can convert the voltage ranging from 0V to 10V. After conversion, the eight high numbers is exported from DB11 ~ DB4, while the low numbers is exported from DB3 ~ DB0. Interface circuit is shown in Fig. 7. The conversion process of AD574 can be seen as setting port address to DPTR → starting the transition → tracking the status of the output signal STS → reading the conversion result.

3.5 The design of display unit

The interface circuit of the MCU and LED digital tube is shown in Fig. 8.

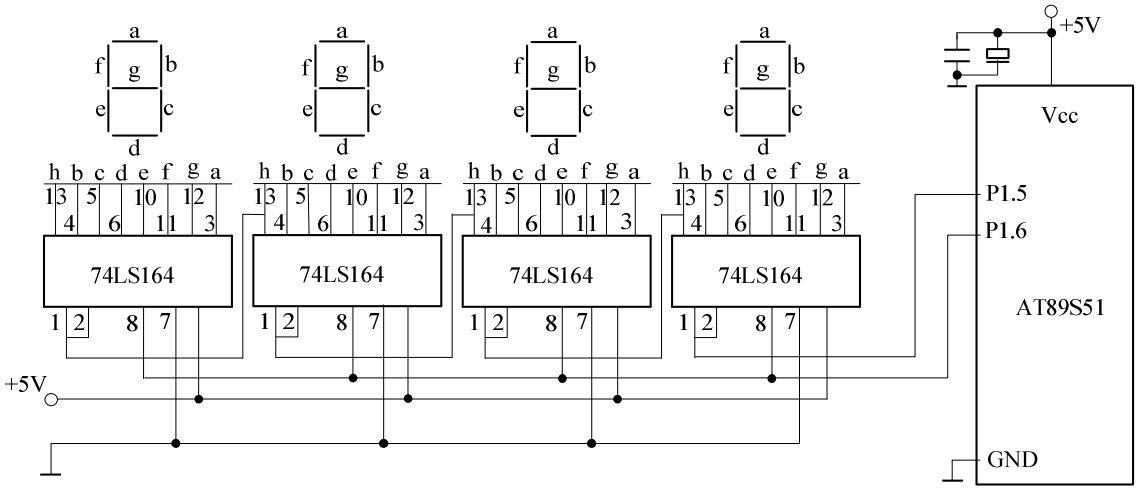

Fig.8 The interface circuit of the MCU and LED digital tube

3.6 The design of alarm unit

The temperature measurement range of this device is - 50 ~ + 150 ℃, so the device must give an alarm when the measured temperature is beyond the scope of measurement. The interface circuit of the MCU and alarm unit is shown in Fig. 9.

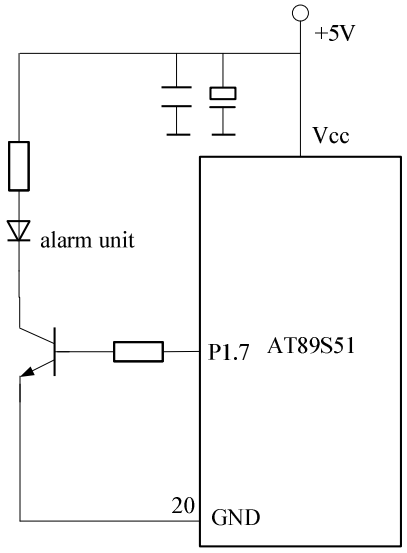

Fig.9 The alarm unit

3.7 The design of serial output unit

The serial output port is completed by MAX220. Each data contains 2 bytes and the baud rate is 9600, which can be accurate to 0.1 □. The interface circuit of the MCU and the serial output unit is shown in Fig. 10.

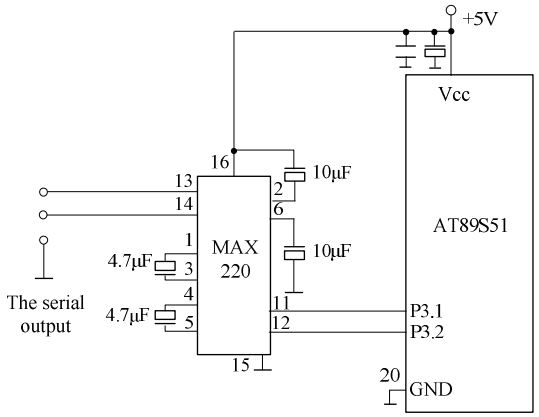

Fig.10 The serial output unit

4 The software design of the system

The main function of the system software is to control the multi-channel logic switch completing the data acquisition and accomplish the bad value processing, digital filtering, the copper thermal resistor calculation, the reverse look-up of the indexing table, the calculation of fractional part between two integral temperature points, the warning

system and the temperature display part, etc. The software design uses block-based design method in order to facilitate the programming and modification. The block-based design is a set together with a family of subsets (repeated subsets are allowed at times) whose members are chosen to satisfy some set of properties that are deemed useful for a particular application. So we often adopt block-based design to exploit complex systems[1-4,24,27-29].

Through analysis, the software program design of this temperature measuring device can be divided into the program initialization, the bad value processing subprogram, digital filter subprogram, copper thermal resistor calculation subprogram, temperature calculation subprogram, alarm subprogram and display subprogram, etc. Additionally, the block diagram of the software design is presented as Fig. 11.

There are 201 temperature points in the indexing table of Cu_{100} thermal resistor, ranging from -50 ℃ to 150 ℃. The value of the Cu_{100} thermal resistor of each temperature points adopts 10mΩ as the base unit, which exists in two bytes using hexadecimal code. The temperature points were made into indexing table according to the sequence from low temperature to high temperature, which were stored in the memory with the memory address increasing.

With the fitting function of Matlab software, we get the temperature characteristic curve of the value of the copper thermal resistor with temperature, where the $R^2 \approx 1$, indicating that the linear relationship is relative good. The scatter diagram and the fitting curve of the Cu_{100} thermal resistor indexing table with the temperature are shown as Fig.12.

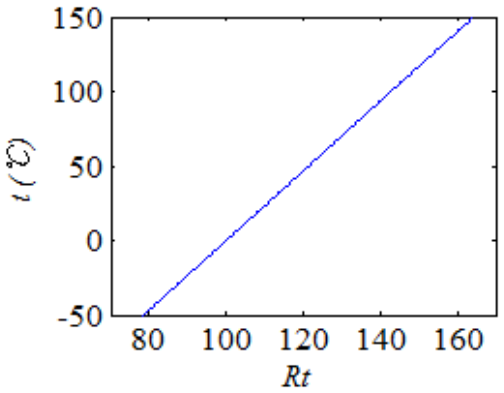

Fig.12 The scatter diagram and the fitting curve of the Cu_{100} thermal resistor indexing table with the temperature

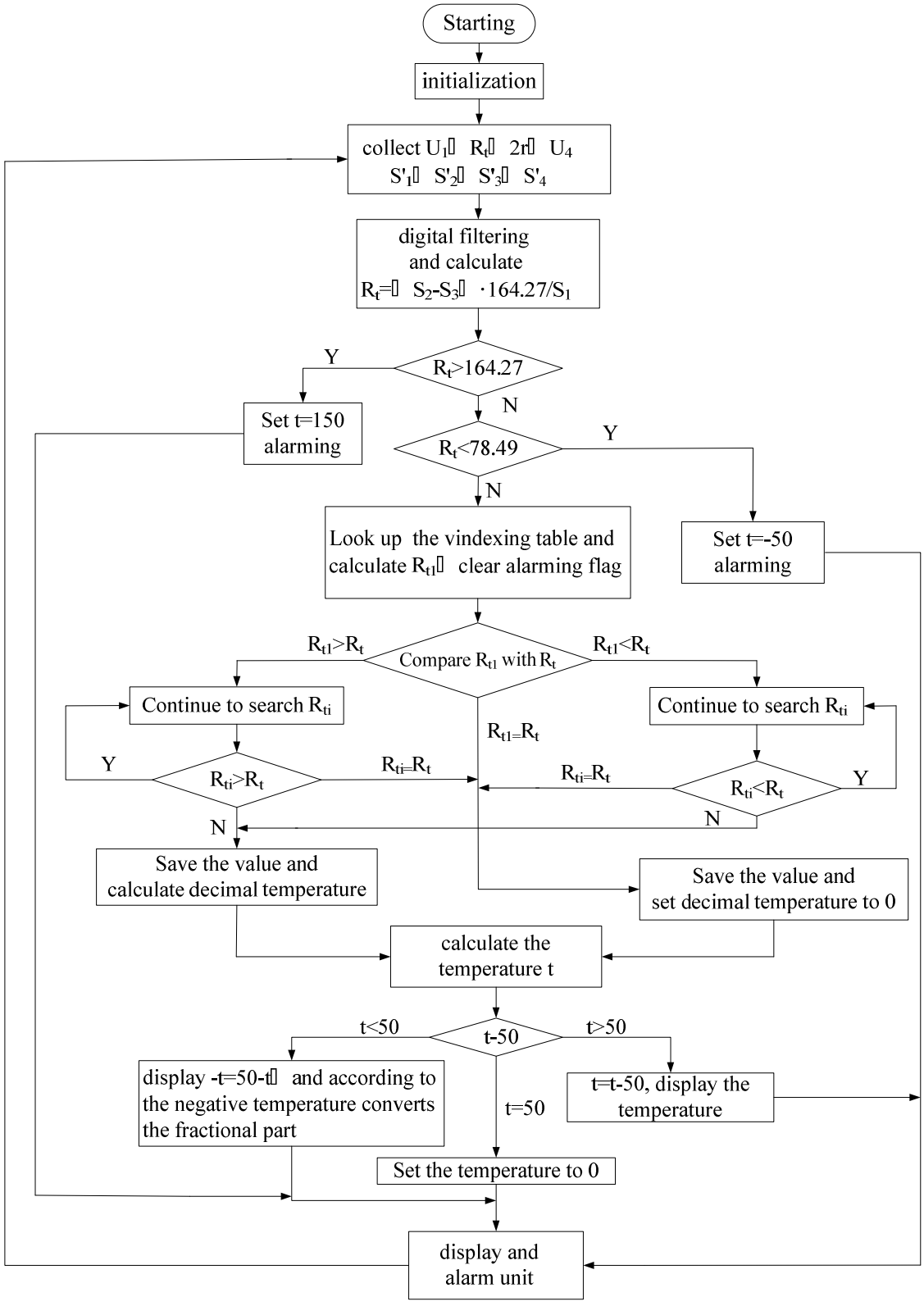

Fig.11 The block diagram of the software design

The formula of the characteristic curve in Fig.12 is shown as

$$t = 2.334 \cdot R_t - 233.34 \qquad (25)$$

Where the unit of R_t and t are Ω and respectively.

The error of the fitting curve and characteristic curve of the copper thermal resistor is relatively

small. The maximum temperature error is 0.16 ℃, less than 1 ℃, between the same copper thermal resistor values, so we can find the whole temperature points without missing.

We can get the value of R_t based on the formula (17). If the value of R_t equals to the value in the Cu_{100} thermal resistor indexing table, the temperature value is the corresponding temperature value which is requested. Otherwise, we should calculate the decimal part of the temperature with the linear interpolation method. The decimal part Δt can be expressed as formula (26)

$$\Delta t = \frac{R_t - R_t(t_z)}{R(t_z+1) - R_t(t_z)} \times 1℃ \qquad (26)$$

where $R_t(t_z)$ is the maximal integer thermal resistor value which is not greater than R_t, while R_t (t_z + 1) is the minimum integer thermal resistor value which is not less than R_t , namely, the value of R_t is between $R_t(t_z)$ and R_t (t_z + 1). If the accuracy of Δt is 0.1℃, the final temperature value for the measurement can be expressed as formula (27)

$$t = t_z + \Delta t \qquad (27)$$

5 The error analysis

From formula (17) we can get the combined standard uncertainty of R_t as formula (28)

$$\begin{aligned} u(R_t) &= [(\frac{\partial R_t}{\partial S_1})^2 u^2(S_1) + (\frac{\partial R_t}{\partial S_2})^2 u^2(S_2) + \\ &(\frac{\partial R_t}{\partial S_3})^2 u^2(S_3) + (\frac{\partial R_t}{\partial R_0})^2 u^2(R_0)]^{\frac{1}{2}} \\ &= [(-\frac{S_2 - S_3}{S_1^2} \cdot R_0)^2 u^2(S_1) + (\frac{R_0}{S_1})^2 u^2(S_2) + \\ &(-\frac{R_0}{S_1})^2 u^2(S_3) + (\frac{S_2 - S_3}{S_1})^2 u^2(R_0)]^{\frac{1}{2}} \end{aligned} \qquad (28)$$

S_1 represents the calibrating signal sampling value with the temperature changing and the minimum value of S_1 is S_1= (273.15/323.2uA) ×4096=3462 at 0℃. S_2 represents the copper thermal resistor signal sampling value and the maximum value of S_2 is 4096. S_2 represents the line resistor signal sampling value. If we approximate 2r as 10Ω, S_3 can be expressed as S_3=10Ω×4096/174.27Ω=235.04. $u(S_1)$ 、$u(S_2)$、$u(S_3)$ represent the standard uncertainty of AD574 whose mean value is 1/ ($2\times4096\sqrt{3}$) =7.04E-5. $u(R_0)$ represent the standard uncertainty of R_0 whose value is 164.27Ω (the maximum error is 0.01Ω). By choosing the confidence probability of normal distribution as 0.9973, we can get $u(R_0)$=0.01/3Ω=3.33E^{-3} Ω.

After calculating the minimum value of S_1 , the maximum value of S_2 ,S_3 ,$u(R_0)$, we can get $u(R_t)$ (the combined standard uncertainty of R_t). By choosing the confidence probability of normal distribution as 0.9973, we can get the extended combined standard uncertainty of R_t, which can be expressed as U=3×$u(R_t)$=0.011Ω.

From the Cu_{100} thermal resistor indexing table, we can find the minimum difference of thermal resistor value between two integer temperature points is 0.39Ω, which means that the maximum of copper resistor temperature conversion coefficient is 1℃/0.39Ω. The total measuring error is determined by the error of R_t (0.011Ω) and the rounding error of R_t (the maximum rounding error of Cu_{100} is 0.005Ω) when calculating. We convert the resistor error to the limit error of temperature which can be expressed as δ_{R_t} =0.028℃ , δ_b =0.013℃ respectively. Finally, the limit temperature error of the device can be expressed as formula (29)

$$\begin{aligned} \delta &= \sqrt{\delta_1^2 + \delta_2^2} = \sqrt{0.028^2 + 0.013^2} \\ &= 0.031℃ \end{aligned} \qquad (29)$$

Formula (29) is the theoretical limit error of the device, which can meet the general industrial design requirements.

6 Conclusion

The purpose of this paper is designing a copper resistance (Cu100) linear temperature measurement device, mainly used for the temperature control of industrial processes. The device is made up of signal acquisition unit, signal amplification unit, A/D converter, digital display unit, serial ports and other sectors, mainly to complete the data acquisition, logic control, bad value processing, digital filtering, the calculation of thermal resistance, look-up table, calculation, warning, serial output and display. The System uses AD590M constant current source instead of the constant current source, providing

current. Under the control of the AT89S51 MCU, the standard resistance uses the standard signal to calibrate the system, then conduct signal sampling, calculation of the copper resistance value and the temperature values corresponding to the reverse look-up of the indexing table, thus achieving a true sense of the linearization. The device greatly reduces the temperature drift and nonlinearity of the amplifier in the measurement process, realizing the whole temperature measurement range of the copper resistance. The theoretical error of the device is less than 0.1 □ to meet the requirements in most of industrial processes.

References:

[1] Yue, Cai Qing, Based on MCU AT89S52 temperature control system, *Applied Mechanics and Materials*, Vol.441, 2014, pp. 875-878.

[2] Oberoi, D.S.; Dhingra, Harinder, Simple Temperature Indicator Uses RISC-Based MCU, *Electronic Design*, Vol.51, No.19, 2003, pp.67-68.

[3] Reading, M., The use of modulated temperature programs in thermal methods, *Journal of Thermal Analysis and Calorimetry*, Vol.64, No.1, 2001, pp.7-14.

[4] Azzouzi, M.; Neri, F., An introduction to the special issue on advanced control of energy systems, *WSEAS Transactions on Power Systems*, Vol.8, No.3, 2013, pp.103.

[5] Ciufudean, C., Nri, F., Open research issues on Multi-Models for Complex Technological Systems, *WSEAS Transactions on Power Systems*, Vol. 13, 2014, in press.

[6] Neri, F., Open research issues on Computational Techniques for Financial Applications, *WSEAS Transactions on Power Systems*, Vol. 13, 2014, in press.

[7] Pekař, L., Neri, F., An introduction to the special issue on advanced control methods: Theory and application, *WSEAS Transactions on Systems*, Vol.12, No.7, 2013, pp.337-338.

[8] Bojkovic, Z.; Neri, F., An introduction to the special issue on advances on interactive multimedia systems, *WSEAS Transactions on Systems*, Vol.12, No.6, 2013, pp. 301-303.

[9] An, Young-Jae; Ryu, Kyungho; Jung, Dong-Hoon; Woo, Seung-Han; Jung, Seong-Ook, An energy efficient time-domain temperature sensor for low-power on-chip thermal management, *IEEE Sensors Journal,* Vol.14, No.1, 2014, pp. 104-110.

[10] Doroshin, A. V.; Neri, F., Open research issues on Nonlinear Dynamics, Dynamical Systems and Processes, *WSEAS Transactions on Systems*, Vol.13, 2014, in press.

[11] Guarnaccia, C., Neri, F., An introduction to the special issue on recent methods on physical polluting agents and environment modeling and simulation, *WSEAS Transactions on Systems,* Vol.12, No.2, 2013, pp. 53-54.

[12] Doroshin, A.V., Exact solutions in attitude dynamics of a magnetic dual-spin spacecraft and a generalization of the lagrange top, *WSEAS Transactions on Systems,* Vol.12, No. 10, 2013, pp. 471-482.

[13] Volos, C.; Neri, F., An introduction to the special issue: Recent advances in defense systems: Applications, methodology, technology, *WSEAS Transactions on Systems*, Vol.11, No.9, 2012, pp. 477-478.

[14] Hájek, P., Neri, F., An introduction to the special issue on computational techniques for trading systems, time series forecasting, stock market modeling, financial assets modeling, *WSEAS Transactions on Business and Economics*, Vol. 10, No. 4, 2013, pp. 201-292.

[15] Doroshin, A.V., Synthesis of attitude motion of variable mass coaxial bodies, *WSEAS Transactions on Systems and Control*, Vol. 13, 2014, in press.

[16] Karthikeyan, P., Neri, F., Open research issues on Deregulated Electricity Market: Investigation and Solution Methodologies, *WSEAS Transactions on Systems,* Vol. 3, No. 1, 2008, pp. 50-61.

[17] Panoiu, M., Neri, F., Open research issues on Modeling, Simulation and Optimization in Electrical Systems, *WSEAS Transactions on Systems,* Vol. 13, 2014, in press.

[18] Lv, Sisi, Study on low temperature performance evaluation index of asphalt mixture based on bending test at low temperature, *Applied Mechanics and Materials*, Vol. 193-194, 2012, pp. 427-430.

[19] Johnston, A.H.; Swimm, R.T.; Thorbourn, D.O., Total dose effects on bipolar integrated circuits at low temperature, *IEEE Transactions on Nuclear Science,* Vol.59, No.6, 2012, pp. 2995-3003.

[20] Sun, Rong-Gao; Wan, Zhong; Sun, De-Chao,. Based on embedded database greenhouse temperature and humidity intelligent control system, *WSEAS Transactions on Circuits and Systems*, Vol.8, No.1, 2009, pp.41-52.

[21] Wang, Chenluan, A thermostat fuzzy control system based on MCU, *3rd International Symposium on Intelligent Information*

Technology Application, IITA 2009, Vol.1, 2009, pp. 462-463.

[22] Yi, Soon Jai; Jeong, Hang Geun; Cho, Seong Ik, Temperature compensated crystal oscillator based on current conveyor and thermistor network, *WSEAS Transactions on Circuits and Systems*, Vol.6, No.3, 2007, pp. 296-301.

[23] Lin, Shieh-Shing; Horng, Shih-Cheng; Hsu, Hen-Chia; Chen, Jia-Hau; Hsieh, Tseng-Lin; Ho, Chih-Hao; Lin, Kuang-Yao, A design of a class of temperature stabilization system and implementation, *WSEAS Transactions on Circuits and Systems*, Vol.8, No.6, 2009, pp. 498-507.

[24] Liu, Guo-qiang, A temperature-measuring system on the gun-barrel bore of armor-artillery base on 80C196 MCU, *Advanced Materials Research*, Vol.562-564, 2012, pp. 1920-1923.

[25] Wang, Haizhen; Duan, Zhengang;Wang, Jian; Lian, Xiaoqin, A design of boiler temperature monitoring system based on MCU, *2011 International Conference on Electrical and Control Engineering, ICECE 2011 - Proceedings*, 2011, pp. 3765-3768.

[26] Han, Dawoon.; Jang, You-Cheol; Oh, Sung-Nam; Chand, Rohit; Lim, Ki-Tae; Kim, Kab-Il; Kim, Yong-Sang, MCU based real-time temperature control system for universal microfluidic PCR chip, *Microsystem Technologies*, 2013, pp.1-6.

[27] Lin, Jin; Tong, Zhao, Granary temperature and humidity detection system based on MCU, *Advanced Materials Research,* Vol. 605-607, No.19, 2013, pp. 941-944.

[28] Muntean, M.; Neri, F., Foreword to the special issue on collaborative systems, WSEAS Transactions on Systems*,* Vol. 11, No.11, 2012, pp. 617.

[29] Pekař, L.; Neri, F., An introduction to the special issue on time delay systems: Modelling, identification, stability, control and applications WSEAS Transactions on Systems, *WSEAS Transactions on Systems,* Vol. 11, No.10, 2012, pp. 539-540.

Fault Detection and Diagnosis in Non-Linear Process using Multi Model Adaptive H^{∞} Filter

M. MANIMOZHI, R. SARAVANAKUMAR
School of Electrical Engineering
VIT University
Vellore – 632014, Tamilnadu
India
mmanimozhi@vit.ac.

Abstract: - Kalman Filter (KF) is widely used in process industries as state estimator to diagnose the faults either in the sensor, actuator or in the plant because of its recursive nature. But, due to increase in non-linearity and exogenous perturbations in the monitored plant, it is often difficult to use a simple KF as state estimator for nonlinear process monitoring purposes. Thus, the first objective of this paper is to design an Adaptive Linear H^{∞} Filter ($ALH^{\infty}F$) using gain scheduling algorithm to estimate nonlinear process states in the presence of unknown noise statistics and unmodeled dynamics. Next the designed $ALH^{\infty}F$ is used to detect sensor and actuator faults which may occur either sequentially or simultaneously using Multi Model $ALH^{\infty}F$ ($MMALH^{\infty}F$). The proposed estimator is demonstrated on Continuously Stirred Tank Reactor (CSTR) process to show the efficacy. And the performance of $MMALH^{\infty}F$ is compared with MMALKF. The proposed $MMALH^{\infty}F$ is detecting and isolating the faults exactly in the presence of unknown noise statistics and unmodeled dynamics.

Key-Words: - CSTR, Process Monitoring, Kalman Filter, Multi Model Adaptive Linear H^{∞} Filter, Residual generation, State Estimation.

.

1 Introduction

Due to increase in complexity, non-linearity and exogenous perturbations, it is often difficult to use a simple Kalman filter as state estimator for process monitoring purposes. To use linear estimator or controller for the non-linear applications multiple local linear model approach is used to represent the non-linear model. Each local linear model is valid around particular operating point. To get the global linear model all the local linear models are fused using gain scheduling algorithm at current operating point [1].

Process monitoring has become an essential task because of process automation with minimal manual intervention. To ensure the quality of the product, optimal utilization of the plant safety and to control the pollution level it becomes mandatory. Kalman filter is widely used in process industries as state estimator to diagnose the faults either in the sensor, actuator or in the plant because of its recursive nature. Kalman filter is based on the assumption that the state and the measurement noises are uncorrelated and zero mean Gaussian noise with known covariance, and it is suitable for linear applications only [2]. The Kalman filter fails if either the noise statistics are unknown, if there is a plant model-mismatch or the process is non-linear and in the presence of unmodeled dymanics. For non-linear systems the widely used estimator is Extended Kalman Filter (EKF). EKF linearizes all nonlinear transformations and substitutes Jacobian matrices in the KF equations [3]. But the nonlinear estimation methods are computationally complex. Most of the existing algorithms are designed for sequential faults and not for simultaneous faults.

To overcome all these difficulties, first the Adaptive Linear H^{∞} Filter ($ALH^{\infty}F$) is designed using gain scheduling algorithm to use the H^{∞} filter for non-linear state estimation in the presence of unknown noise statistics and unmodeled dynamics. Next, multiple $ALH^{\infty}Fs$ are designed with different hypothesis to isolate sensor and actuator faults which may occur either sequentially or simultaneously [4]. And the performance of $MMALH^{\infty}F$ is compared with MMALKF in the presence of unknown noise statistics and unmodeled dynamics. The following section deals with the design of H^{∞} Filter and section 3 and 4 deals with the design of $ALH^{\infty}F$ and $MMALH^{\infty}F$ respectively. The process used for simulation studies is presented in section 5. Simulation results are presented in

section 6 and conclusion reached is given in section 7.

2. H$^\infty$ Filter

The H$^\infty$ filter design is based on linear quadratic game theory approach. The filter is designed to estimate the process states in the presence of unknown noise statistics and unmodeled dynamics. Consider the following linear stochastic time invariant discrete-time system.

$$x_{k+1} = \Phi_x x_k + \Phi_u u_k + w_k \quad (1)$$

$$y_k = \Phi_y x_k + v_k \quad (2)$$

Where $x_k \in R^n$ represents state vector, $w_k \in R^m$ represents the process noise vector, $y_k \in R^p$ represents measurement vector and $v_k \in R^p$ represents measurement noise vector. Φ_x, Φ_u and Φ_y are system matrices of appropriate dimension. The linear combination of state x_k is given by,

$$Z_k = L_k x_k \quad (3)$$

Where L_k is a user defined matrix. State variables are estimated based on measurement history till (N-1) sampling instant. Basically the H$^\infty$ filter is a one step ahead predictor, it tries to estimate the states with small estimation error $e_k = Z_k - \hat{Z}_k$. Using game theory approach the H$^\infty$ filter will try to satisfy the following performance criterion.

$$J = \frac{\sum_{k=0}^{N-1} \left\| Z_k - \hat{Z}_k \right\|_S^2}{\left\| x_0 - \hat{x}_0 \right\|_{p_0^{-1}}^2 + \sum_{k=0}^{N-1} \left(\left\| w_k \right\|_{Q^{-1}}^2 + \left\| v_k \right\|_{R^{-1}}^2 \right)} \quad (4)$$

Where $\hat{x}_0$ is an apriori estimate of x_0. P_0, Q, R and S are symmetric, positive definite weighting matrices chosen by designer based on process dynamics. The estimate Z_k should satisfy,

$$J < \frac{1}{\theta} \quad (5)$$

Where $\theta > 0$ represents the desired level of noise attenuation. The H$^\infty$ filter can be interpreted as minmax problem. The performance criterion given in (4) becomes

$$\min_{\hat{Z}_k} \max_{v_k, w_k, x_0} J = -\frac{1}{\theta} \left\| x_0 - \hat{x}_0 \right\|_{p_0^{-1}}^2 + \sum_{k=0}^{N-1} \left[\left\| Z_k - \hat{Z}_k \right\|_S^2 - \frac{1}{\theta} \left(\left\| w_k \right\|_{Q^{-1}}^2 + \left\| v_k \right\|_{R^{-1}}^2 \right) \right] \quad (6)$$

The performance criterion can be made less than $\frac{1}{\theta}$ with the following estimation strategy [5,6]

$$\bar{S} = L^T S L \quad (7)$$

$$K = P[I - \theta \bar{S} P + \Phi_y{}^T R^{-1} \Phi_y P]^{-1} \Phi_y{}^T R^{-1} \quad (8)$$

$$\hat{x}_{k+1} = \Phi_x{}^T \hat{x}_k + \Phi_x K (y_k - \Phi_y \hat{x}_k) \quad (9)$$

$$P = \Phi_x P[I - \theta \bar{S} P + \Phi_y{}^T R^{-1} \Phi_y P]^{-1} \Phi_x{}^T + Q \quad (10)$$

If designer is interested in second element of Z_k then the corresponding $S(2,2)$ should be chosen large relative to other element.

3. Adaptive Linear H$^\infty$ Filter

Let us consider a nonlinear stochastic system represented by the following state and output equations:

$$x_{k+1} = f(x_k, u_k, w_k) \quad (11)$$

$$y_k = h(x_k, u_k, v_k) \quad (12)$$

The nonlinear system is linearized around different operating points using Taylor series expansion. The linear system around operating points $(\bar{x}_i, \bar{u}_i)$ is given as follows,

$$x_{(k+1)i} = \Phi_{xi}(x_k - x_i) + \Phi_{ui}(u_k - u_i) + w_k \quad (13)$$

$$y_{ki} = \Phi_{yi} x_{ki} + v_k \quad (14)$$

The nonlinear system is represented by a fused linear model using gain scheduling technique at a given operating point. For a given input vector u_k the fused linear model is represented as follows:

$$x_{k+1} = \sum_{i=1}^{N} g_i [\Phi_{xi}(x_k - \bar{x}_i) + \Phi_{ui}(u_k - \bar{u}_i) + \bar{x}_i] \quad (15)$$

$$y_k = \Phi_{yi} x_k \quad (16)$$

To cover the entire operating horizon, five operating points has been selected (i=1 to 5). Let q_c , is the actual value of the measured process variable at current sampling instant and g_i is the weighting factor .

If $(q_c \geq q_{c5})$, then

$$g_1 = g_2 = g_3 = g_4 = 0 \quad and \quad g_5 = 1 \quad (17)$$

If $(q_{c4} < q_c \leq q_{c5})$, then

$$g_1 = g_2 = g_3 = 0, \quad g_4 = \frac{q_c - q_{c4}}{q_{c5} - q_{c4}} \quad and \quad g_5 = 1 - g_4 \quad (18)$$

If $(q_{c3} < q_c \leq q_{c4})$, then

$$g_1 = g_2 = g_5 = 0, \quad g_3 = \frac{q_c - q_{c3}}{q_{c4} - q_{c3}} \quad and \quad g_4 = 1 - g_3 \quad (19)$$

If $(q_{c2} < q_c \leq q_{c3})$, then

$$g_1 = g_4 = g_5 = 0, \quad g_2 = \frac{q_c - q_{c2}}{q_{c3} - q_{c2}} \quad and \quad g_3 = 1 - g_2 \quad (20)$$

If $(q_{c1} < q_c \le q_{c2})$, then

$$g_1 = \frac{q_c - q_{c1}}{q_{c2} - q_{c1}}, g_2 = 1 - g_1 \quad and \quad g_3 = g_4 = g_5 = 0 \quad (21)$$

If $(q_c \le q_{c1})$, then

$$g_1 = 1 \ \ and \ \ g_2 = g_3 = g_4 = g_5 = 0 \quad (22)$$

The weighting factors are in the range of [0 1].

This approach consists of five local linear estimators and a scheduler. The local linear observer is designed using H^{∞} Filter. At a particular operating point, the local estimator is given below.

$$K_i = P_i[I - \theta \bar{S}P + \Phi_{yi}{}^T R^{-1} \Phi_{yi} P_i]^{-1} \Phi_{yi}{}^T R^{-1} \quad (23)$$

$$\hat{x}_{i(k+1)} = \Phi_{xi}{}^T \hat{x}_k + \Phi_{xi} K_i (y_k - \Phi_{yi} \hat{x}_k) \quad (24)$$

$$P_i = \Phi_{xi} P_i [I - \theta \bar{S} P_i + \Phi_{yi}{}^T R^{-1} \Phi_{yi} P_i]^{-1} \Phi_{xi}{}^T + Q \quad (25)$$

At each sampling instant the scheduler will assign weights (gain scheduling) for each local linear estimator and the weighted sum of the output will be the estimate of the current state. The scheduler assigns weight based on scheduling variable. The scheduling variable may be input variable or state variable or some auxiliary variable, the scheduling variable considered here is coolant flow rate q_c of the process. The ALH$^{\infty}$F (global estimator) dynamics will be weighted sum of individual LH$^{\infty}$F and it is given below.

$$\hat{x}_{k+1} = \sum_{i=1}^{N} g_i \left\{ \Phi_{xi}^T \hat{x}_{ik} + K_i \left[(y_k - \bar{y}_i) - \Phi_{yi} \hat{x}_{ki} + \bar{x}_i \right] \right\} \quad (26)$$

4. Multi Model Adaptive Linear H$^{\infty}$ Filter

MMALH$^{\infty}$F approach uses multiple ALH$^{\infty}$F. Each ALH$^{\infty}$F is designed based on specific hypothesis to detect a specific fault. The fault considered here is soft fault of fixed bias. The same approach can be used to detect dritf like faults. This approach is capable of detecting multiple sequential as well as multiple simultaneous faults which may occur either in sensors or in actuators [7].

The estimator 1 designed to estimator sensor bias and it is hypothesized with a sensor bias of magnitude B_S , then the measurement equation is given by,

$$y_k = \Phi_{yi} x_k + v_k + B_S \quad (27)$$

Estimator 2 is designed to detect actuator bias and it is hypothesized with a actuator bias of magnitude B_a , then the state equation is given by,

$$x_{k+1} = \Phi x_k + \Phi_u (u_k + B_a) + w_k \quad (28)$$

All the ALH$^{\infty}$F except the one using correct hypothesis will produce large estimation error. By monitoring the residuals of each ALH$^{\infty}$F, the faulty element can be detected and isolated. The proposed MMALH$^{\infty}$F scheme is shown in Fig. 1. Each ALH$^{\infty}$F consists of five LH$^{\infty}$Fs developed at different operating points. The weights are calculated by using coolant flow rate of the process as scheduling variable. The LH$^{\infty}$F outputs are weighted and added to get the global output estimate($\hat{y}$). The process output is compared with the ALH$^{\infty}$F output to generate residuals. Under fault free condition the magnitude of the residuals are maximum. If fault occurs in any of the sensor or actuator, the estimators except the one using the correct hypothesis will produce large estimation error. If the ALH$^{\infty}$F is designed for -5% bias and the bias occurred is less than or above 0.5%, then the residual generated will be different from the one during the normal operating condition. By closely observing the innovations, the faults which occurs either sequentially or simultaneously can be isolated and the time of occurance can also be detected.

5. Continuously stirred Tank Reactor (CSTR)

A simulated CSTR process was considered to test the efficacy of the proposed method. The schematic of the system is shown in Fig 2. An irreversible exothermic reaction A → B occurs in a constant-volume reactor that is cooled by a single coolant stream The two state variables of the process are concentration and temperature. The first principle model of the system is given by the following equations.

$$\frac{dC_A(t)}{dt} = \frac{q(t)}{V}(C_{A0}(t) - C_A(t)) - k_0 C_A(t) \exp\left(\frac{-E}{RT(t)}\right) \quad (29)$$

$$\frac{dT(t)}{dt} = \frac{q(t)}{V}(T_0(t) - T(t)) - \frac{(-\Delta H) k_0 C_A(t)}{\rho C_p} \exp\left(\frac{-E}{RT(t)}\right) + \frac{\rho_c C_{pc}}{\rho C_p} q_c(t) \left\{ 1 - \exp\left(\frac{-hA}{q_c(t) \rho C_p}\right) \right\} T_{c0}(t) - T(t) \quad (30)$$

The steady state operating point data used in the simulation studies is given in Table 1[8,9]. The continuous linear state space model is obtained by linearizing the differential equations (29) and (30) around nominal operating point $\bar{C}_A$ and $\bar{T}$. The

state vector is $x(t)=[C_A;T]$ and the input vector is $u(t)=[q_C]$.

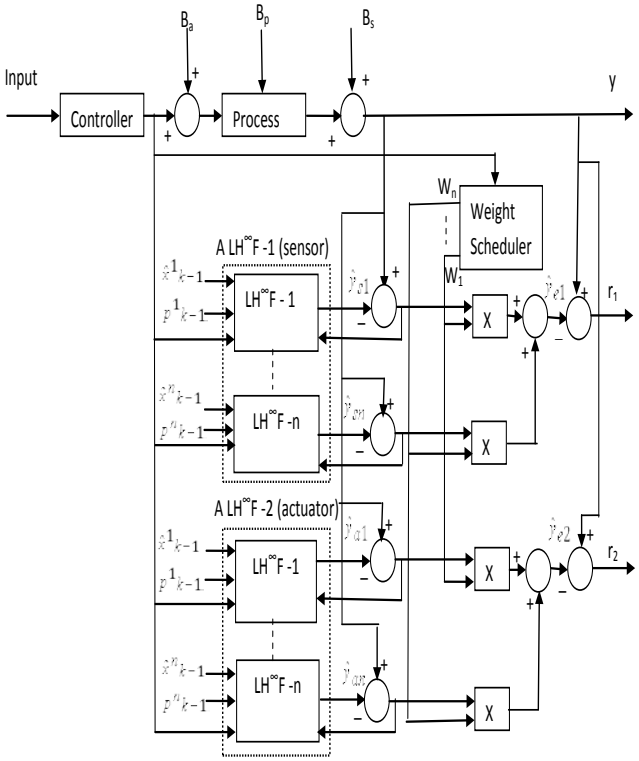

Fig. 1: Structure of the proposed MMALH$^{\infty}$F

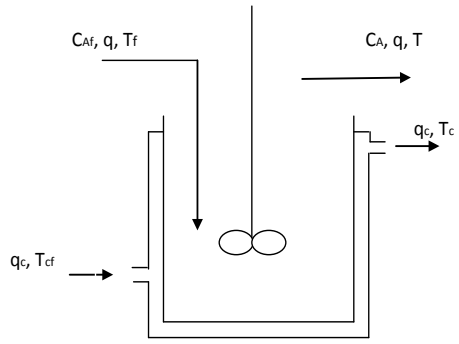

Fig. 2: Schematic of CSTR

6. Simulation Results

The CSTR process is simulated using first principles model as given in (29) and (30) and the true state variables are computed by solving the nonlinear differential equations using Matlab 7.1. The dynamic behavior of the CSTR process is not same at different operating points and the process is nonlinear.

6.1 Fused Linear Model: To validate the performance of ALKF (local estimators designed using linear kalman filter are fused using gain scheduling algorithm) and ALH$^{\infty}$F, the process states are estimated using these estimators and compared with the rigorous non-linear model. The process and measurement noise covariance are assumed to be 0.25% of coolant flow rate and 0.5% of state variables respectively. Fig.3 shows the variation in coolant flow rate introduced. Fig.4 and Fig.5 shows the estimation of system states when the noise sequences are uncorrelated using ALKF and ALH$^{\infty}$F. It has been observed that both ALKF and ALH$^{\infty}$F exactly estimates the system states without dynamic and steady state error in the presence of uncorrelated noise. Fig.6 and Fig.7 shows the estimation of system states when the measurement noise sequences are correlated. It has been observed that the performance ALH$^{\infty}$F is better than the ALKF when the noise sequences are correlated. The ALKF tracks the changes with dynamic and steady state error. Fig.8 and Fig.9 shows the residual generated when the noise sequences are correlated. Table 2 shows the performance comparison of ALKF and ALH$^{\infty}$F when the noise sequences are uncorrelated, correlated and after introducing distrubances in the feed temperature. It has been observed that the ALH$^{\infty}$F outperforms the ALKF when the noise sequences are correlated and in the presence of unmodeled dynamics.

Table 1: Nominal operating condition for CSTR

Process variable	Normal Value
Tank volume (V)	100 L
Feed flow rate (q)	100.0 L/ min
Feed concentration (C_{Af})	1 mol/ L
Feed temperature (T_f)	350.0 K
Coolant flow rate (q_c)	103 L/ min
Inlet coolant temperature (T_{cf})	350.0 K
Liquid density (ρ, ρ_c)	1 * 10^3 g/L
Specific heats(C_p, C_{pc})	1 cal/(g k)
Reaction rate constant(k_0)	7.2 * 10^{10} $min-1$
Activation energy term (E/R)	1 * 10^4 K
Heat of reaction (-ΔH)	-2 * 10^5 cal/ mol
Heat transfer term (hA)	7 * 10^5 cal/(min k)
product concentration (C_A)	0.0989 mol/ L
Reactor temperature (T)	438.7763 K

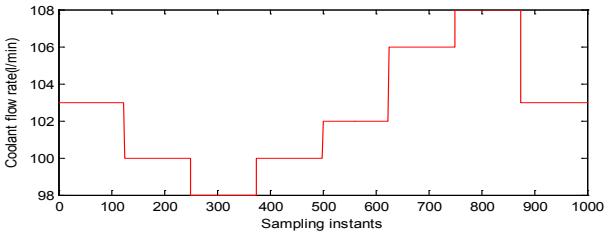

Fig. 3: Coolant flow rate (L/min)

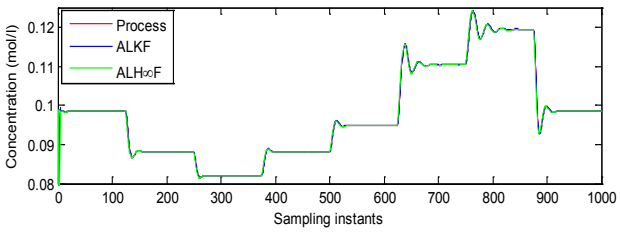

Fig. 4: Estimation of product concentration (mol/L) when the noise sequences are uncorrelated

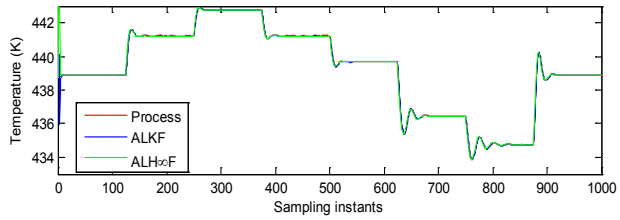

Fig. 5: Estimation of reactor temperature (K) when the noise sequences are uncorrelated

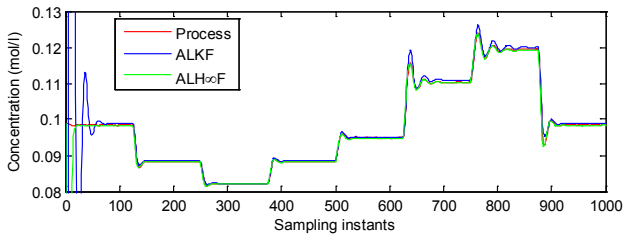

Fig. 6: Estimation of product concentration (mol/L) when the noise sequences are correlated

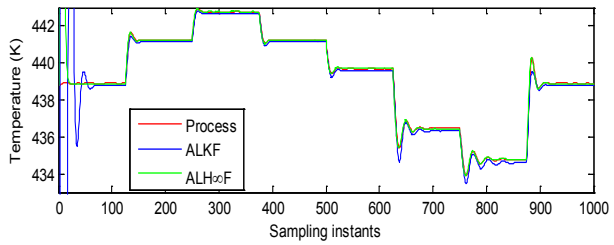

Fig.7. Estimation of reactor temperature (K) when the noise sequences correlated

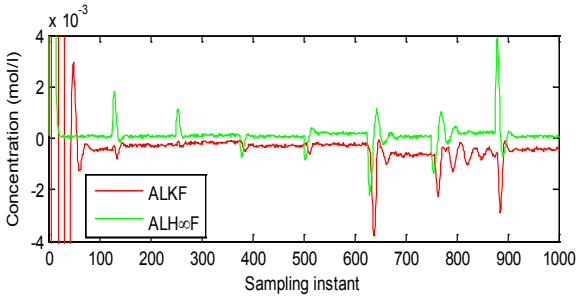

Fig. 8: Product concentration error when the noise sequences are correlated (mol/L)

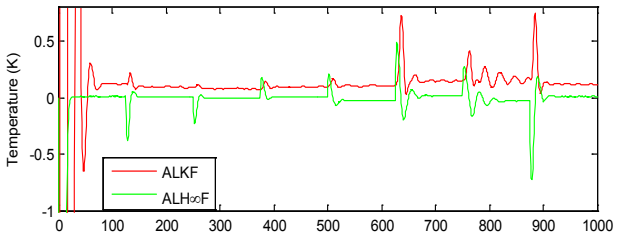

Fig. 9: Reactor temperature error when the noise sequences are correlated

6.2 Sensor and actuator bias detection: Estimator1 is designed to detect bias in C_A sensor and T sensor and hypothesized with -5% sensor bias. Estimator2 is designed to detect bias in the actuator and hypothesized with 0% bias which manipulates q_c . The designed MMALH$^{\infty}$F has been used to detect the biases which may occur either in the sensors or in the actuator.

The magnitude of fault occurred is estimated from the magnitude of residual generated and the time of occurance of fault is the time at which the residual changes its trend, and the fault is confirmed by comparing the mean of the residual over a period of time with the threshold value. While analysing the efficacy of MMALH$^{\infty}$F the coolant flow rate is fixed at 100 L/min, the corresponding steady state values are [0.0885; 441.1475]. And the Estimator1 is hypothesized with -5% bias so, in the absence of bias in the sensors, the residual generated by the estimator1 is [0.0044; 22.057]. Estimator2 is hypothesized with 0% actuator bias so, in the absence of both sensor and actuator bias the residual generated by estimator2 should be [0; 0]. Fig. 10, Fig.11 and Fig.12 shows the residuals generated by estimator1 and estimator2 after introducing -2% of bias in both sensors at 50th sampling instant. Actuator bias will be reflected in both state variables, and any one state variable is sufficient to estimate the actuator bias. So, here temperature residual is considered. From Fig.13 and 14 it is clear that the H$^{\infty}$ Filter converges quickly compared to KF. And the kalman gain smaller than H$^{\infty}$ filter gain, so we can conclude that the KF rely more on process model and less on measurement and H$^{\infty}$ rely more on measurement and less on process model.

7. Conclusion

In this paper MMALH$^{\infty}$F is proposed which uses local linear H$^{\infty}$ filters. Local H$^{\infty}$ filters are fused using gain scheduling algorithm to estimate nonlinear process states in the presence of unmodeled dynamics and disturbances. To isolate faults which ocurrs sequentially or simultaneously multiple model estimators are used. The efficiency

of the proposed MMALH$^{\infty}$F is denonstrated on CSTR process to detect sequential and simultaneous faults. The MMALH$^{\infty}$F is detecting and isolating the faults in the presence of unmodeled dynamics as well as in the presence of unknown noise statistics and it outperforms the MMALKF. The H$^{\infty}$ Filter estimate depends more on measurement and less on process model, so it is not suitable for magnitude estimation of actuator faults. Magnitude of actuator fault can be estimated by setting threshold using MMALH$^{\infty}$F.

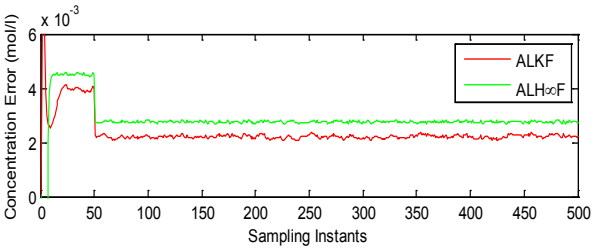

Fig. 10: Estimator1 concentration residual when -2% of bias is present in both sensors

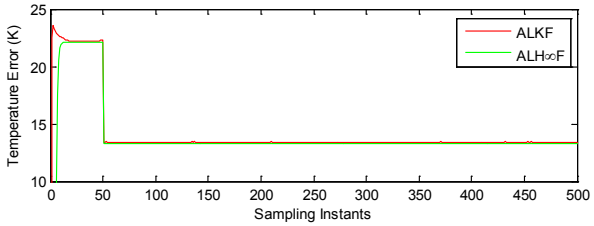

Fig. 11: Estimator1 temperature residual when -2% of bias is present in both sensors

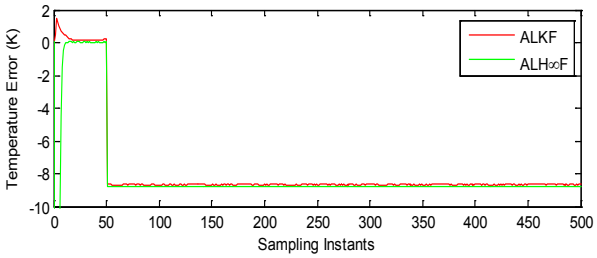

Fig. 12: Estimator2 temperature residual when -2% of bias is present in both sensors

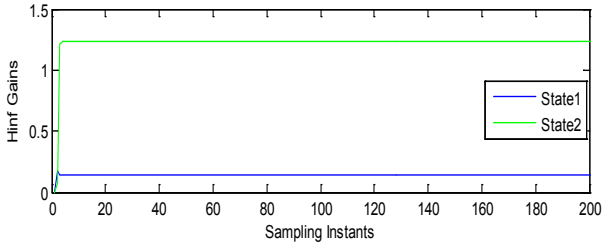

Fig. 13: H$^{\infty}$ Filter gains

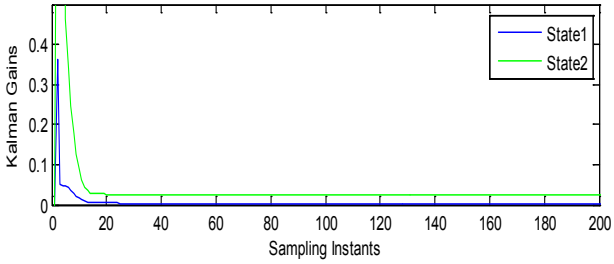

Fig. 14: Kalman Filter gains

Table 2: Performance comparison of ALKF and ALH$^{\infty}$F

Noise Information	RMSE			
	State 1 - C_A		State 2 - T	
	MMALKF	MMALH$^{\infty}$F	MMALKF	MMALH$^{\infty}$F
Uncorrelated Noise	0.0032	8.1724*10^{-4}	1.2536	0.0823
Correlated Noise	0.0044	0.0014	1.7904	0.0880
Uncorrelated Noise with Disturbance in T_f (350 K to 352 K)	0.0062	0.0011	2.2590	0.2208

Table 3: Estimated residual in the presence of sensors and actuator faults

% of bias	Estimated residual by estimator1	Estimated temperature residual by estimator2
No bias	[0.004425; 22.057]	0.0000
-1% bias in actuator	[0.004425; 22.057]	0.8525
-2% bias in actuator	[0.004425; 22.057]	1.6525
-3% bias in actuator	[0.004425; 22.057]	2.3091
-1% bias in both sensors	[0.00354 ; 17.646]	-4.4114
-2% bias in both sensors	[0.00265 ; 13.234]	-8.8228
-3% bias in both sensors	[0.00177 ; 8.823]	-13.2342
-1% bias in both sensors & actuator	[0.00354 ; 17.646]	-3.5589
-2% bias in both sensors & actuator	[0.00265 ; 13.234]	-7.1703
-3% bias in both sensors & actuator	[0.00177 ; 8.823]	-10.9251
-3% bias in both sensors & actuator	[0.000; 0.000]	-18.2048

Table 4: Sequential and simultaneous bias detection using MMALKF and MMALH$^{\infty}$F

% of bias introduced			Mean value of the residual generated					
Sensor1 (C_A in mol/l)	Sensor2 (T in K)	Actuator (q_c in l/min)	Estimator 1 for sensor bias detection (hypothesized with --5% bias)				Estimator 2 for actuator bias detection (hypothesised with 0% bias)	
			State 1 - C_A		State 2 - T		State 2 - T	
			MMALKF	MMALH$^{\infty}$F	MMALKF	MMALH$^{\infty}$F	MMALKF	MMALH$^{\infty}$F
0%	0%	0%	0.0040	0.0045	22.2214	22.0935	0.1640	0.0362
0%	0%	-1%	0.0011	0.0045	22.9369	22.2087	0.8795	0.1514
0%	0%	-2%	-0.0015	0.0046	23.6430	22.3047	1.5857	0.2474
0%	0%	-3%	-0.0041	0.0047	24.3496	22.3766	2.2923	0.3193
-1%	-1%	0%	0.0031	0.0036	17.8064	17.6780	-4.2509	-4.3793
-2%	-2%	0%	0.0022	0.0028	13.4075	13.2675	-8.6498	-8.7899
-3%	-3%	0%	0.0013	0.0019	8.9836	8.8512	-13.0737	-13.2062
-1%	-1%	-1%	$2.735*10^{-4}$	0.0037	18.5214	17.7884	-3.5360	-4.2689
-2%	-2%	-2%	-0.0032	0.0029	14.7917	13.4505	-7.2657	-8.6070
-3%	-3%	-3%	-0.0065	0.0023	11.0452	9.0709	-11.0122	-12.8865
-5%	-5%	-5%	-0.013	0.0015	3.5649	0.2248	-18.492	-21.5326

References:

[1] D. Danielle and D. Cooper, "A Practical Multiple Model Adaptive Strategy for Multivariable Model Predictive Control," *Control Engineering Practice*, vol 11, pp.649-664, 2003.

[2] V. Venkatasubramanian, R. Rengaswamy, K. Yin, and S. N. Kavuri, "A review of process fault detection and diagnosis, Part I: Quantitative model-based methods", *Elsevier. Computers & Chemical Engineering*, vol. 27, pp. 293-311, 2003.

[3] Y.C. Shi, K. Sun, L.P. Huang, and Y.D. Li, "Online identification of permanent magnet flux based on extended Kalman filter for IPMSM drive with position sensorless control", *IEEE Transactions on Industrial Electronics*, 59(11):4169–4178, 2012.

[4] Takahisa Kobayashi, Donald L. Simon, "Application of A Bank of Kalman Filter for

Aircraft Engine Fault Diagnostics", NASA/TM – 2003 – 212526
[5] Xuemin Shen and Li Deng, "Game Theory Approach to Discrete H_∞ Filter Design," *IEEE Trans. on signal processing,* vol. 45, no. 4, April 1997
[6] Dan Simon, "Optimal state estimation," John Wiley & sons, New Jersey, 2006
[7] J. Prakash, S.C.Patwardhan, S.Narasimhan, "A supervisory approach to fault tolerant control of linear multivariable systems," *Industrial Engineering Chemistry Research.* Vol.41, pp. 2270-2281, 2002.
[8] M. pottmann, D. E. Seborg, "Identification of Non-linear process Using Reciprocal Multi quadratic Functions," *Journal of Process Control*, vol.2, pp. 189 – 203, 1992.
[9] Manimozhi, M., Snigdha, G., Nagalakshmi, S., Saravanakumar, R., "State Estimation and Sensor Bias Detection using Adaptive Linear Kalamn Filter", *International Review on Modelling and Simulation*, 6(3); 1005-1010, 2013.
[10] W. L. Luyben, *Process Modeling Simulation and Control for Chemical Engineers*. McGraw-Hill, 2nd edition, 1989.
[11] Doroshin, A. V., Neri, F., "Open research issues on Nonlinear Dynamics, Dynamical Systems and Processes". *WSEAS Transactions on Systems*, 13, in press, 2014.
[12] Ciufudean, C., Neri, F., " Open research issues on Multi-Models for Complex Technological Systems". *WSEAS Transactions on Systems*, 13, in press, 2014.
[13] Neri, F., "Open research issues on Computational Techniques for Financial Applications". *WSEAS Transactions on Systems*, 13, in press, 2014.
[14] Karthikeyan, P., Neri, F. "Open research issues on Deregulated Electricity Market: Investigation and Solution Methodologies". *WSEAS Transactions on Systems*, 13, in press, 2014.
[15] Panoiu, M., Neri, F., " Open research issues on Modeling, Simulation and Optimization in Electrical Systems". *WSEAS Transactions on Systems*, 13, in press, 2014.
[16] Neri, F., "Open research issues on Advanced Control Methods: Theory and Application". *WSEAS Transactions on Systems*, 13, in press, 2014.
[17] Hájek, P., Neri, F., "An introduction to the special issue on computational techniques for trading systems, time series forecasting, stock market modeling, financial assets modeling", *WSEAS Transactions on Business and Economics*, 10 (4), pp. 201-292, 2013.
[18] Azzouzi, M., Neri, F., "An introduction to the special issue on advanced control of energy systems", *WSEAS Transactions on Power Systems*, 8 (3), p. 103, 2013.
[19] Bojkovic, Z., Neri, F., " An introduction to the special issue on advances on interactive multimedia systems", *WSEAS Transactions on Systems*, 12 (7), pp. 337-338, 2013.
[20] Pekař, L., Neri, F., "An introduction to the special issue on advanced control methods: Theory and application", *WSEAS Transactions on Systems*, 12 (6), pp. 301-303, 2013.
[21] Guarnaccia, C., Neri, F. , "An introduction to the special issue on recent methods on physical polluting agents and environment modeling and simulation", *WSEAS Transactions on Systems*, 12 (2), pp. 53-54, 2013.
[22] Neri, F., "An introduction to the special issue on computational techniques for trading systems, time series forecasting, stock market modeling, and financial assets modeling", *WSEAS Transactions on Systems*, 11 (12), pp. 659-660, 2012.
[23] Muntean, M., Neri, F.," Foreword to the special issue on collaborative systems",*WSEAS Transactions on Systems*, 11 (11), p. 617, 2012.
[24] Pekař, L., Neri, F., "An introduction to the special issue on time delay systems: Modelling, identification, stability, control and applications", *WSEAS Transactions on Systems*, 11 (10), pp. 539-540, 2012.
[25] Volos, C., Neri, F., "An introduction to the special issue: Recent advances in defense systems: Applications, methodology, technology", *WSEAS Transactions on Systems*, 11 (9), pp. 477-478, 2012.
[26] Doroshin, A.V., "Exact solutions in attitude dynamics of a magnetic dual-spin spacecraft and a generalization of the lagrange top", *WSEAS Transactions on Systems*, 12(10), pp. 471-482, 2013.
[27] Doroshin, A.V., " Synthesis of attitude motion of variable mass coaxial bodies", *WSEAS Transactions on Systems and Control*, 3 (1), pp. 50-61, 2008.

Permanence and Asymptotically Periodic Solution for A Cyclic Predator-Prey Model With Sigmoidal Type Functional Response

CHANGJIN XU
Guizhou University of Finance and Economics
Guizhou Key Laboratory of Economics System Simulation
Longchongguan Street 276, 550004 Guiyang
CHINA
xcj403@126.com

QIMING ZHANG
Hunan University of Technology
College of science
Beijing Street 42, 412007 Zhuzhou
CHINA
zhqm20082008@sina.com

Abstract: This paper is concerned with a cyclic predator-prey system with Sigmoidal type functional response. By using the differential inequality theory, some sufficient conditions are derived for the permanence of the system. By constructing a suitable Liapunov function, we obtain that the system has a unique asymptotically periodic solution which is globally asymptotically stable. Some numerical simulations that illustrate our analytical predictions are carried out. The paper ends with a brief conclusion.

Key–Words: Predator-prey system, Permanence, Sigmoidal type functional response, Asymptotically periodic solution, Liapunov function; Global stability

1 Introduction

In recent years, the interest in study of the dynamical properties occurring in the predator-prey system with delay has been growing rapidly. For example, Li and Ye [1] had made discussion about the multiple positive almost periodic solutions to an impulsive non-autonomous Lotka-Volterra predator-prey system with harvesting terms. Zhang and Luo [2] analyzed the multiple periodic solutions of a delayed predator-prey system with stage structure for the predator. Dai et al. [3] focused on the multiple periodic solutions for impulsive Gause-type ratio-dependent predator-prey systems with non-monotonic numerical responses. Wang and Fan [4] studied the multiple periodic solutions for a non-autonomous delayed predator-prey model with harvesting terms. Zhang et al. [5] studied the multiplicity of positive periodic solutions to a generalized delayed predator-prey system with stocking. For more investigation about predator-prey models or related topic, one can see [6-67]. It shall be pointed out that all the papers mentioned above are concerned with periodic coefficients. However, the asymptotically periodic system describe our real word more realistic and more accurate than the periodic ones, but the research work about asymptotically periodic predator-prey is scare at present. Recently, Wei and Wang [68] investigated a asymptotically periodic solution multispecies competition predator-prey model with Hilling III functional response. Yang and Chen [69] studied the uniformly strong persistence of a nonlinear asymptotically periodic multispecies competition predator-prey system with general functional response.

In this paper, we will deal with the following cyclic predator-prey system with Sigmoidal type functional response

$$\begin{cases} \dot{x}_1(t) = x_1(t)\Big[r_1(t) - a_1(t)x_1(t) \\ \qquad - \dfrac{d_1(t)x_1(t)x_2(t)}{c_1(t) + b_1(t)x_1(t) + x_1^2(t)} \\ \qquad + \dfrac{k_3(t)d_3(t)x_3^2(t)}{c_3(t) + b_3(t)x_3(t) + x_3^2(t)}\Big], \\ \dot{x}_2(t) = x_2(t)\Big[r_2(t) - a_2(t)x_2(t) \\ \qquad - \dfrac{d_2(t)x_2(t)x_3(t)}{c_2(t) + b_2(t)x_2(t) + x_2^2} \\ \qquad + \dfrac{k_1(t)d_1(t)x_1^2(t)}{c_1(t) + b_1(t)x_1(t) + x_1^2(t)}\Big], \\ \dot{x}_3(t) = x_3(t)\Big[r_3(t) - a_3(t)x_3(t) \\ \qquad - \dfrac{d_3(t)x_1(t)x_3(t)}{c_3(t) + b_3(t)x_3(t) + x_3^2(t)} \\ \qquad + \dfrac{k_2(t)d_2(t)x_2^2(t)}{c_2(t) + b_2(t)x_2(t) + x_2^2(t)}\Big], \end{cases} \tag{1}$$

where x_2 is the predator of x_1, x_3 is the predator

of x_2 and x_1 is the predator of x_3, they have dependent density and Sigmoidal functional response. $a_i(t), b_i(t), c_i(t), d_i(t), k_i(t), r_i(t)(i = 1, 2, 3)$ are continuous nonnegative and bounded function within $[0, +\infty)$. Moreover, $a_i(t), c_i(t)(i = 1, 2, 3) > 0$.

Now we define $R_+ = [0, +\infty)$ and introduce the concept of the asymptotically function.

Definition 1 *If $f \in C(R_+, R)$, where $f(t) = g(t) + \alpha(t)$, $g(t)$ is continuous T-periodic function and $\lim_{t\to+\infty} \alpha(t) = 0$, then $f(t)$ is called asymptotically T-periodic function.*

Throughout this paper, we always assume that
(H1) $a_i(t), b_i(t), c_i(t), d_i(t), k_i(t), r_i(t)(i = 1, 2, 3)$ are all continuous positive, bounded asymptotically periodic functions.

This paper is organized as follows. In Section 2, the permanence of system (1) are studied by using the differential inequality theory. In Section 3, the existence and uniqueness of asymptotically periodic solution are investigated by constructing a suitable Liapunov function. Some numerical simulations that illustrate our analytical predictions are carried out in Section 4. A brief conclusion is drawn in Section 5.

2 Permanence

For convenience in the following discussing, we always use the notations:

$$f^l = \inf_{t\in R} f(t), \quad f^u = \sup_{t\in R} f(t),$$

where $f(t)$ is a continuous function. The initial value condition of system (1) is $x_i(0) = \phi_i(0) > 0(i = 1, 2, 3)$. In order to obtain the main result of this paper, we shall first state some definitions and several lemmas which will be useful in the proving the main result.

Definition 2 *We say that system (1) is permanence if there are positive constants m and M such that for each positive solution $(x_1(t), x_2(t), x_3(t))$ of system (1) satisfies*

$$m \le \lim_{t\to+\infty} \inf x_i(t) \le \lim_{t\to+\infty} \sup x_i(t) \le M,$$

where $i = 1, 2, 3$.

Definition 3 *The solution $X(t, t_0, \phi)$ is called ultimately bounded. If there exists $B > 0$ such that for any $t_0 \ge 0, \phi \in C$, there exists $T = T(t_0, \phi) > 0$ when $t \ge t_0 + T, |X(t, t_0, \phi)| \le B$.*

Lemma 4 [70] *If $a > 0, b > 0$ and $\dot{x} \ge x(b - ax)$, when $t \ge 0$ and $x(0) > 0$, we have*

$$\lim_{t\to+\infty} \inf x(t) \ge \frac{b}{a}.$$

If $a > 0, b > 0$ and $\dot{x} \le x(b - ax)$, when $t \ge 0$ and $x(0) > 0$, we have

$$\lim_{t\to+\infty} \sup x(t) \le \frac{b}{a}.$$

Now we state our permanence result for system (1).

Lemma 5 *The set $R^n_+ = \{(x_1, x_2, x_3)|x_i > 0, i = 1, 2, 3.\}$ is the positively invariant set of system (1).*

Proof: It follows from the initial value condition $x_i(0) = \phi_i(0 > 0(i = 1, 2, 3)$ that

$$\begin{cases} x_1(t) = x_1(0)\exp\left\{\int_0^t \left[r_1(s) - a_1(s)x_1(s) - \dfrac{d_1(s)x_1(s)x_2(s)}{c_1(s) + b_1(s)x_1(s) + x_1^2(s)} + \dfrac{k_3(s)d_3(s)x_3^2(s)}{c_3(s) + b_3(s)x_3(s) + x_3^2(s)}\right]ds\right\}, \\ x_2(t) = x_2(0)\exp\left\{\int_0^t \left[r_2(s) - a_2(s)x_2(s) - \dfrac{d_2(s)x_2(s)x_3(s)}{c_2(s) + b_2(s)x_2(s) + x_2^2(s)} + \dfrac{k_1(s)d_1(s)x_1^2(s)}{c_1(s) + b_1(s)x_1(s) + x_1^2(s)}\right]ds\right\}, \\ \dot{x}_3(t) = x_3(0)\exp\left\{\int_0^t \left[r_3(s) - a_3(s)x_3(s) - \dfrac{d_3(s)x_1(s)x_3(s)}{c_3(s) + b_3(s)x_3(s) + x_3^2(s)} + \dfrac{k_2(s)d_2(s)x_2^2(s)}{c_2(s) + b_2(s)x_2(s) + x_2^2(s)}\right]ds\right\}. \end{cases} \tag{2}$$

The proof of Lemma 5 is complete.

Theorem 6 *Let M_1, M_2, M_3 are defined by (3),(5) and (7), respectively. In addition to the condition (H1), suppose that the following condition*

$$(H2)\ b_1^l r_1^l > d_1^u M_2, b_2^l r_2^l > d_2^u M_3, b_3^l r_3^l > d_3^u M_1$$

hold, then system (1) is permanent, that is, there exist positive constants $m_i, M_i(i = 1, 2, 3)$ which are independent of the solution of system (1), such that for any positive solution $(x_1(t), x_2(t), x_3(t))$ of system (1) with the initial condition

$$x_i(0) \ge 0(i = 1, 2, 3),$$

one has

$$m_i \le \lim_{t\to+\infty} \inf x_i(t) \le \lim_{t\to+\infty} \sup u(t) \le M_i.$$

Proof: It is easy to see that system (1) with the initial value condition $(x_1(0), x_2(0), x_3(0))$ has positive solution $(x_1(t), x_2(t), x_3(t))$ passing through $(x_1(0), x_2(0), x_3(0))$. Let $(x_1(t), x_2(t), x_3(t))$ be any positive solution of system (1) with the initial condition $(x_1(0), x_2(0), x_3(0))$. It follows from the first equation of system (1) that

$$\begin{aligned}\frac{dx_1(t)}{dt} &= x_1(t)\Big[r_1(t) - a_1(t)x_1(t) \\ &\quad - \frac{d_1(t)x_1(t)x_2(t)}{c_1(t) + b_1(t)x_1(t) + x_1^2(t)} \\ &\quad + \frac{k_3(t)d_3(t)x_3^2(t)}{c_3(t) + b_3(t)x_3(t) + x_3^2(t)}\Big] \\ &\leq x_1(t)\Big[r_1(t) - a_1(t)x_1(t) \\ &\quad + k_3(t)d_3(t)\Big] \\ &\leq x_1(t)\left[r_1^u + k_3^u d_3^u - a_1^l x_1(t)\right].\end{aligned}$$

It follows from Lemma 4 that

$$\lim_{t\to+\infty} \sup x_1(t) \leq \frac{r_1^u + k_3^u d_3^u}{a_1^l} := M_1. \qquad (3)$$

For any positive constant $\varepsilon_1 > 0$, it follows (3) that there exists a $T_1 > 0$ such that for all $t > T_1$,

$$x_1(t) \leq M_1 + \varepsilon. \qquad (4)$$

By the second equation of system (1) that

$$\begin{aligned}\frac{dx_2(t)}{dt} &= x_2(t)\Big[r_2(t) - a_2(t)x_2(t) \\ &\quad - \frac{d_2(t)x_2(t)x_3(t)}{c_2(t) + b_2(t)x_2(t) + x_2^2} \\ &\quad + \frac{k_1(t)d_1(t)x_1^2(t)}{c_1(t) + b_1(t)x_1(t) + x_1^2(t)}\Big] \\ &\leq x_2(t)\Big[r_2(t) - a_2(t)x_2(t) \\ &\quad + k_1(t)d_1(t)\Big] \\ &\leq x_2(t)\left[r_2^u + k_1^u d_1^u - a_2^l x_2(t)\right].\end{aligned}$$

It follows from Lemma 4 that

$$\lim_{t\to+\infty} \sup x_2(t) \leq \frac{r_2^u + k_1^u d_1^u}{a_2^l} := M_2. \qquad (5)$$

For any positive constant $\varepsilon > 0$, it follows (5) that there exists a $T_2 > 0$ such that for all $t > T_2$,

$$x_2(t) \leq M_2 + \varepsilon. \qquad (6)$$

By the third equation of system (1) that

$$\begin{aligned}\frac{dx_3(t)}{dt} &= x_3(t)\Big[r_3(t) - a_3(t)x_3(t) \\ &\quad - \frac{d_3(t)x_1(t)x_3(t)}{c_3(t) + b_3(t)x_3(t) + x_3^2(t)} \\ &\quad + \frac{k_2(t)d_2(t)x_2^2(t)}{c_2(t) + b_2(t)x_2(t) + x_2^2(t)}\Big] \\ &\leq x_2(t)\Big[r_3(t) - a_3(t)x_3(t) \\ &\quad + k_2(t)d_2(t)\Big] \\ &\leq x_2(t)\left[r_3^u + k_2^u d_2^u - a_3^l x_3(t)\right].\end{aligned}$$

It follows from Lemma 4 that

$$\lim_{t\to+\infty} \sup x_3(t) \leq \frac{r_3^u + k_2^u d_2^u}{a_3^l} := M_3. \qquad (7)$$

For any positive constant $\varepsilon > 0$, it follows (7) that there exists a $T_3 > T_2 > 0$ such that for all $t > T_3$,

$$x_3(t) \leq M_3 + \varepsilon. \qquad (8)$$

For $t \geq T_3$, from (6) and the first equation of system (1), we have

$$\begin{aligned}\frac{dx_1(t)}{dt} &= x_1(t)\Big[r_1(t) - a_1(t)x_1(t) \\ &\quad - \frac{d_1(t)x_1(t)x_2(t)}{c_1(t) + b_1(t)x_1(t) + x_1^2(t)} \\ &\quad + \frac{k_3(t)d_3(t)x_3^2(t)}{c_3(t) + b_3(t)x_3(t) + x_3^2(t)}\Big] \\ &\geq x_1(t)\Big[r_1(t) - a_1(t)x_1(t) \\ &\quad - \frac{d_1(t)x_2(t)}{b_1(t)}\Big] \\ &\geq x_1(t)\Big[r_1^l - a_1^u x_1(t) \\ &\quad - \frac{d_1^u(M_2 + \varepsilon)}{b_1^l}\Big].\end{aligned}$$

Thus, as a direct corollary of Lemma 4, one has

$$\lim_{t\to+\infty} \inf x_1(t) \geq \frac{b_1^l r_1^l - d_1^u(M_2 + \varepsilon)}{a_1^u b_1^l}. \qquad (9)$$

Setting $\varepsilon \to 0$, it follows that

$$\lim_{t\to+\infty} \inf x_1(t) \geq \frac{b_1^l r_1^l - d_1^u M_2}{a_1^u b_1^l} := m_1. \qquad (10)$$

For $t \geq T_3$, from (8) and the second equation of system (1), we have

$$\begin{aligned}\frac{dx_2(t)}{dt} &= x_2(t)\Big[r_2(t) - a_2(t)x_2(t) \\ &\quad - \frac{d_2(t)x_2(t)x_3(t)}{c_2(t)+b_2(t)x_2(t)+x_2^2} \\ &\quad + \frac{k_1(t)d_1(t)x_1^2(t)}{c_1(t)+b_1(t)x_1(t)+x_1^2(t)}\Big] \\ &\geq x_2(t)\Big[r_2(t) - a_2(t)x_2(t) \\ &\quad - \frac{d_2(t)x_3(t)}{b_2(t)}\Big] \\ &\geq x_2(t)\Big[r_2^l - a_2^u x_2(t) \\ &\quad - \frac{d_2^u(M_3+\varepsilon)}{b_2^l}\Big]. \end{aligned} \tag{11}$$

It follows Lemma 2.1 and (11) that

$$\lim_{t\to+\infty}\inf x_2(t) \geq \frac{b_2^l r_2^l - d_2^u(M_3+\varepsilon)}{a_2^u b_2^l}. \tag{12}$$

Setting $\varepsilon \to 0$ in (12) leads to

$$\lim_{t\to+\infty}\inf x_2(t) \geq \frac{b_2^l r_2^l - d_2^u M_3}{a_2^u b_2^l} := m_2. \tag{13}$$

For $t \geq T_3 > T_1 > 0$, from (4) and the second equation of system (1), we have

$$\begin{aligned}\frac{dx_3(t)}{dt} &= x_3(t)\Big[r_3(t) - a_3(t)x_3(t) \\ &\quad - \frac{d_3(t)x_1(t)x_3(t)}{c_3(t)+b_3(t)x_3(t)+x_3^2(t)} \\ &\quad + \frac{k_2(t)d_2(t)x_2^2(t)}{c_2(t)+b_2(t)x_2(t)+x_2^2(t)}\Big] \\ &\geq x_3(t)\Big[r_3(t) - a_3(t)x_3(t) \\ &\quad - \frac{d_3(t)x_1(t)x_3(t)}{b_3(t)}\Big] \\ &\geq x_3(t)\Big[r_3^l - a_3^u x_3(t) \\ &\quad - \frac{d_3^u(M_1+\varepsilon)}{b_3^l}\Big]. \end{aligned}$$

It follows Lemma 4 that

$$\lim_{t\to+\infty}\inf x_3(t) \geq \frac{b_3^l r_3^l - d_3^u(M_1+\varepsilon)}{a_3^u b_3^l}. \tag{14}$$

Setting $\varepsilon \to 0$ in (2.13) leads to

$$\lim_{t\to+\infty}\inf x_3(t) \geq \frac{b_3^l r_3^l - d_3^u M_1}{a_3^u b_3^l} := m_3. \tag{15}$$

In view of (3),(5),(7),(10), (13) and (15), we can conclude that system (1) is permanent. The proof of Theorem 6 is complete.

Denote

$$\Omega = \{(x_1,x_2,x_3)^T \in R_+ | m_i \leq x_i \leq M_i, i = 1,2,3\}.$$

Corollary 7 *The set Ω is the ultimately bounded set of system (1).*

3 Existence and uniqueness of asymptotically periodic solution

Let us consider the asymptotically periodic system as follows

$$\frac{dx}{dt} = f(t, x_t), \tag{16}$$

where $f \in C([-r,0], R^n)$ and for any $x_t \in C$. Define $x_t(\theta) = x(t+\theta), \theta \in [-r,0]$. For any $x = (x_1, x_2, \cdots, x_n) \in R^n$, we define $|x| = \sum_{i=1}^n |x_i|$, from the above proof, we can see that there exists $H > 0$ such that $|x| \leq nM_i < H$. For any $\phi \in C$, define $||\phi|| = \sup_{-r\leq\theta\leq 0}|\phi(\theta)|$. Let $C_H = \{\phi \in C, ||\phi|| < H\}$ and $\bar{S}_H = \{x \in R^n, |x| < H\}$. In order to focus on the existence and uniqueness of asymptotically periodic solution of system (16), we consider the adjoint system

$$\begin{cases} \dfrac{dx}{dt} = f(t, x_t), \\ \dfrac{dy}{dt} = f(t, y_t). \end{cases} \tag{17}$$

Then we begin with our analysis with Lemma 3.1.

Lemma 8 (Yuan [71]) *Let $V \in C(R_+ \times S_H \times S_H, R_+)$ satisfy*
(i) $a(|x-y|) \leq V(t,x,y) \leq b(|x-y|)$, where $a(r)$ and $b(r)$ are continuously positively increasing functions;
(ii) $|V(t,x_1,y_1) - V(t,x_2,y_2)| \leq l(|x_1-x_2|+|y_1-y_2|)$, where l is a constant and satisfies $l > 0$;
(iii) there exists continuous non-increasing function $P(s)$, such that for $s > 0, P(s) > s$. And as $P(V(t,\phi(0),\phi(0))) > V(t+\theta,\phi(\theta),\phi(\theta)), \theta \in [-r,0]$, it follows that $V'_{(17)}(t,\phi(0),\phi(0)) \leq -\delta V(t,\phi(0),\phi(0))$, where δ is a constant and satisfies $\delta > 0$. Furthermore, system (16) has a solution

$\xi(t)$ for $t \geq t_0$ and satisfies $||\xi_t|| \leq H$. Then system (16) has a unique asymptotically periodic solution, which is uniformly asymptotically stable.

Theorem 9 *Let $\theta_1, \theta_2, \theta_3$ and δ are defined by (24), (25), (26) and (27), respectively. In addition to the conditions (H1) and (H2), assume further that $\delta > 0$ is satisfied, then there exists a unique asymptotically periodic solution of system (1) wich is uniformly asymptotically stable.*

Proof: By Theorem 6 (or Corollary 7), we know that the solution of system (1) is ultimately bounded. Ω is the region of ultimately bounded. We consider the adjoint system of system (1) as follows

$$\begin{cases} \dot{x}_1(t) = x_1(t)\Big[r_1(t) - a_1(t)x_1(t) \\ \quad - \frac{d_1(t)x_1(t)x_2(t)}{c_1(t)+b_1(t)x_1(t)+x_1^2(t)} \\ \quad + \frac{k_3(t)d_3(t)x_3^2(t)}{c_3(t)+b_3(t)x_3(t)+x_3^2(t)}\Big], \\ \dot{x}_2(t) = x_2(t)\Big[r_2(t) - a_2(t)x_2(t) \\ \quad - \frac{d_2(t)x_2(t)x_3(t)}{c_2(t)+b_2(t)x_2(t)+x_2^2} \\ \quad + \frac{k_1(t)d_1(t)x_1^2(t)}{c_1(t)+b_1(t)x_1(t)+x_1^2(t)}\Big], \\ \dot{x}_3(t) = x_3(t)\Big[r_3(t) - a_3(t)x_3(t) \\ \quad - \frac{d_3(t)x_1(t)x_3(t)}{c_3(t)+b_3(t)x_3(t)+x_3^2(t)} \\ \quad + \frac{k_2(t)d_2(t)x_2^2(t)}{c_2(t)+b_2(t)x_2(t)+x_2^2(t)}\Big], \\ \dot{u}_1(t) = u_1(t)\Big[r_1(t) - a_1(t)u_1(t) \\ \quad - \frac{d_1(t)u_1(t)u_2(t)}{c_1(t)+b_1(t)u_1(t)+u_1^2(t)} \\ \quad + \frac{k_3(t)d_3(t)u_3^2(t)}{c_3(t)+b_3(t)u_3(t)+u_3^2(t)}\Big], \\ \dot{u}_2(t) = u_2(t)\Big[r_2(t) - a_2(t)u_2(t) \\ \quad - \frac{d_2(t)u_2(t)u_3(t)}{c_2(t)+b_2(t)u_2(t)+u_2^2} \\ \quad + \frac{k_1(t)d_1(t)u_1^2(t)}{c_1(t)+b_1(t)u_1(t)+u_1^2(t)}\Big], \\ \dot{u}_3(t) = u_3(t)\Big[r_3(t) - a_3(t)u_3(t) \\ \quad - \frac{d_3(t)u_1(t)u_3(t)}{c_3(t)+b_3(t)u_3(t)+u_3^2(t)} \\ \quad + \frac{k_2(t)d_2(t)u_2^2(t)}{c_2(t)+b_2(t)u_2(t)+u_2^2(t)}\Big]. \end{cases} \tag{18}$$

For $X(t) = (x_1(t), x_2(t), x_3(t))$ and $U(t) = (u_1(t), u_2(t), u_3(t))$ are the solutions of system (18) in $\Omega \times \Omega$. Let $x_i^*(t) = \ln x_i(t), u_i^*(t) = \ln u_i(t), i = 1, 2, 3$. Now we construct a Lyapunov functional as follows

$$V(t) = \sum_{i=1}^{3} |x_i^*(t) - u_i^*(t)|. \tag{19}$$

Taking $a(r) = b(r) = \sum_{i=1}^{3} |x_i^*(t) - u_i^*(t)|$ and using the inequality $||a| - |b|| \leq |a - b|$, we can easily prove that (i) and (ii) in Lemma 8 hold true. In the sequel, we will investigate (iii) of Lemma 8. It follows from (16) that

$$\begin{aligned} D^+V(t) &= \sum_{i=1}^{3}\left(\frac{\dot{x}_i(t)}{x_i(t)} - \frac{\dot{u}_i(t)}{u_i(t)}\right) \\ &\times \text{sign}(x_i(t) - u_i(t)) \\ &\leq -a_1^l|x_1(t) - u_1(t)| \\ &+ \left[\frac{d_1(t)x_1(t)x_2(t)}{c_1(t) + b_1(t)x_1(t) + x_1^2(t)}\right. \\ &\left. - \frac{d_1(t)u_1(t)u_2(t)}{c_1(t) + b_1(t)u_1(t) + u_1^2(t)}\right] \\ &+ \left[\frac{k_3(t)d_3(t)x_3^2(t)}{c_3(t) + b_3(t)x_3(t) + x_3^2(t)}\right. \\ &\left. - \frac{k_3(t)d_3(t)u_3^2(t)}{c_3(t) + b_3(t)u_3(t) + u_3^2(t)}\right] \\ &- a_2^l|x_2(t) - u_2(t)| \\ &+ \left[\frac{d_2(t)x_2(t)x_3(t)}{c_2(t) + b_2(t)x_2(t) + x_2^2}\right. \\ &\left. - \frac{d_2(t)u_2(t)u_3(t)}{c_2(t) + b_2(t)u_2(t) + u_2^2}\right] \\ &+ \left[\frac{k_1(t)d_1(t)x_1^2(t)}{c_1(t) + b_1(t)x_1(t) + x_1^2(t)}\right. \\ &\left. - \frac{k_1(t)d_1(t)u_1^2(t)}{c_1(t) + b_1(t)u_1(t) + u_1^2(t)}\right] \\ &- a_3^l|x_3(t) - u_3(t)| \\ &+ \left[\frac{d_3(t)x_1(t)x_3(t)}{c_3(t) + b_3(t)x_3(t) + x_3^2(t)}\right. \\ &\left. - \frac{d_3(t)u_1(t)u_3(t)}{c_3(t) + b_3(t)u_3(t) + u_3^2(t)}\right] \\ &+ \left[\frac{k_2(t)d_2(t)x_2^2(t)}{c_2(t) + b_2(t)x_2(t) + x_2^2(t)}\right. \\ &\left. - \frac{k_2(t)d_2(t)u_2^2(t)}{c_2(t) + b_2(t)u_2(t) + u_2^2(t)}\right] \\ &\leq \left[-a_1^l + \frac{c_1^M d_1^M M_2 + d_1^M M_1^2 M_2}{(c_1^l + b_1^l m_1 + m_1^2)^2}\right] \end{aligned}$$

$$
\begin{aligned}
&\times|x_1(t)-u_1(t)|\\
&+\left[\frac{c_1^M d_1^M M_1+d_1^M b_1^M M_1^2+d_1^M M_1^3}{(c_1^l+b_1^l m_1+m_1^2)^2}\right]\\
&\times|x_2(t)-u_2(t)|\\
&+\left[\frac{2k_3^M c_3^M d_3^M M_3+2k_3^M b_3^M d_3^M M_3^2}{(c_3^l+b_3^l m_3+m_3^2)^2}\right]\\
&\times|x_3(t)-u_3(t)|\\
&+\left[-a_2^l+\frac{d_2^M c_2^M M_3+d_2^M M_2^2 M_3}{(c_2^l+b_2^l m_2+m_2^2)^2}\right]\\
&\times|x_2(t)-u_2(t)|\\
&+\left[\frac{d_2^M c_2^M M_2+d_2^M b_2^M M_2^2+d_2^M M_2^3}{(c_2^l+b_2^l m_2+m_2^2)^2}\right]\\
&\times|x_3(t)-u_3(t)|\\
&+\left[-a_3^l+\frac{d_3^M c_3^M M_1+2d_3^M M_3 M_1}{(c_3^l+b_3^l m_3+m_3^2)^2}\right]\\
&\times|x_3(t)-u_3(t)|\\
&+\left[\frac{d_3^M c_3^M M_3+2d_3^M b_3^M M_3+2d_3^M M_3^2}{(c_3^l+b_3^l m_3+m_3^2)^2}\right]\\
&\times|x_1(t)-u_1(t)|. \qquad (20)
\end{aligned}
$$

Nothing that

$$
\begin{aligned}
&|x_i(t)-u_i(t)|\\
&=|\exp(x_i^*(t))-\exp(u_i^*(t))|\\
&=\exp(\xi_i(t))||x_i^*(t)-u_i^*(t)|, \qquad (21)
\end{aligned}
$$

where $\xi_i(t)$ lies between $x_i(t)$ and $u_i(t)$. Then we have

$$
\begin{aligned}
&m_i|x_i^*(t)-u_i^*(t)|\\
&\le|x_i(t)-u_i(t)|\\
&\le M_i|x_i^*(t)-u_i^*(t)|, i=1,2,3. \qquad (22)
\end{aligned}
$$

It follows from (20)and (22) that

$$
\begin{aligned}
D^+V(t)&\le\left[-a_1^l+\frac{c_1^M d_1^M M_2+d_1^M M_1^2 M_2}{(c_1^l+b_1^l m_1+m_1^2)^2}\right]\\
&\times m_1|x_1^*(t)-u_1^*(t)|\\
&+\left[\frac{c_1^M d_1^M M_1+d_1^M b_1^M M_1^2+d_1^M M_1^3}{(c_1^l+b_1^l m_1+m_1^2)^2}\right]\\
&\times M_2|x_2^*(t)-u_2^*(t)|\\
&+\left[\frac{2k_3^M c_3^M d_3^M M_3+2k_3^M b_3^M d_3^M M_3^2}{(c_3^l+b_3^l m_3+m_3^2)^2}\right]\\
&\times M_3|x_3^*(t)-u_3^*(t)|\\
&+\left[-a_2^l+\frac{d_2^M c_2^M M_3+d_2^M M_2^2 M_3}{(c_2^l+b_2^l m_2+m_2^2)^2}\right]\\
&\times m_2|x_2^*(t)-u_2^*(t)|\\
&+\left[\frac{d_2^M c_2^M M_2+d_2^M b_2^M M_2^2+d_2^M M_2^3}{(c_2^l+b_2^l m_2+m_2^2)^2}\right]\\
&\times M_3|x_3^*(t)-u_3^*(t)|\\
&+\left[-a_3^l+\frac{d_3^M c_3^M M_1+2d_3^M M_3 M_1}{(c_3^l+b_3^l m_3+m_3^2)^2}\right]\\
&\times m_3|x_3^*(t)-u_3^*(t)|\\
&+\left[\frac{d_3^M c_3^M M_3+2d_3^M b_3^M M_3+2d_3^M M_3^2}{(c_3^l+b_3^l m_3+m_3^2)^2}\right]\\
&\times M_1|x_1^*(t)-u_1^*(t)|\\
&=-\theta_1|x_1^*(t)-u_1^*(t)|\\
&-\theta_2|x_2^*(t)-u_2^*(t)|\\
&-\theta_3|x_3^*(t)-u_3^*(t)|, \qquad (23)
\end{aligned}
$$

where

$$
\begin{aligned}
\theta_1&=\left[a_1^l-\frac{c_1^M d_1^M M_2+d_1^M M_1^2 M_2}{(c_1^l+b_1^l m_1+m_1^2)^2}\right]m_1\\
&-\left[\frac{d_3^M c_3^M M_3+2d_3^M b_3^M M_3+2d_3^M M_3^2}{(c_3^l+b_3^l m_3+m_3^2)^2}\right]\\
&\times M_1, \qquad (24)\\
\theta_2&=\left[a_2^l-\frac{d_2^M c_2^M M_3+d_2^M M_2^2 M_3}{(c_2^l+b_2^l m_2+m_2^2)^2}\right]m_2\\
&-\left[\frac{c_1^M d_1^M M_1+d_1^M b_1^M M_1^2+d_1^M M_1^3}{(c_1^l+b_1^l m_1+m_1^2)^2}\right]\\
&\times M_2, \qquad (25)\\
\theta_3&=\left[a_3^l-\frac{d_3^M c_3^M M_1+2d_3^M M_3 M_1}{(c_3^l+b_3^l m_3+m_3^2)^2}\right]m_3\\
&-\left[\frac{2k_3^M c_3^M d_3^M M_3+2k_3^M b_3^M d_3^M M_3^2}{(c_3^l+b_3^l m_3+m_3^2)^2}\right]\\
&\times M_3\\
&-\left[\frac{d_2^M c_2^M M_2+d_2^M b_2^M M_2^2+d_2^M M_2^3}{(c_2^l+b_2^l m_2+m_2^2)^2}\right]\\
&\times M_3. \qquad (26)
\end{aligned}
$$

Let

$$\delta=\min\{\theta_1,\theta_2,\theta_3\}. \qquad (27)$$

It follows from (23) and (27) that

$$D^+V(t)\le-\delta V(t). \qquad (28)$$

Then (iii) of Lemma 3.1 is fulfilled. Therefore system (1) has a unique positive asymptotically periodic solution in domain Ω, which is uniformly asymptotically stable. The proof is complete.

4 Numerical example

To illustrate the theoretical results, we present some numerical simulations. Let us consider the following cyclic predator-prey system with Sigmoidal type functional response:

$$\begin{cases} \dot{x}_1(t) = x_1(t)\Big[r_1(t) - a_1(t)x_1(t) \\ \qquad - \dfrac{d_1(t)x_1(t)x_2(t)}{c_1(t) + b_1(t)x_1(t) + x_1^2(t)} \\ \qquad + \dfrac{k_3(t)d_3(t)x_3^2(t)}{c_3(t) + b_3(t)x_3(t) + x_3^2(t)}\Big], \\ \dot{x}_2(t) = x_2(t)\Big[r_2(t) - a_2(t)x_2(t) \\ \qquad - \dfrac{d_2(t)x_2(t)x_3(t)}{c_2(t) + b_2(t)x_2(t) + x_2^2} \\ \qquad + \dfrac{k_1(t)d_1(t)x_1^2(t)}{c_1(t) + b_1(t)x_1(t) + x_1^2(t)}\Big], \\ \dot{x}_3(t) = x_3(t)\Big[r_3(t) - a_3(t)x_3(t) \\ \qquad - \dfrac{d_3(t)x_1(t)x_3(t)}{c_3(t) + b_3(t)x_3(t) + x_3^2(t)} \\ \qquad + \dfrac{k_2(t)d_2(t)x_2^2(t)}{c_2(t) + b_2(t)x_2(t) + x_2^2(t)}\Big], \end{cases} \tag{29}$$

where

$$\begin{cases} b_1(t) = 20 + 0.2\sin t, b_2(t) = 10 + 0.4\cos t, \\ b_3(t) = 15 + 0.3\sin t, a_1(t) = 10 + \sin t, \\ a_2(t) = 11 + \cos t, a_3(t) = 12 - \cos t, \\ r_1(t) = 10 + 0.3\sin t, r_2(t) = 12 + 0.2\cos t, \\ r_3(t) = 13 - 0.2\sin t, d_1(t) = 0.2 + 0.2\cos t, \\ d_2(t) = 0.2 + 0.1\sin t, d_3(t) = 0.1 + 0.1\cos t, \\ k_1(t) = 1 + \sin t, k_2(t) = 1 + \sin t, \\ k_3(t) = 1 + \sin t. \end{cases}$$

Then

$$\begin{cases} b_1^l = 19.8, b_1^l = 9.6, b_3^l = 14.7, \\ r_1^l = 9.7, r_2^l = 11.8, r_3^l = 12.8, \\ a_1^l = 9, a_2^l = 10, a_3^l = 11, \\ r_1^u = 10.3, r_2^u = 12.2, r_3^u = 13.2, \\ d_1^u = 0.4, d_2^u = 0.3, d_3^u = 0.2, \\ M_1 = 1.1889, M_2 = 1.3, M_3 = 1.2181. \end{cases}$$

It is easy to check that the coefficients of system (29) satisfy all the conditions in Theorem 9. The phase diagram of system (29) is illustrated in Figures 1-3. Numerical simulations show that system (29) has a unique positive periodic solution which is globally asymptotically stable.

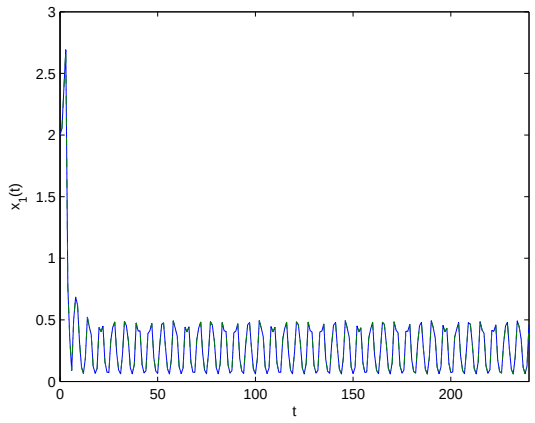

Fig.1. The dynamical behavior of the solution $(x_1(t), x_2(t), x_3(t))$ of system (29).

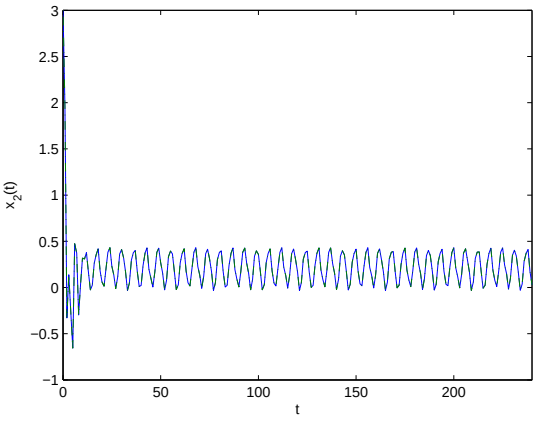

Fig.2. The dynamical behavior of the solution $(x_1(t), x_2(t), x_3(t))$ of system (29).

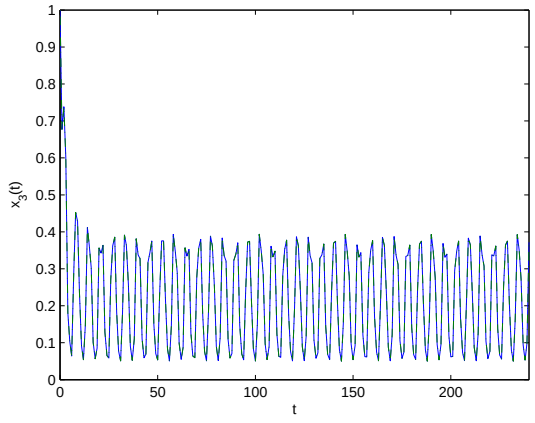

Fig.3. The dynamical behavior of the solution $(x_1(t), x_2(t), x_3(t))$ of system (29).

5 Conclusions

In this paper, we have analyzed a cyclic predator-prey system with Sigmoidal type functional response. Applying the differential inequality theory, we obtain some sufficient conditions for the permanence of the system. By constructing a suitable Liapunov function, we find that under some suitable conditions, the system has a unique asymptotically periodic solution which is globally asymptotically stable. Numerical simulations show the feasibility of our main results.

Acknowledgements: The research was supported by This work is supported by National Natural Science Foundation of China(No.11261010, No.11101126), Soft Science and Technology Program of Guizhou Province(No.2011LKC2030), Natural Science and Technology Foundation of Guizhou Province(J[2012]2100), Governor Foundation of Guizhou Province([2012]53), Natural Science and Technology Foundation of Guizhou Province(2014), Natural Science Innovation Team Project of Guizhou Province ([2013]14) and Doctoral Foundation of Guizhou University of Finance and Economics (2010).

References:

[1] Y.K. Li, and Y. Ye, Multiple positive almost periodic solutions to an impulsive non-autonomous Lotka-Volterra predator-prey system with harvesting terms, *Commun. Nonlinear Sci. Numer. Simul.* 18, 2013, pp. 3190–3201.

[2] Z.Q. Zhang, and J.B. Luo, Multiple periodic solutions of a delayed predator-prey system with stage structure for the predator, *Nonlinear Anal.: Real World Appl.* 11, 2010, pp. 4109–4120.

[3] B.X. Dai, Y. Li, and Z.G. Luo, Multiple periodic solutions for impulsive Gause-type ratio-dependent predator-prey systems with non-monotonic numerical responses, *Appl. Math. Compu.* 217, 2011, pp. 7478–7487.

[4] L.L. Wang, and Y.H. Fan, Multiple periodic solutions for a non-autonomous delayed predator-prey model with harvesting terms, *Appl. Math. Comput.* 217, 2011, pp. 9552–9561.

[5] Z.Q. Zhang, Z.T. Hou, and L. Wang, Multiplicity of positive periodic solutions to a generalized delayed predator-prey system with stocking, *Nonlinear Anal.* 68, 2008, pp. 2608–2622.

[6] M. Fan, K. Wang, and D.Q. Jiang, Existence and global attractivity of positive periodic solutions of periodic n-species Lotka-Volterra competition systems with several deviating arguments, *Math. Biosci.* 160, 1999, pp. 47–61.

[7] Z.J. Liu, R.H. Tan, Y.P. Chen, and L.S. Chen, On the stable periodic solutions of a delayed two-species model of faculative mutualism, *Appl. Math. Comput.* 196, 2008, pp. 105–117.

[8] D.W. Hu, and Z.Q. Zhang, Four positive periodic solution to a Lotka-Volterra cooperative system with harvesting terms, Nonlinear Anal.: Real World Appl., 11, 2010, pp. 1115-1121.

[9] Y.K. Li, and G.T. Xu, Positive periodic solutions for an integrodifferential model of mutualism, *Appl. Math. Lett.* 14, 2001, pp. 525–530.

[10] Y.H. Xia, J.D. Cao, and S.S. Cheng, Multiple periodic solutions of a delayed stage-structured predator-prey model with non-monotone functional responses, *Appl. Math. Modelling* 31, 2007, pp. 1947–1959.

[11] Z.Q. Zhang, and H.L. Wang, Existence and global attractivity of positive periodic solutions for a generalized predator-prey system with time delay, *Math. Comput. Modelling* 44, 2006, pp. 188–203.

[12] Y.H. Fan, and L.L. Wang, Multiplicity of periodic solutions for a delayed ratio-dependent predator-prey model with Holling type III functional response and harvesting terms, *J. Math. Anal. Appl.* 365, 2010, pp. 525–540.

[13] F.Q. Zhang, and C.W. Zheng, Positive periodic solutions for the neutral ratio-dependent predator-prey model, *Comput. Mat. Appl.* 61, 2011, pp. 2221-2226.

[14] K. Wang, Periodic solutions to a delayed predator-prey model with Hassell-Varley type functional response, *Nonlinear Anal.: Real World Appl.* 12, 2011, pp. 137–145.

[15] Z.W. Cai, L.H. Huang, and H.B. Chen, Positive periodic solution for a multispecies competition-predator system with Holling III functional response and time delays, *Appl. Math. Comput.* 217, 2011, pp. 4866-4878.

[16] B. Sahoo, S. Poria, Effects of supplying alternative food in a predator-prey model with harvesting, *Appl. Math. Comput.* 234, 2014, pp. 150–166.

[17] H.W. Yin, X.Y. Xiao, X.Q. Wen, and K. Liu, Pattern analysis of a modified Leslie-Gower predator-prey model with Crowley-Martin functional response and diffusion, *Comput. Math. Appl.* 67, 2014, pp. 1607–1621.

[18] Y. Zhang, Q.L. Zhang, and X.G. Yan, Complex dynamics in a singular LeslieCGower predator-prey bioeconomic model with time delay and stochastic fluctuations, *Phys. A* 404, 2014, pp. 180–191.

[19] Q. Liu, Y.L. Liu, and X. Pan, Global stability of a stochastic predator-prey system with infinite delays, *Appl. Math. Comput.* 235, 2014, pp. 1–7.

[20] Y.H. Huang, and P.X. Weng, Periodic traveling wave train and point-to-periodic traveling wave for a diffusive predator-prey system with Ivlev-type functional response, *J. Math. Anal. Appl.* 417, 2014, pp. 376–393.

[21] Z. Ling, L. Zhang, Z.G. Lin, Turing pattern formation in a predator-prey system with cross diffusion, *Appl. Math. Modelling*, in Press, 2014.

[22] J.D. Flores, and E. González-Olivares, Dynamics of a predator-prey model with Allee effect on prey and ratio-dependent functional response, *Ecological Complexity*, in press, 2014.

[23] P.J. Pal, and P.K. Mandal, Bifurcation analysis of a modified LeslieCGower predator-prey model with Beddington-DeAngelis functional response and strong Allee effect, *Math. Comput. Simul.* 97, 2014, pp. 123–146.

[24] G.D. Zhang, Y. Shen, and B.S. Chen, Bifurcation analysis in a discrete differential-algebraic predator-prey system, *Appl. Math. Modelling*, in press, 2014.

[25] Y.F. Lv, and R. Yuan, Existence of traveling wave solutions for Gause-type models of predator-prey systems Original Research Article *Appl. Math. Comput.* 229, 2014, pp. 70–84.

[26] Z.J. Du, and Z.S. Feng, Periodic solutions of a neutral impulsive predator-prey model with Beddington-DeAngelis functional response with delays, *J. Comput. Appl. Math.* 258, 2014, pp. 87–98.

[27] O. Makarenkov, Topological degree in the generalized Gause preyCpredator model *J. Math. Anal. Appl.* 410, 2014, pp. 525–540.

[28] X.X. Liu, Impulsive periodic oscillation for a predatorCprey model with Hassell-Varley-Holling functional response Original Research Article *Appl. Math. Modelling* 38, 2014, pp. 1482–1494.

[29] S. Bhattacharya, M. Martcheva, and X.Z. Li, A predator-prey-disease model with immune response in infected prey, *J. Math. Anal. Appl.* 411, 2014, pp. 297-313.

[30] S. Shabani, Diffusive Holling type-II predator-prey system with harvesting of prey, *J. Math. Anal. Appl.* 410, 2014, pp. 469–482.

[31] L.N. Guin, Existence of spatial patterns in a predatorCprey model with self- and cross-diffusion, *Appl. Math. Comput.* 226, 2014, pp. 320–335.

[32] B.S.R.V. Prasad, M. Banerjee, P.D.N. Srinivasu, Dynamics of additional food provided predator-prey system with mutually interfering predators, *Math. Biosci.* 246, 2013, pp. 176–190.

[33] M. Javidi, and N. Nyamoradi, Dynamic analysis of a fractional order preyCpredator interaction with harvesting, *Appl. Math. Modelling* 37, 2013, pp. 8946–8956.

[34] M.M. Molina, M.A. Moreno-Armendáriz, and J.C.S. Tuoh Mora, On the spatial dynamics and oscillatory behavior of a predator-prey model based on cellular automata and local particle swarm optimization, *J. Theor. Biol.* 336, 2013, pp 173–184.

[35] M. Liu, and C.Z. Bai, On a stochastic delayed predator-prey model with Levy jumps, *Appl. Math. Compu.* 228, 2014, pp. 563–570.

[36] M. Fras, and M. Gosak, Spatiotemporal patterns provoked by environmental variability in a predator-prey model, *Biosystems* 114, 2013, pp. 172–177.

[37] A.J. Terry, A predator-prey model with generic birth and death rates for the predator, *Math. Biosci.* 248, 2014, pp. 57–66.

[38] Y.K. Li, and Y. Ye, Multiple positive almost periodic solutions to an impulsive non-autonomous Lotka-Volterra predator-prey system with harvesting terms, *Commun. Nonlinear Sci. Numer. Simul.* 18, 2013, pp. 3190–3201.

[39] H.K. Kim, and H. Baek, The dynamical complexity of a predator-prey system with Hassell-Varley functional response and impulsive effect,*Math. Comput. Simul.* 94, 2013, pp. 1–14.

[40] J. Zhou, and J.P. Shi, The existence, bifurcation and stability of positive stationary solutions of a diffusive Leslie-Gower predator-prey model with Holling-type II functional responses, *J. Math. Anal. Appl.* 405, 2013, pp. 618–630.

[41] C. Miao, and Y. Ke, Positive periodic solutions of a generalized Gilpin-Ayala competitive system with time delays, *WSEAS Trans. Math.*, 12 (3), 2013, pp.277–285.

[42] L. Zhang, Y. Li, Q. Ren, and Z. Huo, Global dynamics of an SEIRS epidemic model with constant immigration and immunity, *WSEAS Trans. Math.*, 12 (5), 2013, pp.630–640.

[43] K. Zhuang, and H. Zhu, Stability and bifurcation analysis for an improved HIV model with time delay and cure rate, *WSEAS Trans. Math.*, 12 (8), 2013, pp.860–869.

[44] K. Zhao, and L. Ding, Multiple periodic solutions for a general class of delayed cooperative systems on time scales, *WSEAS Trans. Math.*, 12 (10), 2013, pp.957–966.

[45] Y. Pei, Y. Liu, and C. Li, Dynamic study of mathe-matical models on antibiotics and immunologic adjuvant against Toxoplasmosis, *WSEAS Trans. Math.*, 11 (11), 2012, pp.1018–1027.

[46] C. Miao, and Y. Ke, Positive periodic solutions of a generalized Gilpin-Ayala competitive system with time delays, *WSEAS Trans. Math.*, 12 (3), 2013, pp.277–285.

[47] A. V. Doroshin, and F. Neri, Open research issues on Nonlinear Dynamics, Dynamical Systems and Processes, *WSEAS Trans. Syst.*, 13, 2014, in press.

[48] C. Ciufudean, and F. Neri, Open research issues on Multi-Models for Complex Technological Systems, *WSEAS Trans. Syst.*, 13, 2014, in press.

[49] F. Neri, Open research issues on Computational Techniques for Financial Applications, *WSEAS Trans. Syst.*, 13, 2014, in press.

[50] P. Karthikeyan, and F. Neri, Open research issues on Deregulated Electricity Market: Investigation and Solution Methodologies, *WSEAS Trans. Syst.*, 13, 2014, in press.

[51] M. Panoiu, and F. Neri, Open research issues on Modeling, Simulation and Optimization in Electrical Systems, *WSEAS Trans. Syst*, 13, 2014, in press.

[52] F. Neri, Open research issues on Advanced Control Methods: Theory and Application, *WSEAS Trans. Syst.*, 13, 2014, in press.

[53] P. Hajek, and F. Neri, An introduction to the special issue on computational techniques for trading systems, time series forecasting, stock market modeling, financial assets modeling, *WSEAS Transa. Bus. Econ.*, 10, 2013, pp. 201-292.

[54] M. Azzouzi, and F. Neri, An introduction to the special issue on advanced control of energy systems, *WSEAS Trans. Power Syst.*, 8, 2013, pp. 103.

[55] Z. Bojkovic, and F. Neri, An introduction to the special issue on advances on interactive multimedia systems, *WSEAS Trans. Syst.*, 12, 2013, pp. 337-338.

[56] L. Pekar, and F. Neri, An introduction to the special issue on advanced control methods: Theory and application, *WSEAS Trans. Syst.*, 12, 2013, pp. 301–303.

[57] C. Guarnaccia, and F. Neri, An introduction to the special issue on recent methods on physical polluting agents and environment modeling and simulation, *WSEAS Trans. Syst.*, 12, 2013, pp. 53–54.

[58] F. Neri, An introduction to the special issue on computational techniques for trading systems, time series forecasting, stock market modeling, and financial assets modeling *WSEAS Trans. Syst.*, 11, 2012, pp. 659–660.

[59] M. Muntean, and F. Neri, Foreword to the special issue on collaborative systems, *WSEAS Trans. Syst.*, 11, 2012, pp. 617.

[60] L. Pekar, and F. Neri, An introduction to the special issue on time delay systems: Modelling, identification, stability, control and applications, *WSEAS Trans. Syst.*, 11, 2012, pp. 539–540.

[61] C. Volos, and F. Neri, An introduction to the special issue: Recent advances in defense systems: Applications, methodology, technology, *WSEAS Trans. Syst.*, 11, 2012, pp. 477–478.

[62] A.V. Doroshin, Exact solutions in attitude dynamics of a magnetic dual-spin spacecraft and a generalization of the lagrange top, *WSEAS Trans. Syst.*, 12, 2013, pp. 471–482.

[63] A.V. Doroshin, Synthesis of attitude motion of variable mass coaxial bodies, *WSEAS Trans. Syst. Control* 3, 2008, pp. 50–61.

[64] L. Zhang, Y. Li, Q. Ren, and Z. Huo, Global dynamics of an SEIRS epidemic model with constant immigration and immunity, *WSEAS Trans. Math.*, 12, 2013, pp.630–640.

[65] K. Zhuang, and H. Zhu, Stability and bifurcation analysis for an improved HIV model with time delay and cure rate, *WSEAS Trans. Math.*, 12, 2013, pp.860–869.

[66] K. Zhao, and L. Ding, Multiple periodic solutions for a general class of delayed cooperative systems on time scales, *WSEAS Trans. Math.*, 12, 2013, pp.957–966.

[67] Y. Pei, Y. Liu, and C. Li, Dynamic study of mathe-matical models on antibiotics and immunologic adjuvant against Toxoplasmosis, *WSEAS Trans. Math.*, 11, 2012, pp.1018–1027.

[68] F.Y. Wei, K. Wang, Uniform persistence of asymptotically periodic multispecies competition predator-prey systems with Holling III type of functional response, *Appl. Math. Comput.* 170, 2005, pp. 994–998.

[69] Y. Yang, and W.C. Chen, Uniformly strong persistence of an nonlinear asymptotically periodic multispecies competition predator-prey system with general functional response, *Appl. Math. Comput.* 183, 2006, pp. 423–426.

[70] F. Montes de Oca, and M. Vivas, Extinction in a two dimensional Lotka-Volterra sysstem with infinite delay, *Nonlinear Anal.: Real World Appl.* 7, 2006, pp. 1042–1047.

[71] R. Yuan, Existence of almost periodic solutions of functional differential equations of neutral type, *J. Math. Anal. Appl.* 165, 1992, pp. 524–538.

LMI based bounded output feedback control for uncertain systems

ÉVA GYURKOVICS
Budapest University of Technology
and Economics
Institute of Mathematics
Műegyetem rkp. 3, H-1521, Budapest
HUNGARY
gye@math.bme.hu

TIBOR TAKÁCS
KIH
Department for Research

Múzeum u. 17, H-1088, Budapest
HUNGARY
tibor.takacs@kih.gov.hu

Abstract: The paper provides conditions for constrained dynamic output feedback controller to be cost guaranteeing and assuring asymptotic stability for both continuous and discrete-time systems with quadratically constrained nonlinear/uncertain elements. The conditions are formulated in the form of matrix inequalities, which can be rendered to be linear fixing one of the scalar parameters. An abstract multiplier method is applied. Numerical examples illustrate the application of the proposed method.

Key–Words: robust control; dynamic output feedback; guaranteed cost; uncertain systems; LMI

1 Introduction

Treatment of nonlinearities in dynamical and control systems is one of the research focuses of control theory (see e.g. [7], [10], [29], [31], [32]). The areas of applications of nonlinear control theory cover physics, engineering (see [3], [6], [8], [9], [13], [26], [30], [32], [39] from the recent literature) and also economics (e.g. [19], [21], [27], [28]). The performance of control systems may not be satisfactory because of the presence of exogenous disturbances and of system uncertainties stemming from the mismatch of the model and the real dynamics. A performance index assigned to the system cannot be minimized at the presence of unknown uncertainties, however it is possible to design a controller guaranteeing that the performance index will not exceed a certain bound, and it stabilizes the system for any admissible uncertainties and disturbances (see e.g., [2], [14], [15], [17], [20], [23], [35], [38], [41] and the references therein). It is favorable, if such robust controls can be given in feedback form. However, the state of the system is often not available for feedback. An extended static output feedback is applied e.g. by [33] for continuous-time systems using both the output and its derivatives in the construction of the controller. The same approach is applied to discrete-time systems with polytopic uncertainties in [34]. Paper [40] applies a dynamic output feedback for T-S fuzzy systems with norm bounded uncertainties. A dynamic output feedback can still guarantee an adequate level of system performance and stability (see also [18]). The present paper applies the latter approach for both discrete and continuous-time systems with a broad class of admissible system nonlinearities/uncertainties. The control is also supposed to be quadratically constrained (cf. [4] on stabilization of uncertain linear systems by bounded inputs).

A recently published paper [22] gave a sufficient condition for the existence of robust stabilizing observer-based dynamic output feedback control by solving linear matrix inequalities (LMIs). Unfortunately, this paper contains a technical error. The present paper proposes a method eliminating the mistake, and extends the range of solvable problems in several aspects. In our paper both continuous and discrete-time systems are discussed. We consider quadratically constrained uncertainties. This representation includes, among many others, the norm bounded uncertainty considered in [24] and [22], as a special case. In fact, this approach proposed originally by ([1]) and further developed by ([16]) as an abstract multiplier method allows to treat both uncertainties and system nonlinearities in a common framework, therefore the proposed method of design can be applied to a broad class of dynamic systems. Furthermore, exogenous disturbances are also taken into consideration. The control is also supposed to be quadratically constrained. It is assumed furthermore, that the exact initial state is not known, but it lies in a given ball.

The paper is organized as follows. The problem will be stated, and some preliminary results will be recalled in Section 2. The main results for continuous and discrete time systems will be presented in Section 3. Two numerical examples illustrate the results in

Section 4. Finally, the conclusion will be drawn.

Standard notations are used. The transpose of matrix A is denoted by A^T, I_n is the identity matrix of size $n \times n$, and $P > 0$ (≥ 0) denotes the positive (semi-) definiteness of P. The maximum eigenvalue of the symmetric matrix P is $\lambda_M(P)$. Symbol ∇V stands for the gradient of the multivariable function V, symbol $\otimes$ is used for Kronecker-product, while $\oplus$ is the direct sum. The notation of time-dependence is omitted, if it does not cause any confusion. For the sake of brevity, asterisks replace the blocks in hypermatrices, and matrices in expressions that are inferred readily by symmetry (e.g. $\begin{bmatrix} A & B \\ * & C \end{bmatrix}$ stands for $\begin{bmatrix} A & B \\ B^T & C \end{bmatrix}$, and $(*)PX$ stands for X^TPX). In general, we shall write n_v for the number of coordinates of a vector v, i.e. $v \in \mathbf{R}^{n_v}$.

2 Problem statement and preliminaries

Consider system

$$\delta x = Ax + Bu + E_x w + H_x p_x, \tag{1}$$

$$y = Cx + H_y p_y + E_y w, \tag{2}$$

$$\zeta^T = \left(x^T C_\zeta^T \; u^T D_\zeta^T\right), \tag{3}$$

$$q_x = A_q x + B_q u + G_x p_x, \tag{4}$$

$$q_y = C_q x + D_q u + G_y p_y, \tag{5}$$

where $x \in \mathbf{R}^{n_x}$ is the state, $u \in \mathbf{R}^{n_u}$ is the input, $w \in \mathbf{R}^{n_w}$ is the exogenous disturbance, δx stands for $\dot{x}$ in the continuous-time and x^+ in the discrete-time case. The measured output is $y \in \mathbf{R}^{n_y}$, and $\zeta \in \mathbf{R}^{n_\zeta}$ represents the penalty output, where D_ζ is assumed to be nonsingular.

Uncertainty constraints. All system nonlinearities/uncertainties are represented by functions p_x and p_y possibly depending on t, x and u. Functions q_x and q_y are the uncertain outputs. The only available information about $p^T = \left(p_x^T, p_y^T\right) \in \mathbf{R}^{l_p}$ and $q^T = \left(q_x^T, q_y^T\right) \in \mathbf{R}^{l_q}$ is that their values are constrained by the set $\Omega = \Omega_1 \times ... \times \Omega_s$,

$$\Omega_i = \left\{ \begin{bmatrix} p_i \\ q_i \end{bmatrix} \in \mathbf{R}^{l_{p_i}+l_{q_i}} : \begin{bmatrix} p_i \\ q_i \end{bmatrix}^T \begin{bmatrix} Q_{0i} & S_{0i} \\ S_{0i}^T & R_{0i} \end{bmatrix} \begin{bmatrix} p_i \\ q_i \end{bmatrix} \geq 0 \right\}, \tag{6}$$

$i = 1, ..., s$, where $Q_{0i} = Q_{0i}^T$, $R_{0i} = R_{0i}^T \geq 0$ and S_{0i} are constant matrices, $p \in \mathbf{R}^{l_p}$, and $q \in \mathbf{R}^{l_q}$ are partitioned appropriately. We shall use the notations $Q_0 = \text{diag}\{Q_{01}, ..., Q_{0s}\}$, $R_0 = \text{diag}\{R_{01}, ..., R_{0s}\}$, $S_0 = \text{diag}\{S_{01}, ..., S_{0s}\}$. We note that the positive semi-definiteness of R_0 assures that the system (1)-(5) is well posed, i.e. for any (x, u) there is a p so that $\left[p^T, \; q^T\right]^T \in \Omega$. It is worth noting that the considered model of uncertainties involves several types of uncertainties frequently investigated in the literature. For example, if $Q_0 = 0$, $S_0 = I$ and $R_0 = 0$, then one speaks about positive real uncertainty, if $Q_0 = -I$, $S_0 = 0$ and $R_0 = I$, then one has norm-bounded uncertainties, (thus, the uncertainty of [24] and [22] can be obtained as a special case), and if $Q_0 = \frac{1}{2}(K_1^T K_2 + K_2^T K_1)$, $S_0 = \frac{1}{2}(K_1 + K_2)^T$ and $R_0 = I$, then one faces the case of sector-bounded uncertainties.

Control constraints. The control is supposed to be quadratically constrained, i.e.

$$u^T Q_u u \leq 1 \tag{7}$$

must be satisfied for a given matrix $Q_u = Q_u^T > 0$.

State constraints. Since the state is not measured, its initial value is not supposed to be known, but it is assumed that

$$\|x_0\|^2 \leq \rho,$$

where ρ is a given positive constant. We remark however that the initial state x_0 may supposed to be known.

Constraints on disturbances. The disturbances are produced by an exosystem, the input of which is the penalty output ζ of the original system, the output is w, and (ζ, w) satisfy the inequality

$$\|w\|_{S_L}^2 = w^T S_L w \leq \gamma_\Delta \|\zeta\|^2$$

with a given positive definite and symmetric matrix S_L and with $\gamma_\Delta < 1$.

Assign the *cost function*

$$J(x_0, u, w) = \begin{cases} \int_0^\infty L(x(t), u(t), w(t))dt, \\ \qquad\qquad \text{if } t \in \mathbf{R}, \\ \sum_{t=1}^\infty L(x(t), u(t), w(t)), \\ \qquad\qquad \text{if } t \in \mathbf{Z} \end{cases} \tag{8}$$

to system (1)-(2), where

$$L(x, u, w) = x^T Q_L x + u^T R_L u - w^T S_L w$$

with $Q_L = C_\zeta^T C_\zeta$, $R_L = D_\zeta^T D_\zeta$ and S_L given above. Thus, it follows from their definitions that Q_L, R_L

and S_L are symmetric, Q_L is positive semidefinite, R_L and S_L are positive definite matrices.

The aim is to keep the value of the cost function by the appropriate choice of the control as low as possible for all realizations of the uncertainties and the external perturbations. Because of the presence of uncertainties a minimum (or minimax) value of the cost cannot be achieved; one can only expect a guaranteed upper bound of it. The corresponding guaranteed cost control has to be determined in feedback form. Since the state is not available for feedback, a dynamic output feedback is sought. We look for the controller in the following form:

$$\delta\hat{x} = A_c\hat{x} + L_c y, \qquad \hat{x}(0) = 0, \tag{9}$$

$$u = K_c\hat{x} \tag{10}$$

where $\hat{x} \in \mathbf{R}^{n_x}$.

Introduce the new variable $z = \left(x^T, \hat{x}^T\right)^T$. With this notation, $u = \kappa z$, where $\kappa = (0, K_c)$, and the augmented closed-loop system is

$$\delta z = \mathcal{A}z + \mathcal{E}w + \mathcal{H}p, \tag{11}$$

$$q = \mathcal{A}_q z + \mathcal{G}p, \tag{12}$$

where $\mathcal{G} = \text{diag}\{G_x, G_y\}$,

$$\mathcal{A} = \begin{bmatrix} A & BK_c \\ L_cC & A_c \end{bmatrix},\ \mathcal{A}_q = \begin{bmatrix} A_q & B_qK_c \\ C_q & D_qK_c \end{bmatrix}, \tag{13}$$

$$\mathcal{E} = \begin{bmatrix} E_x \\ L_cE_y \end{bmatrix}, \qquad \mathcal{H} = \begin{bmatrix} H_x & 0 \\ 0 & L_cH_y \end{bmatrix}. \tag{14}$$

Set $\mathcal{K} = \text{diag}\{I_{n_x}, K_c\}$. The running cost of the augmented closed-loop system is

$$\mathcal{L}(z, w) = z^T\overline{Q}_L z - w^T S_L w,$$

where $\overline{Q}_L = \mathcal{K}^T\text{diag}\{Q_L, R_L\}\mathcal{K}$.

To formulate the notion of guaranteeing cost controller, consider an arbitrary nonlinear/uncertain system

$$\delta z = f(z, u, w, p), \tag{15}$$

$$q = g(z, u, p), \qquad \left[p^T, q^T\right]^T \in \Omega,$$

and a function $\mathcal{V} : \mathbf{R}^{n_z} \to \mathbf{R}^+$.

For system (15) introduce the following notation:

$$\mathcal{V}^*_{(15)}(z, u, w, p) = \\ = \begin{cases} \nabla\mathcal{V}^T(z)\, f(z, u, w, p), & \text{if } t \in \mathbf{R}, \\ \mathcal{V}(f(z, u, w, p)) - \mathcal{V}(z), & \text{if } t \in \mathbf{Z}. \end{cases}$$

Definition 1 *Consider the nonlinear/uncertain system (15) with cost function of the type (8) and with a given set of nonlinearities/uncertainties Ω. The state-feedback $u = k(z)$ is a* guaranteeing cost robust minimax strategy *if there exists a function $\mathcal{V} : \mathbf{R}^{n_z} \to \mathbf{R}^+$ such that*

$$\sup_{\left[p^T,\, q^T\right]^T \in \Omega} \{\mathcal{V}^*_{(15)}(z, k(z), w, p) + L(z, k(z), w)\} < 0 \tag{16}$$

holds for all z and w, $\left[z^T,\ w^T\right] \neq \left[0^T,\ 0^T\right]$. In this case $\mathcal{V}(z_0)$ is called a guaranteed cost.

Remark 2 (A) *Similar definitions of guaranteed cost are frequently used in the literature (see e.g. [23], [42], [14], and the references therein). The rationality of this definition is explained by Theorem 7 given below.*
(B) *Observe that a cost guaranteeing control with special choice of matrices Q_L, R_L and S_L is an H_∞ control with the penalty output (3).*

The main problem is to find an appropriate $\mathcal{V}$ and a feedback $k(z)$ because of the need of maximization over Ω. The main idea of the multiplier method is that an equivalent inequality will be solved over a linear space at the expense of introducing a new matrix variable. The method assures that the feasibility set of the new inequality is the same as that of the original problem. In this way, the investigation of the inequality and of the uncertainty bounding set is separated and the problem becomes tractable. Paper [16] presented an abstract multiplier method. We recall here the basic definitions and the lemma to be used. Let $\mathcal{Q} \subset \mathbf{R}^l$ be given.

Definition 3 *([1], [16]) A symmetric matrix M is called a* multiplier matrix *for $\mathcal{Q}$ if $\xi^T M\xi \geq 0$ for all $\xi \in \mathcal{Q}$. If this inequality is strict, then M is called a* positive multiplier matrix *for $\mathcal{Q}$. The set $\mathcal{M}^+$ of positive multiplier matrices for $\mathcal{Q}$ is called a* sufficiently rich set of positive multipliers *for $\mathcal{Q}$, if for any positive multiplier $\overline{M}$ for $\mathcal{Q}$ there exists an element $M \in \mathcal{M}^+$ such that $M \leq \overline{M}$.*

Consider positive constants τ_i and ε_i, $i = 1, ..., s$ and set

$$\underline{\tau} = \text{diag}\left\{\tau_1 I_{l_{p_1}}, ..., \tau_s I_{l_{p_s}}\right\},$$

$$\underline{\underline{\tau}} = \text{diag}\left\{\tau_1 I_{l_{q_1}}, ..., \tau_s I_{l_{q_s}}\right\},$$

$$\underline{\varepsilon} = \text{diag}\left\{\varepsilon_1 I_{l_{p_1}}, ..., \varepsilon_s I_{l_{p_s}}\right\},$$

$$\underline{\underline{\varepsilon}} = \text{diag}\left\{\varepsilon_1 I_{l_{q_1}}, ..., \varepsilon_s I_{l_{q_s}}\right\}.$$

We note that, if $s = 1$, matrices $\underline{\tau}$, $\underline{\underline{\tau}}$, $\underline{\varepsilon}$ and $\underline{\underline{\varepsilon}}$ consist of a single block, thus two scalar parameters can be used instead. In order to avoid the repetition of big formulas, we shall use the matrix notations in the special case of $s = 1$, as well.

Lemma 4 *([17]) The set*

$$\mathcal{M}^+ = \left\{ M:\ M = \begin{bmatrix} \underline{\tau} Q_0 + \underline{\varepsilon} & \underline{\tau} S_0 \\ S_0^T \underline{\tau} & \underline{\underline{\tau}} R_0 + \underline{\underline{\varepsilon}} \end{bmatrix}, \right. \\ \left. \tau_i, \varepsilon_i > 0,\ i = 1, ..., s \right\} \quad (17)$$

consists of positive multiplier matrices for Ω. If $s = 1$, then $\mathcal{M}^+$ is sufficiently rich.

The recently published paper [22] gave a sufficient condition for the existence of robust stabilizing feedback based on a Luenberger type observer for continuous-time systems with norm-bounded uncertainties. The condition was formulated as an LMI. It was stated that the given LMI contains three adjustable parameters. In fact, there is only one free parameter. The source of the error was that authors failed to multiply the 6th and the 8th term from the left hand side and the 7th and 9th term from the right hand side by P^{-1} in equation (10). If the Schur complement is applied two more times after the correct congruence transformation, it turns out that only parameter ε_1 is adjustable. This certainly results in a lower $\alpha_{\max}$ in the second numerical example of that paper. We made several experiments for fixed $\varepsilon_4 = 0.01$ and for different values of ε_2 and ε_3 with changing magnitudes. It was found that $\alpha_{\max} < 0.98$ for the considered parameter combination.

The present paper solves a more general problem. Both continuous and discrete-time systems are examined with a far broader class of uncertainties/nonlinearities, and exogenous disturbances are considered, too. Also state and control constraints can a priori be given.

3 Main results

Assumption 1 *Inequalities* (1) $R_0 \geq 0$ *and*

(2) $Q_0 + \mathcal{G}^T S_0^T + S_0 \mathcal{G} + \mathcal{G}^T R_0 \mathcal{G} < 0$
hold true.

The second inequality of the Assumption 1 implies that $\left[p^T,\ p^T \mathcal{G}^T\right]^T \in \Omega$ if and only if $p = 0$, thus the origin is an equilibrium point of the unperturbed uncertain/nonlinear system. Moreover, the set of uncertain input vectors satisfying $\left[p^T, q^T\right]^T \in \Omega$ is bounded if q is defined by (4)-(5) and (x, u) comes from a bounded set, which is also a reasonable requirement. Similar conditions are applied e.g. in [41].

Set $N = 5n_x + n_u + n_w + l_p + l_q$, $\Xi = \mathrm{diag}\{Q_L, R_L, -S_L\}$. Introduce the $2n_x \times 2n_x$ matrix

$$\phi = \begin{cases} \phi_c = \begin{bmatrix} 0 & I \\ I & 0 \end{bmatrix}, & \text{if } t \in \mathbf{R}, \\ \phi_d = \begin{bmatrix} -I & 0 \\ 0 & I \end{bmatrix}, & \text{if } t \in \mathbf{Z}, \end{cases}$$

and the matrices

$$\mathcal{L}_1^T = \begin{bmatrix} I & \mathcal{A}^T & \mathcal{K}^T & 0 & 0 & \mathcal{A}_q^T \\ 0 & \mathcal{E}^T & 0 & I & 0 & 0 \end{bmatrix}, \\ \mathcal{L}_0^T = \begin{bmatrix} 0 & \mathcal{H}^T & 0 & 0 & I & \mathcal{G}^T \end{bmatrix}. \quad (18)$$

Lemma 5 *Suppose that Assumption 1 holds true for the set Ω given by (6). The dynamic output feedback controller (9)-(10) defined by the matrices A_c, L_c, K_c yields a guaranteeing cost robust minimax strategy $k(z) = \kappa z$ and $\mathcal{V}(z_0)$ is the guaranteed cost with $\mathcal{V}(z_0) = z_0^T P z_0$, $P = P^T > 0$ if there exists an $M \in \mathcal{M}^+$ such that P, M satisfy the matrix inequality*

$$\left[*\right] \mathit{diag}\left\{\phi \otimes P,\ \Xi,\ M\right\} \left[\mathcal{L}_1, \mathcal{L}_0\right] < 0, \quad (19)$$

where $\mathcal{L}_1$, $\mathcal{L}_0$ correspond to matrices A_c, L_c, K_c as defined by (13), (14) and (18). The existence of $M \in \mathcal{M}^+$ is also necessary, if the uncertainty is unstructured, i.e. if $s = 1$.

Proof. Introduce function $F : \mathbf{R}^{2n_x + n_w + n_p} \to \mathbf{R}$ with the definition

$$F(z, w, p) = \left[*\right] \left[*\right] \left[\phi \otimes P\right] \begin{bmatrix} I & 0 & 0 \\ \mathcal{A} & \mathcal{E} & \mathcal{H} \end{bmatrix} \begin{bmatrix} z \\ w \\ p \end{bmatrix} \\ + \left[*\right] \left[*\right] \Xi \begin{bmatrix} \mathcal{K} & 0 & 0 \\ 0 & I & 0 \end{bmatrix} \begin{bmatrix} z \\ w \\ p \end{bmatrix}$$

Then inequality (16) with respect to (11) is equivalent to

$$\sup_{\left[p^T,\ q^T\right]^T \in \Omega} F(z, w, p) < 0 \quad (20)$$

for all z and w, $\left[z^T,\ \ w^T\right] \neq \left[0^T,\ \ 0^T\right]$.

Set $\Psi = \mathrm{diag}\{\phi \otimes P,\ \Xi,\ 0\}$ and $\mathcal{B}_0 = \mathrm{im}\mathcal{L}_0$, $\mathcal{B}_1 = \mathrm{im}\mathcal{L}_1$, $\mathcal{B} = \mathrm{im}\left(\mathcal{L}_1, \mathcal{L}_0\right)$. Then $\mathcal{B} = \mathcal{B}_1 \oplus \mathcal{B}_0$ and $\mathcal{B}_1 \cap \mathcal{B}_0 = \{0\}$. A straightforward calculation shows that $F(z, w, p) = y^T \Psi y$, if $y \in \mathcal{B}$, i.e. if $y = \mathcal{L}_1 \left[z^T \quad w^T\right]^T + \mathcal{L}_0\, p$. Set

$$V = \begin{bmatrix} 0 & 0 & 0 & 0 & I & 0 \\ 0 & 0 & 0 & 0 & 0 & I \end{bmatrix} \in \mathbf{R}^{(l_p + l_q) \times N},$$

and

$$\mathcal{B}_\Omega = \left\{ y \in \mathcal{B} \subset \mathbf{R}^N : \quad Vy \in \Omega \right\}.$$

Thus inequality (20) is equivalent to

$$y^T \Psi y < 0 \quad \text{for all } y \in \mathcal{B}_\Omega,\ y \neq 0. \tag{21}$$

It was proven in ([16]) that inequality (21) holds true if there exists an $M \in \mathcal{M}^+$ such that

$$\Psi + V^T M V < 0 \qquad \text{for all } y \in \mathcal{B},$$

which is identical to (19). The necessity of the existence of $M \in \mathcal{M}^+$ with this property has been proven in ([16]), as well. □

Remark 6 *Since $\hat{x}(0)$ is fixed, the guaranteed cost depends on $x(0)$ only. Moreover, since any matrix in $\mathcal{M}^+$ is determined by two scalar parameters τ and ε, the existence of an appropriate $M \in \mathcal{M}^+$ is equivalent to the existence of these two scalar parameters.*

In what follows, we shall show that a guaranteeing cost controller in the sense of Definition 1 yields an upper bound of the cost function and a closed-loop system for which the origin is asymptotically stable. This gives the rationality of Definition 1.

Denote the ellipsoid in $\mathbf{R}^{2n_x}$ as

$$\Gamma(P, \alpha) = \left\{ \xi \in \mathbf{R}^{2n_x} : \xi^T P \xi \leq \alpha \right\}.$$

Theorem 7 *Consider the augmented closed-loop system (11)-(12) with Ω satisfying Assumption 1, and suppose that for a given $P = P^T > 0$, inequality (19) holds true. Then $\alpha = \lambda_M(P)\rho$ is an upper bound of the cost function for any admissible initial state, disturbance and uncertainty. Moreover, the ellipsoid $\Gamma(P, \alpha)$ is positively invariant and the origin is asymptotically stable for the closed-loop uncertain system.*

Proof. If inequality (19) holds true then there exists a $\delta > 0$ such that

$$\begin{aligned} \left[*\right] \operatorname{diag}\left\{\phi \otimes P,\ \Xi,\ M\right\} \left[\mathcal{L}_1, \mathcal{L}_0\right] \\ + \ \delta \operatorname{diag}\left\{ \ I_{2n_x}, \quad 0, \quad 0 \ \right\} < 0, \end{aligned}$$

This means in compliance with Lemma 5 that for $k(z) = \kappa z$

$$\begin{aligned} \mathcal{V}^*_{(11)}(z, k(z), w, p) \\ + \ L(z, k(z), w) + \delta \|z\|^2 < 0 \end{aligned} \tag{22}$$

holds true for any $(z, w) \neq (0, 0)$ and for any uncertainty/nonlinearity satisfying $\left[p^T, q^T\right]^T \in \Omega$.

For the sake of definiteness, suppose that we are facing the continuous-time case. (The discrete-time case is completely analogous.) Integrating inequality (22) from 0 to $T > 0$, we obtain that

$$\begin{aligned} \mathcal{V}(z(T)) - \mathcal{V}(z(0)) + \int_0^T z(t)^T \overline{Q}_L z(t) dt \\ - \int_0^T w(t)^T S_L w(t) dt + \delta \int_0^T \|z(t)\|^2 dt < 0. \end{aligned} \tag{23}$$

Omitting the first and the last (nonnegative) terms on the left hand side, we obtain that for all $T > 0$

$$\int_0^T \mathcal{L}(z(t), w(t)) dt < \mathcal{V}(z(0)). \tag{24}$$

For the considered $w(.)$, $\mathcal{L}(z(t), w(t)) \geq 0$ for all t, therefore the integral on the left hand side of (24) is convergent as $T \to \infty$, and it tends to the value of the cost function. Since $\hat{x}(0) = 0$, for any x_0 with $\|x_0\|^2 \leq \rho$, we have that

$$\mathcal{V}(z(0)) \leq \lambda_M(P)\rho = \alpha.$$

From (23) it follows that $\mathcal{V}(z(T)) < \alpha$ for any $T > 0$, thus the ellipsoid $\Gamma(P, \alpha)$ is invariant. Furthermore P is assumed to be positive definite, thus it follows from (22) that function $\mathcal{V}$ is an appropriate Lyapunov-function having a derivative along the solutions of the closed-loop system (11) strictly smaller than $-\delta\|z\|^2$. Therefore the origin is asymptotically stable with a basin of attraction containing $\Gamma(P, \alpha)$.

Corollary 8 *If $z_0^T P z_0 \leq 1$ for any $z_0 = (x_0^T,\ 0^T)^T$ with $\|x_0\|^2 \leq \rho$, then $\Gamma(P, 1)$ is invariant for the closed-loop uncertain system. Moreover, if*

$$\begin{bmatrix} P & * \\ \kappa & Q_u^{-1} \end{bmatrix} \geq 0, \tag{25}$$

then for any $z \in \Gamma(P, 1)$, the control $u = \kappa z$ satisfies the control constraint (7).

Proof. The first part of the statement immediately follows from Theorem 7. The second part follows from (25) using Schur complements. □

We remark that other types of exogenous disturbances can be treated too. For example, disturbances of finite 'energy' are formulated as

$$\int_0^\infty w(t)^2 dt \leq \eta, \qquad \text{if } t \in \mathbf{R},$$

$$\sum_{t=1}^\infty w(t)^2 \leq \eta, \qquad \text{if } t \in \mathbf{Z},$$

where η is a given positive constant. A similar statement can be proven in this case, but the invariant ellipsoid is slightly different.

In what follows we propose methods to determine matrices P, A_c, L_c, K_c, and scalars ε_i, τ_i, $(i = 1, ..., s)$ in the discrete and in the continuous-time case. In order to obtain the matrix inequalities on the basis of which these parameters can be determined, we apply an approach similar to that of [12]. Represent matrix P and its inverse as

$$P = \begin{bmatrix} X & N_1 \\ N_1^T & Z \end{bmatrix}, \quad P^{-1} = \begin{bmatrix} Y & N_2 \\ N_2^T & W \end{bmatrix} \tag{26}$$

with $X = X^T > 0$, $Y = Y^T > 0$, and consider matrices

$$F_1 = \begin{bmatrix} X & I \\ N_1^T & 0 \end{bmatrix}, \quad F_2 = \begin{bmatrix} I & Y \\ 0 & N_2^T \end{bmatrix}, \tag{27}$$

where each block is of dimension $n_x \times n_x$. Clearly,

$$F_1^T P^{-1} F_1 = \begin{bmatrix} X & I \\ I & Y \end{bmatrix}, \quad P^{-1} F_1 = F_2. \tag{28}$$

Introduce furthermore the notations

$$\widetilde{K} = K_c N_2^T, \qquad \widetilde{L} = N_1 L_c, \tag{29}$$

$$\widetilde{A} = XAY + XB\widetilde{K} + \widetilde{L}CY + N_1 A_c N_2^T. \tag{30}$$

Now we derive a matrix inequality equivalent to (19), which is linear in all of the unknown matrices except for parameters τ_i.

3.1 The continuous-time case

In this subsection ϕ is fixed as $\phi = \phi_c$.

Theorem 9 *Inequality (19) holds true for the symmetric and positive definite matrix P partitioned as in (26) and for the coefficient matrices A_c, L_c, K_c of the controller and for the positive scalars τ_i and ε_i if and only if X, Y, $\widetilde{A}$, $\widetilde{L}$, $\widetilde{K}$, ε_i and τ_i $(i = 1, \ldots, s)$ satisfy the following matrix inequalities:*

$$\begin{bmatrix} \Phi_{11} & * \\ \Phi_{21} & \Phi_{22} \end{bmatrix} < 0, \quad \begin{bmatrix} X & I \\ I & Y \end{bmatrix} > 0, \tag{31}$$

$$\Phi_{11} = \begin{bmatrix} \varphi_{11}^{11} & * & * & * \\ \varphi_{21}^{11} & \varphi_{22}^{11} & * & * \\ \varphi_{31}^{11} & \varphi_{32}^{11} & -S_L & * \\ \varphi_{41}^{11} & \varphi_{42}^{11} & 0 & \varphi_{44}^{11} \end{bmatrix},$$

$$\begin{aligned}
\varphi_{11}^{11} &= A^T X + XA + C^T \widetilde{L}^T + \widetilde{L} C, \\
\varphi_{22}^{11} &= AY + B\widetilde{K} + Y^T A^T + \widetilde{K}^T B^T, \\
\varphi_{44}^{11} &= Q_0 \underline{\tau}^{-1} + S_0 \mathcal{G} \underline{\tau}^{-1} + \underline{\tau}^{-1} \mathcal{G}^T S_0^T, \\
\varphi_{21}^{11} &= A + \widetilde{A}^T, \\
\varphi_{31}^{11} &= E_x^T X + E_y^T \widetilde{L}^T, \quad \varphi_{32}^{11} = E_x^T, \\
\varphi_{41}^{11} &= \underline{\tau}^{-1} \begin{bmatrix} H_x^T X \\ H_y^T \widetilde{L}^T \end{bmatrix} + S_0 \begin{bmatrix} A_q \\ C_q \end{bmatrix}, \\
\varphi_{42}^{11} &= \underline{\tau}^{-1} \begin{bmatrix} H_x^T \\ 0 \end{bmatrix} + S_0 \begin{bmatrix} A_q Y + B_q \widetilde{K} \\ C_q Y + D_q \widetilde{K} \end{bmatrix},
\end{aligned}$$

$$\Phi_{21} = \begin{bmatrix} 0 & 0 & 0 & \underline{\tau}^{-1} \\ \varphi_{21}^{21} & \varphi_{22}^{21} & 0 & R_0^{1/2} \mathcal{G} \underline{\tau}^{-1} \\ \varphi_{31}^{21} & \varphi_{32}^{21} & 0 & \mathcal{G} \underline{\tau}^{-1} \\ C_\zeta & C_\zeta Y & 0 & 0 \\ 0 & \widetilde{K} & 0 & 0 \end{bmatrix},$$

$$\begin{aligned}
\varphi_{21}^{21} &= R_0^{1/2} \begin{bmatrix} A_q \\ C_q \end{bmatrix}, \\
\varphi_{22}^{21} &= R_0^{1/2} \begin{bmatrix} A_q Y + B_q \widetilde{K} \\ C_q Y + D_q \widetilde{K} \end{bmatrix}, \\
\varphi_{31}^{21} &= \begin{bmatrix} A_q \\ C_q \end{bmatrix}, \quad \varphi_{32}^{21} \begin{bmatrix} A_q Y + B_q \widetilde{K} \\ C_q Y + D_q \widetilde{K} \end{bmatrix},
\end{aligned}$$

$$\Phi_{22} = \operatorname{diag}\left\{ -\underline{\varepsilon}^{-1}, -\underline{\tau}^{-1}, -\underline{\varepsilon}^{-1}, -I, R_L^{-1} \right\}.$$

Proof. Consider inequality (21) with an arbitrary $M \in \mathcal{M}^+$ given in (18), and multiply the middle block-diagonal matrix from left and right by $L^T L = I$, where L is an appropriate permutation matrix to obtain that

$$\begin{bmatrix} * \end{bmatrix} \begin{bmatrix} 0 & * & * & * & * & * \\ P & 0 & * & * & * & * \\ 0 & 0 & -S_L & * & * & * \\ 0 & 0 & 0 & \underline{\tau} Q_0 + \underline{\varepsilon} & * & * \\ 0 & 0 & 0 & 0 & \Upsilon & * \\ 0 & 0 & 0 & S_0^T \underline{\tau} & 0 & \underline{\underline{\tau}} R_0 + \underline{\underline{\varepsilon}} \end{bmatrix} \times$$

$$\times \begin{bmatrix} I & 0 & 0 \\ \mathcal{A} & \mathcal{E} & \mathcal{H} \\ 0 & I & 0 \\ 0 & 0 & I \\ \mathcal{K} & 0 & 0 \\ \mathcal{A}_{\mathrm{II}} & 0 & \mathcal{G} \end{bmatrix} < 0 \tag{32}$$

with $\Upsilon = \operatorname{diag}\{Q_L, R_L\}$. Applying the definition $Q_L = C_\zeta^T C_\zeta$ and the linearization lemma (see [37])

one obtains that (32) is equivalent to

$$\begin{bmatrix} \mathcal{A}^TP+P\mathcal{A} & * & * & * & * \\ \mathcal{E}^TP & -S_L & * & * & * \\ \mathcal{H}^TP+\underline{\tau}S_0\mathcal{A}_q & 0 & \vartheta+\underline{\varepsilon} & * & * \\ \mathcal{C}_\zeta\mathcal{K} & 0 & 0 & -\mathcal{R}_L^{-1} & * \\ \mathcal{A}_q & 0 & \mathcal{G} & 0 & -(\underline{\underline{\tau}}R_0+\underline{\underline{\varepsilon}}) \end{bmatrix} < 0,$$

where the notations $\vartheta = \underline{\tau}Q_0 + \underline{\tau}S_0\mathcal{G} + \mathcal{G}^TS_0^T\underline{\tau}$ and $\mathcal{C}_\zeta = \text{diag}\{C_\zeta, I\}$ and $\mathcal{R}_L = \text{diag}\{I, R_L\}$ have been used. Now we can apply the Schur complement lemma to get rid of the inverse of $(\underline{\underline{\tau}}R_0 + \underline{\underline{\varepsilon}})$. Then apply the Schur complement again, the congruence transformation with $\text{diag}\{P^{-1}, I, \underline{\tau}^{-1}, I, I, I, I\}$ and notations

$$\theta_1 = \mathcal{A}^TP^{-1} + P^{-1}\mathcal{A}^T, \;\; \theta_2 = \underline{\tau}^{-1}\mathcal{H}^T + S_0\mathcal{A}_qP^{-1}$$
$$\theta_3 = R_0^{1/2}\mathcal{A}_qP^{-1}, \;\; \theta_4 = R_0^{1/2}\mathcal{G}\underline{\tau}^{-1}, \;\; \theta_5 = \mathcal{C}_\zeta\mathcal{K}P^{-1}$$

to derive the equivalent inequality

$$\begin{bmatrix} \theta_1 & * & * & * & * & * & * \\ \mathcal{E}^T & -S_L & * & * & * & * & * \\ \theta_2 & 0 & \varphi_{44}^{11} & * & * & * & * \\ 0 & 0 & \underline{\tau}^{-1} & -\underline{\varepsilon}^{-1} & * & * & * \\ \theta_3 & \theta_4 & 0 & 0 & \underline{\tau}^{-1} & * & * \\ \mathcal{A}_qP^{-1} & 0 & \mathcal{G}\underline{\tau}^{-1} & 0 & 0 & \underline{\underline{\varepsilon}}^{-1} & * \\ \theta_5 & 0 & \mathcal{G}\underline{\tau}^{-1} & 0 & 0 & 0 & -\mathcal{R}_L^{-1} \end{bmatrix} < 0. \quad (33)$$

Multiply (33) by $\text{diag}\{F_1^T, I, I, I, I, I, I\}$ from the left and by its transpose from the right, and take into consideration (27)-(28) to obtain that

$$F_1^T\mathcal{A}F_2 = \begin{bmatrix} \varphi_{11}^{11} & * \\ \varphi_{21}^{11} & \varphi_{22}^{11} \end{bmatrix}, \;\; \mathcal{C}_\zeta\mathcal{K}F_2 = \begin{bmatrix} C_\zeta & C_\zeta Y \\ 0 & \widetilde{K} \end{bmatrix},$$
$$\mathcal{E}^TF_1 = \left[\varphi_{31}^{11}, \varphi_{32}^{11}\right],$$
$$\underline{\tau}^{-1}\mathcal{H}F_1 + S_0\mathcal{A}_qF_2 = \left[\varphi_{41}^{11}, \varphi_{42}^{11}\right],$$
$$R_0^{1/2}\mathcal{A}_qF_2 = \left[\varphi_{21}^{21}, \varphi_{22}^{21}\right], \;\; \mathcal{A}_qF_2 = \left[\varphi_{31}^{21}, \varphi_{32}^{21}\right]. \;\; \square$$

We observe that the matrix inequality (31) is nonlinear in the unknown parameters τ_i. However, if τ_i's are fixed, this inequality becomes linear in variables X, Y, $\widetilde{K}$, $\widetilde{L}$, $\widetilde{A}$ and ε_i^{-1}, $i = 1, ..., s$. If (31) is feasible, inequality

$$\begin{bmatrix} X & I \\ I & Y \end{bmatrix} > 0,$$

is equivalent to $I - XY < 0$, hence the left hand side is factorizable as $N_1N_2^T = I - XY$, where N_1 and N_2 are invertible, i.e. matrices K_c, L_c and A_c can be expressed uniquely from the solution of (31) employing (29)-(30).

3.2 The discrete-time case

In this subsection ϕ is fixed as $\phi = \phi_d$.

Theorem 10 *Inequality (19) holds true for the symmetric and positive definite matrix P partitioned as in (26) and for the coefficient matrices A_c, L_c, K_c, of the controller and for the positive scalars τ_i and ε_i if and only if X, Y, $\widetilde{A}$, $\widetilde{L}$, $\widetilde{K}$, ε_i and τ_i, $(i = 1, ..., s)$, satisfy the following matrix inequality:*

$$\begin{bmatrix} \psi_{11} & * & * & * & * & * & * & * \\ 0 & -S_L & * & * & * & * & * & * \\ \psi_{31} & 0 & \psi_{33} & * & * & * & * & * \\ \psi_{41} & \psi_{42} & \psi_{43} & \psi_{44} & * & * & * & * \\ 0 & 0 & I & 0 & -\underline{\varepsilon}^{-1} & * & * & * \\ \psi_{61} & 0 & \mathcal{G} & 0 & 0 & -\underline{\underline{\varepsilon}}^{-1} & * & * \\ \psi_{71} & 0 & R_0^{1/2}\mathcal{G} & 0 & 0 & 0 & -\underline{\tau}^{-1} & * \\ \psi_{81} & 0 & 0 & 0 & 0 & 0 & 0 & -\mathcal{R}_L^{-1} \end{bmatrix} < 0, \quad (34)$$

where

$$\psi_{11} = -\begin{bmatrix} X & I \\ I & Y \end{bmatrix}, \; \psi_{31} = \tau S_0\psi_{71},$$
$$\psi_{33} = \underline{\tau}Q_0 + \underline{\tau}S_0\mathcal{G} + \mathcal{G}^TS_0^T\underline{\tau},$$
$$\psi_{41} = \begin{bmatrix} XA + \widetilde{L}C & \widetilde{A} \\ A & AY + B\widetilde{K} \end{bmatrix},$$
$$\psi_{42} = \begin{bmatrix} XE_x + \widetilde{L}E_y \\ E_x \end{bmatrix},$$
$$\psi_{43} = \begin{bmatrix} XH_x & \widetilde{L}H_y \\ H_x & 0 \end{bmatrix}, \; \psi_{44} = \psi_{11},$$
$$\psi_{61} = \begin{bmatrix} A_q & A_qY + B_q\widetilde{K} \\ C_q & C_qY + D_q\widetilde{K} \end{bmatrix},$$
$$\psi_{71} = R_0^{1/2}\psi_{61}, \quad \psi_{81} = \begin{bmatrix} C_\zeta & C_\zeta Y \\ 0 & \widetilde{K} \end{bmatrix},$$

Proof. The theorem can be proved completely analogously to the previous one, the details are omitted for the lack of space. $\square$

Inequality (34) is nonlinear in he unknown parameters τ_i, but for any fixed values, it is an LMI in the remaining unknown matrices. Observations similar to the continuous-time case can be made concerning the computation of the coefficient matrices of the controller, as well.

3.3 Control constraint LMIs

For a given value of parameters τ_i, Theorems 9 and 10 provide LMIs on the basis of which one can obtain the solution of the formulated problem, if no control constraint is imposed. Next we shall derive additional LMIs to assure the satisfaction of the control

constraint presuming that the initial value x_0 is admissible.

Theorem 11 *Assume that the condition of Corollary 8 is valid. Suppose that in addition to (31) in the continuous-time case and to (34) in the discrete-time case inequalities*

$$X - \frac{1}{\rho} I \leq 0, \tag{35}$$

$$\begin{bmatrix} X & I & 0 \\ I & Y & \widetilde{K}^T \\ 0 & \widetilde{K} & Q_u^{-1} \end{bmatrix} \geq 0 \tag{36}$$

hold true. Then $z(t)^T P z(t) \leq 1$ for any $t \geq 0$, and $u(t) = \kappa z(t)$ satisfies the control constraint (7) for all $t \geq 0$.

Proof. Suppose that P is partitioned according to (26) and $\|x_0\|^2 \leq \rho$, $\hat{x}(0) = 0$. Then we have $z_0^T P z_0 = x_0^T X x_0$, thus it follows from (35) that $z_0^T P z_0 \leq 1$. Therefore, Corollary 8 involves that $z(t)^T P z(t) \leq 1$ for any $t \geq 0$. On the other hand, if

$$z(t)^T \kappa^T Q_u \kappa z(t) \leq z(t)^T P z(t), \tag{37}$$

then (7) holds true for any $t \geq 0$. Inequality (37) holds true, if

$$P - \kappa^T Q_u \kappa \geq 0,$$

which is equivalent to

$$\begin{bmatrix} P & * \\ \kappa & Q_u^{-1} \end{bmatrix} \geq 0. \tag{38}$$

If we apply the congruence transformation for (38) with diag $\left\{ P^{-1} F_1,\ I \right\}$, we get that the latter inequality is equivalent to the required one (36). □

Remark 12 *Every feasible solution of systems (31), (35)-(36) or (34), (35)-(36), provides a cost guaranteeing controller. Several types of objective functions can be assigned to the systems of inequalities. For example, paper [11] proposes to minimize trP to obtain the largest set of admissible states of the augmented system. (Matrix P was kept there as the unknown of the LIMs.) Similar purpose can be achieved by minimizing $\mu := 1/\varrho$.*

4 Numerical examples

Example 1. ([24], [22]) To illustrate the effectiveness of our approach we consider the same example as [24] and [22]. The system is described by the following parameters:

$$A = \begin{bmatrix} 1 & 1 & 1 \\ 0 & -2 & 1 \\ 1 & -2 & -5 \end{bmatrix},\ B = \begin{bmatrix} 1 & 0 \\ 0 & 1 \\ 0 & 0 \end{bmatrix},\ A_q = \begin{bmatrix} 0 & 0 & \alpha \\ 0 & \beta & 0 \\ \gamma & 0 & 0 \end{bmatrix},$$
$$p = \begin{bmatrix} p_x \\ p_y \end{bmatrix} \in \mathbf{R}^4,\ q = \begin{bmatrix} q_x \\ q_y \end{bmatrix} \in \mathbf{R}^4,\ p_i = F_i(t) q_i,$$

with $|F_i(t)| \leq 1,\ i = 1, \ldots, 4$, (i.e. $Q_{0i} = -1$, $S_{0i} = 0$, $R_{0i} = 1$,) and $E_x = 0$, $H_x = I_3$, $C = (1\ 0\ 1)$, $E_y = 0$, $H_y = 1$, $C_q = (0\ \delta\ 0)$ $G_x = 0$, $G_y = 0$. Similarly to [24] and [22], we assumed that $\alpha = \beta = \gamma = \delta$. The maximum value of α achieved by [24] was 1.35, while inequality (31) has a feasible stabilizing solution up to $\alpha_{max} = 3.48$. (The results of the second paper are not comparable, the best result that we could achieve with the corrected inequality and with a wide range of parameter combinations was $\alpha_{max} < 0.98$. Figure 1 illustrates that the dynamic

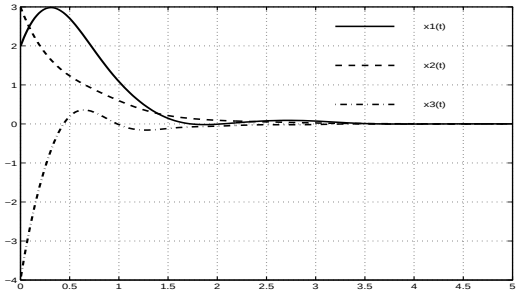

Figure 1: Time evolution of the state variables.

output feedback control obtained with $\alpha_{max} = 3.4$ provides a quick convergence and smaller deviations than in [24], when the initial state and the uncertainties in the simulation are same as there.

Example 2. ([5]) To illustrate the applicability of our approach to nonlinear systems we consider the example of a flexible joint robotic arm investigated e.g. in [5]. The the dynamics of this model contains a sector bounded nonlinearity. [5] constructed a stabilizing predictive control supposing that the state was available for feedback. We applied here the dynamic output feedback control (9)-(10) supposing that only x_1 and x_3 were measured. Moreover, we allowed the effect of exogenous disturbances with $w(t) \in \mathbf{R}$, $E_x^T = \begin{bmatrix} 0 & 1 & 0 & 1 \end{bmatrix}$. In our representation, the prob-

lem to be solved was characterized by matrices

$$A = \begin{bmatrix} 0 & 1 & 0 & 0 \\ -48.6 & -1.25 & 48.6 & 0 \\ 0 & 0 & 0 & 1 \\ 19.5 & 0 & -16.7 & 0 \end{bmatrix}, \; B = \begin{bmatrix} 0 \\ 21.6 \\ 0 \\ 0 \end{bmatrix},$$

$$C = \begin{bmatrix} 1 & 0 & 0 & 0 \\ 0 & 0 & 1 & 0 \end{bmatrix}, \; H_x^T = \begin{bmatrix} 0 & 0 & 0 & -3.33 \end{bmatrix},$$

$A_q = \begin{bmatrix} 0 & 0 & 1 & 0 \end{bmatrix}$, $Q_0 = -1$, $S_0 = 1$, $R_0 = 0$, $Q_u = 1/2.25$, $C_\zeta = \text{diag}\{1, \sqrt{0.1}, 1, \sqrt{0.1}\}$, $R_L = 0.1$, and $p_x = \sin x_3 + x_3$, $q_x = x_3$. The initial state is $x_0 = \begin{pmatrix} 1.2 & 0 & 0 & 0 \end{pmatrix}^T$ and we set $\rho = 1.21$ and $S_L = Q_L$. Figures 2 illustrates that the dynamic

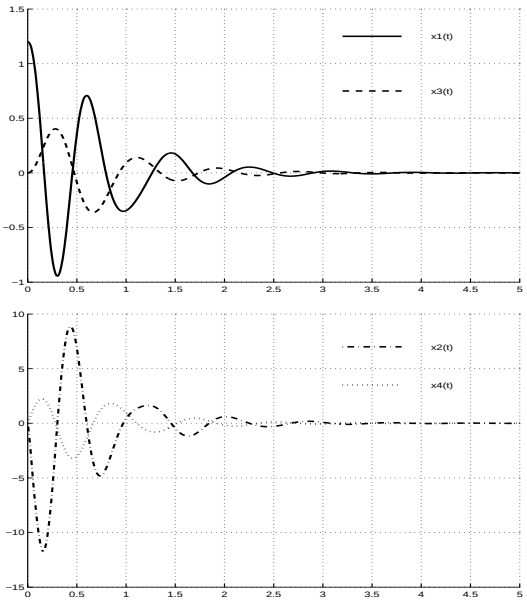

Figure 2: Time evolution of the state variables.

output feedback control still provides a quick convergence at the presence of exogenous disturbances. The disturbances were simulated as $w(t) = 0.1 \sin(t)x(t)$, which was admissible with any $0.01 \leq \gamma_\Delta < 1$.

The computations were made in both examples using YALMIP ([25]) and MATLAB.

5 Conclusion

The paper establishes sufficient (and necessary) conditions for dynamic output feedback to be cost guaranteeing and stabilizing in the case of systems with quadratically constrained nonlinearities/uncertainties. It is shown that this condition was sufficient for the boundedness of the cost and the trajectories, if the constructed dynamic feedback is applied. The considered class of nonlinearities/uncertainties permits to treat a great number of nonlinearity/uncertainty types by the appropriate choice of system parameters. Both the discrete and continuous-time cases are examined. The conditions are formulated as matrix inequalities. When one scalar parameter is fixed, the matrix inequality system to be solved is linear. The proposed method extends the results of a recently published paper in several aspects. Numerical examples illustrate the application of the proposed method.

References

[1] A. B. Açıkmeşe and M. Corless, Stability analysis with quadratic Lyapunov functions: Some necessary and sufficient multiplier conditions, *Systems & Control Letters* 57, 2008, pp. 78–94.

[2] D. Arzelier and D. Peaucelle, Quadratic guaranteed cost control for uncertain dissipative models: a Riccati equation approach, *International Journal of Control* 73, 2000, pp. 762–775.

[3] M. Azzouzi and F. Neri, An introduction to the special issue on advanced control of energy systems, *WSEAS Transactions on Power Systems* 8, 2013, p. 103.

[4] M. Bakošová, A. Vasičkaninová and M. Karšaiová, Robust static output feedback stabilization of an exothermic chemical reactor with input constraints, *Proceedings of the 14th WSEAS International Conference on Systems*, Vol. I, 2010, pp. 341–346.

[5] C. Böhm, S. Yu, R. Findeisen and F. Allgöwer, Predictive control for Lure systems subject to constraints using LIMs, *Proceedings of the European Control Conference*, Budapest, Hungary, 2009, pp. 3389–3394.

[6] Z. Bojkovic and F. Neri, An introduction to the special issue on advances on interactive multimedia systems, *WSEAS Transactions on Systems* 12, 2013, pp. 337–338.

[7] C. Ciufudean, C. and F. Neri, Open research issues on multi-models for complex technological systems, *WSEAS Transactions on Systems* 13, 2014, in press.

[8] A. V. Doroshin, Synthesis of attitude motion of variable mass coaxial bodies, *WSEAS Transactions on Systems and Control* 3, 2008, pp. 50–61.

[9] A. V. Doroshin, Exact solutions in attitude dynamics of a magnetic dual-spin spacecraft and a generalization of the lagrange top, *WSEAS Transactions on Systems* 12, 2013, pp. 471–482.

[10] A. V. Doroshin and F. Neri, Open research issues on nonlinear dynamics, dynamical systems and processes, *WSEAS Transactions on Systems* 13, 2014, in press.

[11] D. Famularo and G. Franzé, Output feedback model predictive control of uncertain norm-bounded linear systems, *International Journal of Robust and Nonlinear Control* 21, 2011, pp. 838–862.

[12] P. Gahinet and P. Apkarian, A linear matrix inequality approach to the H_∞ control problem, *International Journal of Control* 4, 1994, pp. 421–448.

[13] C. Guarnaccia and F. Neri, An introduction to the special issue on recent methods on physical polluting agents and environment modeling and simulation *WSEAS Transactions on Systems* 12, 2013, pp. 53–54.

[14] É. Gyurkovics and T. Takács, Output feedback guaranteeing cost control by matrix inequalities for discrete-time delay systems, *WSEAS Transactions on Systems* 7, 2008, pp. 645–654.

[15] É. Gyurkovics and T. Takács, Some results on guaranteeing cost strategies: Full block multipliers and fictitious games, *European Journal of Control* 14, 2008, pp. 76–86.

[16] É. Gyurkovics and T. Takács, A remark on abstract multiplier conditions for robustness problems, *Systems & Control Letters* 58, 2009, pp. 276–281.

[17] É. Gyurkovics and T. Takács, Application of a multiplier method to uncertain Lur'e-like systems, *Systems & Control Letters* 60, 2011, pp. 854–862.

[18] É. Gyurkovics and T. Takács, Guaranteed cost by bounded dynamic output feedback control, *Proceedings of the 9th European Workshop on Advanced Control and Diagnosis*, Budapest, Hungary, 2011, http://www.conferences.hu/acd2011/.

[19] P. Hájek and F. Neri, An introduction to the special issue on computational techniques for trading systems, time series forecasting, stock market modeling, financial assets modeling, *WSEAS Transactions on Business and Economics* 10, 2013, pp. 201–292.

[20] S. Ibrir, Static output feedback and guaranteed cost control of a class of discrete-time nonlinear systems with partial state measurements, *Nonlinear Analysis: Theory, Methods & Applications* 68, 2008, pp. 1784–1792.

[21] P. Karthikeyan and F. Neri, Open research issues on deregulated electricity market: investigation and solution methodologies, *WSEAS Transactions on Systems* 13, 2014, in press.

[22] H. Kheloufi, A. Zemouche, F. Bedouhene and M. Boutayeb, On LMI conditions to design observer-based controllers for linear systems with parameter uncertainties, *Automatica* 49, 2013, pp. 3700–3704.

[23] M. M. Kogan, Robust H_∞ suboptimal and guaranteed cost state feedback as solutions to linear-quadratic dynamic games under uncertainty, *International Journal of Control* 73, 2000, pp. 219–224.

[24] C.–H. Lien, Robust observer based control of systems with state perturbations via LMI approach, *IEEE Transactions on Automatic Control* 49, 2004, pp. 1365–1370.

[25] J. Löfberg, YALMIP : A Toolbox for Modeling and Optimization in MATLAB. In *Proceedings of the CACSD Conference*, Taipei, Taiwan, 2004. (http://users.isy.liu.se/johanl/yalmip/)

[26] M. Muntean and F. Neri, Foreword to the special issue on collaborative systems *WSEAS Transactions on Systems* 11, 2012, p. 617.

[27] F. Neri, An introduction to the special issue on computational techniques for trading systems, time series forecasting, stock market modeling, and financial assets modeling, *WSEAS Transactions on Systems* 11, 2012, pp. 659–660.

[28] F. Neri, Open research issues on computational techniques for financial applications, *WSEAS Transactions on Systems* 13, 2014, in press.

[29] F. Neri, Open research issues on advanced control methods: theory and application, *WSEAS Transactions on Systems* 13, 2014, in press.

[30] M. Panoiu and F. Neri, Open research issues on modeling, simulation and optimization in electrical systems, *WSEAS Transactions on Systems* 13, 2014, in press.

[31] L. Pekař and F. Neri, An introduction to the special issue on time delay systems: modelling, identification, stability, control and applications, *WSEAS Transactions on Systems* 11, 2012, pp. 539–540.

[32] L. Pekař and F. Neri, An introduction to the special issue on advanced control methods: theory and application, *WSEAS Transactions on Systems* 12, 2013, pp. 301–303.

[33] A. Rios–Bolivar, F. Rivas and G. Mousalli, Extended static output feedback: an H_2-H_∞ setting, *WSEAS Transactions on Systems and Control* 4, 2009, pp. 286–295.

[34] A. Rios–Bolivar and F. Narciso, A robust control by extended static output feedback for discrete-time uncertain linear systems, *Proceedings of the 12th WSEAS International Conference on Automatic Control, Modelling & Simulation*, 2010, pp. 378–383.

[35] D. Rosinová and V. Veselý, Robust PSD controller design, *Proceedings of the* 18^{th} *International Conference on Process Control*, Tatranská Lomnica, Slovakia, 2011, pp. 565–570.

[36] C. W. Scherer, LPV control and full block multipliers, *Automatica* 37, 2001, pp. 361–375.

[37] C. W. Scherer and S. Weiland, Lecture notes DISC course on linear matrix inequalities in control, *www.dcsc.tudelft.nl/ cscherer/lmi/notes99.pdf*, 2004.

[38] V. Veselý and N. Q. Thuan, Design of robust guaranteed cost PID controller for networked control systems (NCSs), *Journal of Electrical Engineering* 61, 2010, pp. 114–119.

[39] C. Volos and F. Neri, An introduction to the special issue. Recent advances in defense systems: applications, methodology, technology, *WSEAS Transactions on Systems* 11, 2012, pp. 477–478.

[40] J. Wei, Y. Dong and Y. Su, Guaranteed cost control of uncertain T-S fuzzy systems via output feedback approach, *WSEAS Transactions on Systems* 10, 2011, pp. 306–317.

[41] S. Xie, L. Xie and C. de Souza, Robust dissipative control for linear systems with dissipative uncertainty, *International Journal of Control* 70, 1998, pp. 169–191.

[42] L. Yu and F. Gao, Output feedback guaranteed cost control for uncertain discrete-time systems using linear matrix inequalities, *Journal of Optimization Theory and Applications* 113, 2002, pp. 621–634.

Dynamical Analysis and Synthesis of Inertia-Mass Configurations of a Spacecraft with Variable Volumes of Liquids in Jet Engine Tanks

ANTON V. DOROSHIN, MIKHAIL M. KRIKUNOV

Space Engineering Department (Division of Flight Dynamics and Control Systems)
Samara State Aerospace University (National Research University)
SSAU, Moscowskoe shosse 34, Samara, Russia 443086
RUSSIAN FEDERATION
doran@inbox.ru; Krikunov_MM@mail.ru

Abstract: - In the article the attitude motion of a spacecraft with variable mass/structure is considered at the variability of the volume of liquids (the fuel and the oxidizer) in tanks of the jet engines. The variability of the liquid's volume is occurred under the action of systems of the extrusion of liquids by the pressure creation and, as a result, by the diaphragm (a thin soft foil) deformation inside the fuel/oxidizer tank. The synthesis of the attitude dynamics is fulfilled by the change of directions of the extrusion of the liquids in tanks – this modifies the inertia-mass parameters (their corresponding time-dependencies) and affects the final motion dynamics. Here we showed that the extrusion in the lateral radial "outside" direction is most preferable in comparison with the longitudinal extrusion (in the direction of jet-vector). It means that the precession cone of the longitudinal axis of the spacecraft (the axis of the jet-engine reactive thrust) is "twisted up" to the precalculated necessary direction of jet-impulse, and it has not "untwisted" phases. This scheme of the liquid extrusion is dynamically optimal, because it allows to improve the active inter-orbital maneuver by the natural/uncontrolled/passive way.

Key-Words: - Spacecraft; Variability of the Volume of Liquids; Tanks of the Jet-Engines; Attitude Dynamics; The Curvature Method; Precession Motion

1. Introduction.

The task of the spacecraft (SC) attitude dynamics investigation/synthesis at the implementation of the active maneuvers is one of the main tasks of the space flight mechanics.

This task is considered in different formulations taking into account many different aspects, including regimes of controlled/uncontrolled regular/chaotic attitude motion of rigid and flexible SC with constant and variable inertia-mass parameter, an implementation of the attitude reorientation using mechanical actuators and thrusters, etc. The corresponding research results are described in many works [e.g. 1-44], which are not limited by the indicated references list.

In this research we give the short description of some features of the SC with two types of the liquids extrusion in spherical jet-engines tanks. We will consider symmetrical bunches of four spherical tanks (for example, two tanks contain the fuel, and other two tanks contain the oxidizer). This scheme is usually used in the upper stages and boosters configurations. So, let us describe the scheme with spherical tanks (fig.1).

The attitude motion of the SC is considered in this research as the angular motion around the fixed point, coincided at the initial time-moment with the initial position of the center of mass of SC [9-11].

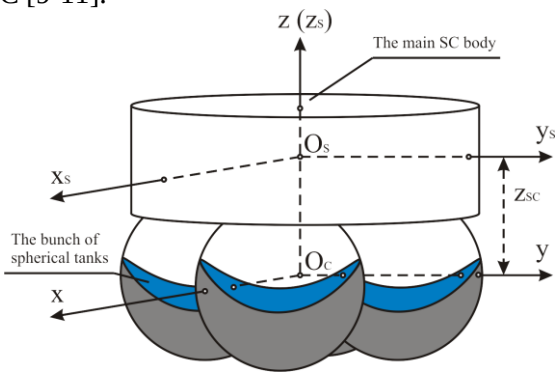

Fig.1 *The bunch/block of spherical tanks*

This mechanical model allows applying the simple type of the definition of the internal geometry (inertia-mass geometry) and corresponding variable inertia-mass parameters.

So, the mathematical model of the attitude motion was built in the works [9-11] for the case of dual-spin spacecraft (with four degrees of freedom). This model represents the dynamical

equations connected with the angular momentum components, and we will use this model in this article without essential modifications at the fixing/elimination of the relative rotation of coaxial bodies.

2. The mathematical model of motion

Let us investigate the free (without the action of any external perturbations) attitude motion of the spacecraft with the variable volume of the liquids (the fuel/oxidizer) in the tanks. The equations [9-11] in the considering case can be reduced to the simple form:

$$\begin{cases} A(t)\dot{p}+\big(C(t)-B(t)\big)qr=0, \\ B(t)\dot{q}+\big(A(t)-C(t)\big)pr=0, \\ C(t)\dot{r}+\big(B(t)-A(t)\big)pq=0, \end{cases} \qquad (1)$$

where $A(t)=B(t), C(t)$ — the variable inertia moments of the SC calculated relatively the point O; and p, q, r — are the angular velocity's components. The total values of the inertia moments are summarized by the terms

$$A(t)=A_S+A_T(t)-M(t)z_C^2(t),$$
$$C(t)=C_S+C_T(t),$$

where A_S, C_S are the constant parts of the inertia moments corresponding to the rigid part of the SC structure (the main SC body including the empty tanks), and A_T, C_T – are the varied (depending on time) parts corresponding to inertia moments of the tanks with momentary "current-freezing" forms of liquids ($M(t)$, $z_C(t)$ – the current values of the mass of the SC and the coordinate of the current position of the center of mass ($z_C(0)=0$).

The angular/attitude/spatial orientation of the SC (fig.2) is described by the Euler's type angles ($\psi\rightarrow\gamma\rightarrow\varphi$).

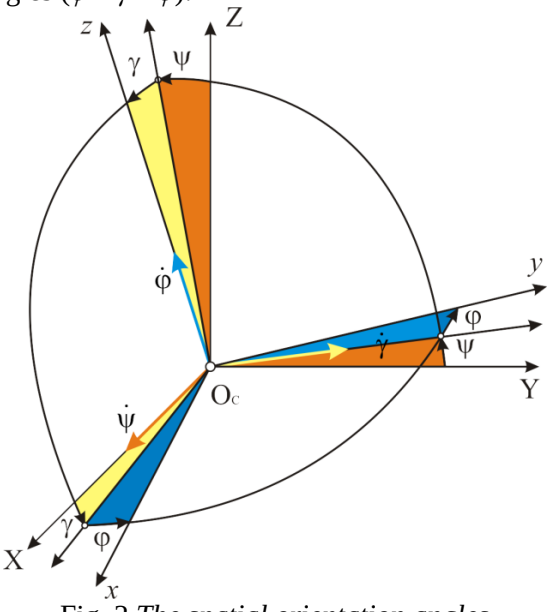

Fig. 2 *The spatial orientation angles*

The kinematical equations for the spatial angles are follows:

$$\dot{\gamma}=p\sin\varphi+q\cos\varphi,$$
$$\dot{\psi}=\frac{1}{\cos\gamma}\big(p\cos\varphi-q\sin\varphi\big), \qquad (2)$$
$$\dot{\varphi}=r-\frac{\sin\gamma}{\cos\gamma}\big(p\cos\varphi-q\sin\varphi\big).$$

It will be quite useful to make the change of the variables [9-11]:

$$p=G(t)\sin F(t),$$
$$q=G(t)\cos F(t). \qquad (3)$$

Then the dynamical equations (1) can be rewritten:

$$\begin{cases} \dot{F}=-\dfrac{1}{A(t)}\big[\big(C(t)-A(t)\big)r\big], \\ G=\text{cosnt}>0, \qquad r=\text{const} \end{cases} \qquad (4)$$

Let us consider the case of the attitude motion of the gyroscopic stabilized SC with the predominance of the longitudinal component of the angular velocity (r) in comparison with the equatorial component:

$$\varepsilon=\sqrt{p^2+q^2}\,/\,|r|<<1.$$

In this case we can rewrite the kinematical equations in the simplified form [9-11]:

$$\dot{\gamma}\cong G\cos\Phi(t), \quad \dot{\psi}\cong G\sin\Phi(t),$$
$$\dot{\varphi}\cong r, \qquad \Phi(t)=F(t)-\varphi(t). \qquad (5)$$

where $\Phi(t)$ is the phase of spatial oscillations. The equations (5) allow to consider the dynamics of the SC longitudinal axis ($O_C z$) with the help of the phase point (the apex of the axis $O_C z$) at the phase-plane $\{\psi\text{-}\gamma\}$. Then the velocity (V) and the acceleration (W) of this phase point, and the curvature (k) of the corresponding trajectory of this point are:

$$V_\gamma=\dot{\gamma},\ V_\psi=\dot{\psi},\ W_\gamma=\ddot{\gamma},\ W_\psi=\ddot{\psi}.$$
$$k^2=\big(\ddot{\gamma}\dot{\psi}-\ddot{\psi}\dot{\gamma}\big)^2\Big/\big(\dot{\gamma}^2+\dot{\psi}^2\big)^3=\dot{\Phi}^2/G^2.$$

For the analysis/synthesis of the dynamics we can apply the qualitative "curvature" method [9-11], which is very useful for the optimization of the form of the hodograph vector of the jet-thrust direction of the SC at the gyroscopic attitude stabilization. This method is based on the evaluation of the roots of the "evolution function" $\tilde{P}(t)$, which describes the evolution of the curvature of the trajectory of the phase point (excluding the multipliers of constant signs):

$$\tilde{P}=\text{const}\cdot k\dot{k}=\dot{\Phi}\ddot{\Phi}G-\dot{G}\dot{\Phi}^2. \qquad (6)$$

Taking into account the equations (4) we can rewrite the expression for the "evolution function" (excluding the multipliers of constant signs):

$$\tilde{P}(t) = \dot{C}A - \dot{A}C \qquad (7)$$

The intervals of the positive sign conservation of this function correspond to the SC's monotonous phases of the angular motion with twisting (Fig.3-a) sections of the longitudinal axis (the trust direction) hodograph (on the plane of parameters γ-ψ). The alternation of the signs of the function (the existence of real roots) results in the alternation of the hodograph's phases. At the Fig.3 it is possible to see the clotoid (Fig.3-b, that corresponds to the existence of one root of $\tilde{P}(t)$) and the complex phase-alternation-spiral (Fig.3-c, that corresponds to the existence of many roots of $\tilde{P}(t)$).

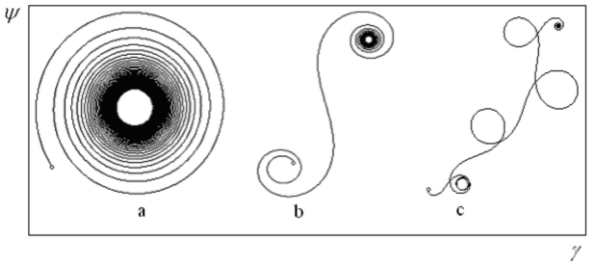

Fig.3 *The hodographs of the longitudinal SC axis (O_Cz) on the tangential plane {ψ-γ}*

These evolutions of the hodographs' affect the inter-orbital transitions' implementation [9] due to the corresponding "travel" of the trust-vector (Fig.4) with the accumulation of the impulses' error.

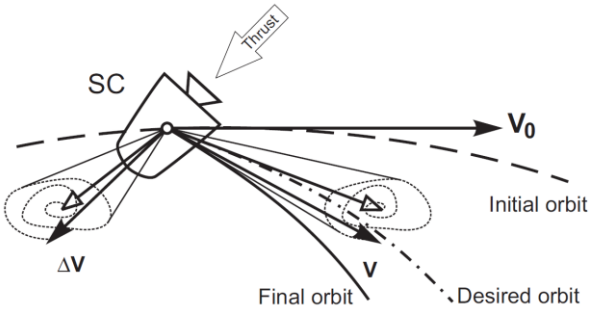

Fig.4 *The influence of the attitude motion on the inter-orbital transitional maneuver*

So, in the purposes of the "positive" dynamics (with the inside twisting hodograph (Fig.3-a)) synthesis the function $\tilde{P}(t)$ has to be positive on the whole time-interval of the motion [9-11].

The following references' frames are used in the research:

1. $O_C xyz$ — the main coordinates frame connected to the main axes of the SC (Fig.1) with the origin in the point O_C of the SC coincided with the initial position of the system's mass center.
2. $O_S x_S y_S z_S$ — the frame connected to the rigid part of the system's structure (the SC without the tanks). Moreover, the frame axes (Fig.1) are collinear with the axes of the main coordinates frame $\left(x \uparrow\uparrow x_S;\ y \uparrow\uparrow y_S;\ z \equiv z_S\right)$.
3. $Ox_0y_0z_0$ — the frame geometrically connected to the tank (coinciding with its main axes) with the origin in the geometrical center of the tank (Fig.5).

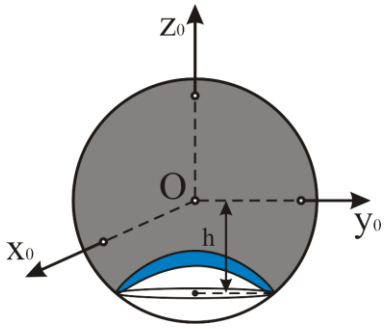

Fig. 5. *The frame connected with the tank*

4. $O_T x_T y_T z_T$ — the frame (Fig. 6) connected to the bunch of the tanks with the origin in the geometrical center of the tanks bunch.

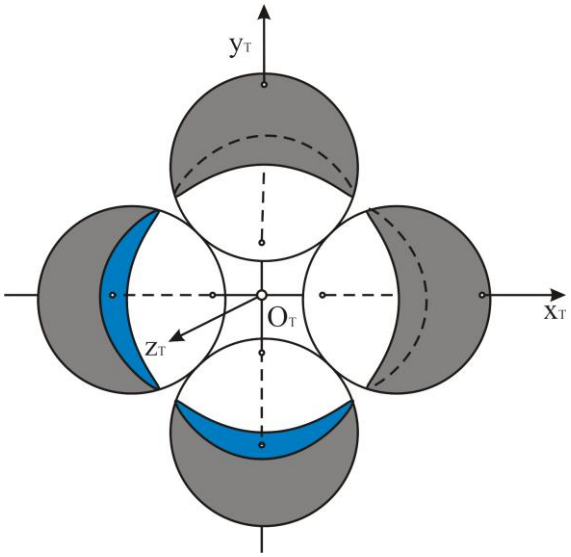

Fig. 6 *The frame connected with the geometrical center of the tanks bunch*

5. $O'x'y'z'$ — the frame with axes which is collinear to the axes $O_C xyz$, and with the origin in the "lowest" point of the SC *O*.

Now we can calculate the inertia moments:

$$A(t) = A_S + A_T(t) - Mz_C^2, \quad C(t) = C_S + C_T(t), \tag{8}$$

where A_S, C_S — are the constant parts of the inertia moments corresponding to the rigid part of the SC structure (the main SC body with the empty tanks), and A_T, C_T – are the varied parts corresponding to inertia moments the tanks (including momentary "current-freezing" forms of liquids and the empty tanks) calculated in the frame $O_C xyz$; $M = M(t)$ — is the mass of SC in the current time-moment; $z_C = z_C(t)$ — is the current coordinate of the SC mass center, that can be calculated as follows

$$z_C = z'_{C_0} - z'_C, \tag{9}$$

$$M = m_S + m_{ET} + m_T(t), \tag{10}$$

where z'_C — is the coordinate of the position of the mass center at present time in the frame $O'x'y'z'$ and $z'_{C_0} = z'_C(0)$ — the coordinate of the center of mass at the initial time moment (also in the frame $O'x'y'z'$); m_S — the constant mass of the rigid part of the SC without the empty tanks; m_{ET} - is the mass of the empty tanks; $m_T(t)$ — is mass of liquids in the tanks at the current time.

The recalculation of the inertia moments of the rigid part of the SC without empty tanks can be fulfilled as follows:

$$A_S = A_{S0} + m_S z_{SC}^2, \quad C_S = C_{S0},$$

где A_{S0}, C_{S0} — the inertia moments of the rigid SC body in the frame $O_S x_S y_S z_S$, with the defined/known values; $z_{SC} = \text{const}$ — is the distance between the mass center of the rigid SC body and point O_C (the initial position of the mass center of the system with the filled tanks).

The inertia moments of the tanks can be find in the form:

$$A_T = A_{T0}(t) + m_T z_T^2, \quad C_T = C_{T0}(t), \tag{11}$$

where $A_{T0}(t)$, $C_{T0}(t)$ — are the inertia moments calculated in the frame $O_T x_T y_T z_T$, and $z_T = z_T(t)$ — is the distance between the mass center of the tanks bunch and the point O_C.

The value z_{SC} also formally follows from the expression:

$$z_{SC} = z'_{C_0} - z'_{SC}, \tag{12}$$

where z'_{KC} — the position of the mass center of the SC's rigid part/structure in the frame $O'x'y'z'$. The value z_T satisfies to the equality:

$$z_T = z'_{C_0} - z'_T, \tag{13}$$

where z'_T is the position of the mass center of the bunch of the tanks in the frame $O'x'y'z'$.

Now it is possible to formally find the position of the system mass center in the frame $O'x'y'z'$:

$$z'_C = \frac{1}{M}\left(z'_{SC} m_S + z'_T m_T\right), \tag{14}$$

For example, we consider the SC with the height of the main rigid part H_S and with the bunch of the tanks with the diameter a. Then we have

$$z'_{SC} = \frac{1}{m_{SC}}\left[m_S\left(a + H_S/2\right) + m_{ET}\frac{a}{2}\right], \quad m_{SC} = m_S + m_{ET}. \tag{15}$$

The defined geometrical values undoubtedly depend on the selected shapes of the tanks. In turn, it is clear that the tanks can have different shapes (spheres, cylinders, conical parts, compound forms). Also methods of the liquids extrusion from the tanks differ from each other. For example, the fuel-tank pressurization with the tissue-type or foil-type diaphragms is quite useful.

Let us consider in this research the spherical tanks equipped with the extrusion systems with the hemispherical foil-type diaphragms edge-stiffened in the line of the internal diameter of the tank – the pressure is injected into the gap between the diaphragm and the internal tank's wall, then the irretrievable foil's deflection forms. Such types of the diaphragms allow to fulfill the liquid extrusion without formation of the free liquid's surface at the conservation of the current reached lens-shaped deformity (Fig.5) of the foil (this lens-shaped deformity/deflection rises with the time, and in limit it coincides with the complete spherical tank).

So, the main considering task is the search of the tanks dispositions providing the realization of the "positive" attitude dynamics of the SC on active sections of the trajectory/orbital motion, when the accuracy of the jet propulsion inter-orbital impulse increases by natural way during the SC precession motion with the spiral-convolving hodograph of the SC longitudinal axis (coinciding with the vector of the jet-engine thrust).

Here the most important part of the task is the selection of the direction of the internal

motion of the extrusive diaphragms inside the tank. We can dispose the extrusive diaphragm inside the tank along the thrust vector ("downward extrusion" – Fig.1); or the diaphragms can be disposed in the orthogonal direction and the liquid will be extruded radially outwards ("radial extrusion" – Fig.6).

It is possible to expect that the attitude dynamics at the radial extrusion will differ from the downward one. Let us to make an investigation of this question.

3. The comparative modeling of the extrusions

3.1. The radial extrusion

Let us consider the attitude motion at the radial extrusion realization (Fig.6).

The inertia moments $A_{T0}(t)$ and $C_{T0}(t)$ in the frame $O_T x_T y_T z_T$ can be calculated as follows:

$$A_{T0}(t) = 2A_F + 2C_F + 2m_T(l^2 - r^2), \quad (16)$$

$$C_{T0}(t) = 4A_F + 4m_T(l^2 - r^2), \quad (17)$$

where $A_F = A_F(t)$ and $C_F = C_F(t)$ — are the inertia moment of the current volume of the liquid in the single tank in the frame $Ox_0y_0z_0$ (Fig.5); $l = l(t)$ — is the distance between the point O_T and the mass center of the current volume of the liquid in one tank along $O_T x_T$; $r = r(t)$ — the distance between the geometrical center of the of the single tank and the mass center of the current volume of the liquid in one tank along $O_T x_T$.

We must additionally comment the process of the liquid extrusion: the foil-type diaphragm deforms under the action of the pressure such way, that the created empty space (between the internal tank's wall and the sagged diaphragm) always has symmetrical lens-type shape (Fig.5).

In this case the inertia moments (16) and (17) have the concretized form:

$$A_F = I_0 - \frac{\pi\rho}{5}\left(\frac{8}{3}R^5 + \frac{1}{4}h^5 - \frac{15}{4}R^4h + \frac{5}{6}R^2h^3\right) - 2m_1h\left(h - z_{C1}\right), \quad (18)$$

$$C_F = I_0 - \frac{\pi\rho}{5}\left(\frac{8}{3}R^5 - h^5 - 5R^4h + \frac{10}{3}R^2h^3\right), \quad (19)$$

where I_0 – the inertia moment of the single full spherical tank completely filled with the liquid; ρ – the liquid density; R – the radius of the tank; $h = h(t)$ – the distance between the geometrical center of the tank and the median plane of the empty lens-type space (Fig.5); m_1 – the mass of the current extruded volume of the liquid in the tank; z_{C1} – the distance between the geometrical center of the of the single tank and the spherical segment (one half of the "lens").

$$I_0 = \frac{2}{5}m_0R^2,\ m_0 = \frac{4}{3}\pi\rho R^3 \quad (20)$$

$$m_1 = 2\pi\rho(R-h)^2\left(\frac{2}{3}R + \frac{1}{3}h\right) \quad (21)$$

$$z_{C1} = \frac{3}{4}\frac{\left(R^2 - h^2\right)^2}{2R^3 - 3R^2h + h^3} \quad (22)$$

The value *l* and *r* are calculated as:

$$r(t) = \frac{m_1}{m_0 - m_1}h(t) \quad (23)$$

$$l(t) = R\sqrt{2} - r(t) \quad (24)$$

$$z'_T = R$$

Let us consider the linear time-dependence of $h(t)$:

$$h(t) = h_0 - h_1 t\,.$$

Now we can plot the graph (Fig.7) for the function of the thrust's hodograph curvature $\tilde{P}(t)$ at the parameters from the table 1.

Table 1 – *The parameters of the SC*

The parameter	The value
ρ, kg/m^3	780
h_0, m	1
h_1, m/s	0.025
R, m	1
A_S, kg·m^2	8600
C_S, kg·m^2	18600
m_S, kg	100
H_S, m	2

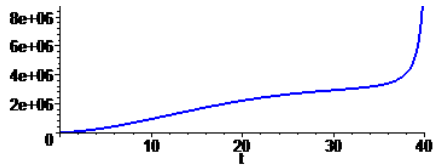

Fig.7 *The thrust's hodograph curvature function* $\tilde{P}(t)$ *at the radial extrusion:*
the function is positive;
and it has no roots

As we can see, the thrust's hodograph curvature function is positive and has no roots. The corresponding hodograph is presented at the figure (Fig.8) – as it was expected this hodograph is spiral-convolving curve and the corresponding attitude dynamics is also "positive" in the above mentioned sense.

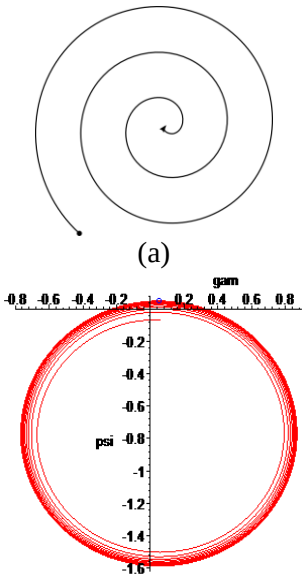

(a)
(b)

Fig.8 *The thrust's hodograph at the radial extrusion of the liquids in the tanks:*
(a) – the schematic monotone type of the hodograph
(b) – the real implementation
(G_0=1.5 [1/s]; F_0=0; r=2 [1/s]; the small blue circle corresponds to the initial position)

3.2. The downward extrusion

Let us now consider the second type of extrusion – the "downward extrusion" (like at the Fig.1). the inertia moments $A_{T0}(t)$ and $C_{T0}(t)$ can be calculated from (11):

$$A_{T0}(t) = 4A_F + 2m_T d^2, \qquad (25)$$

$$C_{T0}(t) = 4C_F + 4m_T d^2, \qquad (26)$$

where $d = R\sqrt{2} = \text{const}$ — is the distance between the point O_T and the geometrical center of the tank.

The inertia moments (16) and (17) in considering case have the form (18) and (19). Also the following values take place:

$$z'_T(t) = R - \frac{m_1(t)}{m_0 - m_1(t)} h(t) \qquad (27)$$

Then the evolution functions $\tilde{P}(t)$ (at the conditions from tab.1) is sign-alternating and has real roots (Fig.9).

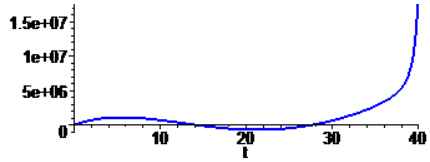

Fig.9 *The thrust's hodograph curvature function* $\tilde{P}(t)$ *at the downward extrusion:*
the function is sign-alternating;
and it has two roots in the open interval t=(0,T)

The corresponding hodograph is presented at the figure (Fig.10) – as it was expected, this hodograph is not monotonously twisting, and it has the first twisting phase (the black section of the schematic hodograph – Fig.10-a), the second untwisting phase (the red section of the schematic hodograph – Fig.10-a) and the third twisting phase (the blue section of the schematic hodograph – Fig.10-a). So, the untwisting phase is realized in the time-interval t=(12..28) where the evolution function is negative) – it characterizes the attitude dynamics as not-positive because inside the "untwisting phase's" time-interval the thrust defocusing takes place, and corresponding jet-impulse is "nebulized in parasite directions".

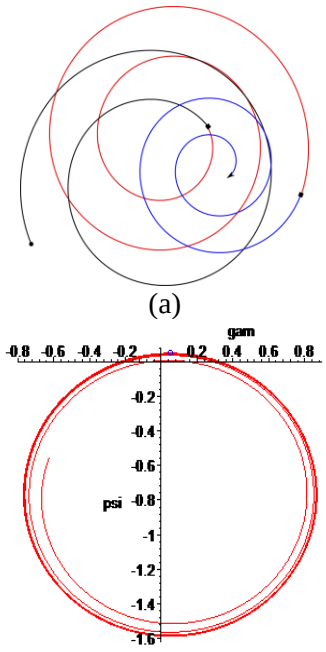

(a)
(b)

Fig.10 *The thrust's hodograph at the downward extrusion of the liquids in the tanks*
(a) – the schematic three-section type of the hodograph
(b) – the real implementation

So, as we can see, the radial type of the extrusion system is optimal in the dynamical sense, when the accuracy of the inter-orbital jet impulse increases by the natural way during the SC precession motion with the spiral-convolving hodograph of the SC longitudinal axis (coinciding with the vector of the jet-engine thrust), that in its turn corresponds to the precessional motion with the twisting nutation cone.

The attitude dynamics at the downwards extrusion is not positive, and we can recommend to change this type of extrusion system on the radial one – this is the main applied/technical result of the fulfilled research.

Conclusion

The attitude dynamics of the SC with the variable volume of the liquids (the fuel and the oxidizer) in the bunch of spherical tanks was investigated based on the qualitative method for the analysis of the curvature of phase trajectories. Two schemes of the extrusion system (the radial and the downward extrusion) were considered.

As it was shown, the attitude dynamics at the downwards extrusion is not positive, that results in the complex trajectory of the apex of the longitudinal axis of the SC (coinciding with the thrust vector of the jet-engine) – this trajectory represents the complex spiral with the twisted and untwisted sections, and the corresponding attitude motion negative affects the jet-engine-impulse.

Owe of the main results of the work is the recommendation of using of the radial extrusion scheme instead the downward scheme. The radial extrusion scheme is optimal in the dynamical sense, when the accuracy of the inter-orbital jet-impulse increases by the natural way during the SC precession motion with the spiral-convolving hodograph of the SC longitudinal axis (coinciding with the vector of the jet-engine thrust), that in its turn corresponds to the precessional motion with the twisting nutation cone.

So, the work additionally confirms the fact that the attitude dynamics of the SC with the variable mass/structure strongly affects its orbital motion.

References

1. A. A. Kosmodem'ianskii, A Course in Theoretical Mechanics, Part 2, Jerusalem, Published for the National Science Foundation, Washington, by the Israel Program for Scientific Translations, 1963.
2. J. Wittenburg, Dynamics of Systems of Rigid Bodies. Stuttgart: Teubner, 1977.
3. F.R. Gantmaher, L.M. Levin, The Theory of Rocket Uncontrolled Flight, Fizmatlit, Moscow, 1959.
4. M. Iñarrea, V. Lanchares, Chaotic pitch motion of an asymmetric non-rigid spacecraft with viscous drag in circular orbit, Int. J. Non-Linear Mech. 41 (2006) 86–100
5. V. Lanchares, M. Iñarrea, J.P. Salas, Spin rotor stabilization of a dual-spin spacecraft with time dependent moments of inertia, Int. J. Bifurcation Chaos 8 (1998) 609–617.
6. M. Iñarrea, V. Lanchares, Chaos in the reorientation process of a dual-spin spacecraft with time-dependent moments of inertia, Int. J. Bifurcation and Chaos. 10 (2000) 997-1018.
7. M. Iñarrea, V. Lanchares, V.M. Rothos, J.P. Salas. Chaotic rotations of an asymmetric body with time-dependent moments of inertia and viscous drag. International Journal of Bifurcation and Chaos, Vol. 13, (2003), 393-409.
8. M. Iñarrea, V. Lanchares, Chaotic pitch motion of an asymmetric non-rigid spacecraft with viscous drag in circular orbit, Int. J. Non-Linear Mech. 41 (2006) 86–100.
9. A.V. Doroshin, Analysis of attitude motion evolutions of variable mass gyrostats and coaxial rigid bodies system, International Journal of Non-Linear Mechanics. Volume 45, Issue 2 (2010) 193-205.
10. A.V. Doroshin, Synthesis of Attitude Motion of Variable Mass Coaxial Bodies, WSEAS TRANSACTIONS on SYSTEMS AND CONTROL, Volume 3 (2008) 50-61.
11. A.V. Doroshin, Evolution of the precessional motion of unbalanced gyrostats of variable structure, Journal of Applied Mathematics and Mechanics, Volume 72, Issue 3 (2008) 259-269.
12. V.S. Aslanov, A.V. Doroshin, G.E. Kruglov, The Motion of Coaxial Bodies of Varying Composition on the Active Leg of Descent, Cosmic Research, Vol.43, No. 3 (2005) 213-221.
13. V.S. Aslanov, V.V. Yudintsev, Dynamics and control of dual-spin gyrostat spacecraft with changing structure. Celestial Mechanics and

Dynamical Astronomy, Volume 115, Issue 1 (2013) 91-105.

14. V.S. Aslanov, The Dynamics and Control of Axial Satellite Gyrostats of Variable Structure. Proceedings of 1st IAA Conference on Dynamics and Control of Space Systems Porto, Portugal 19-21 March 2012, p. 41-54.
15. A.V. Doroshin, Phase Space Research of One Non-autonomous Dynamic System, Proceedings of the 3rd WSEAS/IASME International Conference on DYMAMICAL SYSTEM and CONTROL. Arcachon, France (2007) 161-165.
16. A.V. Doroshin, M.M. Krikunov, Attitude dynamics of a spacecraft with variable structure at presence of harmonic perturbations, Applied Mathematical Modelling, Volume 38, Issues 7–8 (2014) 2073-2089.
17. V.L. Balakin, A.V. Doroshin, M.M. Krikunov, SYNTHESIS OF DYNAMIC MODES OF ATTITUDE MOTION OF SPACECRAFT WITH SOLID PROPELLANT ROCKET ENGINE, The Bulletin of the Samara State Aerospace University (Vestnik SGAU), #5-36 (2012) 13-19.
18. A.V. Doroshin, Exact solutions in attitude dynamics of a magnetic dual-spin spacecraft and a generalization of the Lagrange top, WSEAS Transactions on Systems 12 (10) (2013) 471 – 482.
19. A.V. Doroshin, Exact solutions for angular motion of coaxial bodies and attitude dynamics of gyrostat-satellites, International Journal of Non-Linear Mechanics 50 (2013) PP. 68 – 74.
20. A.V. Doroshin, Modeling of chaotic motion of gyrostats in resistant environment on the base of dynamical systems with strange attractors. Communications in Nonlinear Science and Numerical Simulation, Volume 16, Issue 8 (2011) 3188–3202.
21. A.V. Doroshin, Heteroclinic dynamics and attitude motion chaotization of coaxial bodies and dual-spin spacecraft, Communications in Nonlinear Science and Numerical Simulation, Volume 17, Issue 3 (2012) 1460–1474.
22. A.V. Doroshin, Homoclinic solutions and motion chaotization in attitude dynamics of a multi-spin spacecraft Communications in Nonlinear Science and Numerical Simulation 19(7) (2014) 2528 – 2552.
23. A.V. Doroshin, Chaos and its avoidance in spinup dynamics of an axial dual-spin spacecraft, Acta Astronautica 94(2) (2014) 563 – 576.
24. A.V. Doroshin, Spinup-capture dynamics of multi-rotor nanosatellites and somersaulting robots, (2013) Proceedings of 2013 Science and Information Conference, SAI 2013 PP. 613 – 617.
25. Filippo Neri, Traffic packet based intrusion detection: decision trees and generic based learning evaluation. WSEAS Transactions on Computers, WSEAS Press (Wisconsin, USA), issue 9, vol. 4, 2005, pp. 1017-1024.
26. Filippo Neri, Software agents as a versatile simulation tool to model complex systems. WSEAS Transactions on Information Science and Applications, WSEAS Press (Wisconsin, USA), issue 5, vol. 7, 2010, pp. 609-618.
27. Antonio Gil V. De Brum, Márcio A. A. Fialho, M. L. Selingardi, Nilton D. Borrego, José L. Lourenço, The Brazilian Autonomous Star Tracker – AST, WSEAS Transactions on Systems 12 (10) (2013) 459-470.
28. C. F. de Melo, F. Neri, An Introduction to the Special Issue on Orbital Dynamics and Spacecraft Attitude Control, WSEAS Transactions on Systems 12 (10) (2013) 457-458.
29. Kozlov V. V. Methods of qualitative analysis in the dynamics of a rigid body. Gos. Univ., Moscow; 1980. 241 pp.
30. Robert G. Melton, Hybrid methods for determining time-optimal, constrained spacecraft reorientation maneuves, Acta Astronautica, Volume 94, Issue 1, 2014, Pages 294-301.
31. Ilya Ioslovich, Arbitrary fuel-optimal attitude maneuvering of a non-symmetric space vehicle in a vehicle-fixed coordinate frame, Automatica, Volume 39, Issue 3, 2003, Pages 557-562

32. Jaime Rubio Hervas, Mahmut Reyhanoglu, Thrust-vector control of a three-axis stabilized upper-stage rocket with fuel slosh dynamics, Acta Astronautica, Volume 98, 2014, Pages 120-127

33. Suman Chakravorty and Jaime Ramirez, Fuel Optimal Maneuvers for Multispacecraft Interferometric Imaging Systems, Journal of Guidance, Control, and Dynamics, Vol. 30, No. 1 (2007), pp. 227-236.

34. W. E. Vander Velde and J. He, Design of space structure control systems using on-off thrusters, Journal of Guidance, Control, and Dynamics, Vol. 6, No. 1 (1983), pp. 53-60.

35. A. D. Challoner, Determination of spacecraft liquid fill fraction, AIAA Guidance, Navigation and Control Conference, Monterey, CA, Aug. 9-11, 1993, Technical Papers. Pt. 1 (A93-51301 22-63), p. 254-264.

36. V. Coverstone-Carroll, J. E. Prussing, Optimal cooperative power-limited rendezvous with propellant constraints, 1992 AIAA/AAS Astrodynamics Conference, Hilton Head Island, SC, Aug. 10-12, 1992, Technical Papers (A92-52051 22-13). Washington, American Institute of Aeronautics and Astronautics, 1992, p. 246-255.

37. Mauro Massari and Franco Bernelli-Zazzera, Optimization of Low-Thrust Reconfiguration Maneuvers for Spacecraft Flying in Formation, Journal of Guidance, Control, and Dynamics, Vol. 32, No. 5 (2009), pp. 1629-1638.

38. B. Wie and P. M. Barba, Quaternion feedback for spacecraft large angle maneuvers, Journal of Guidance, Control, and Dynamics, Vol. 8, No. 3 (1985), pp. 360-365.

39. John I. Hochstein, Alfredo E. Patag, T. P. Korakianitis, and David J. Chato, Pulsed thrust propellant reorientation - Concept and modeling, Journal of Propulsion and Power, Vol. 8, No. 4 (1992), pp. 770-777.

40. Karl D. Bilimoria and Bong Wie, Time-optimal three-axis reorientation of a rigid spacecraft, Journal of Guidance, Control, and Dynamics, Vol. 16, No. 3 (1993), pp. 446-452.

41. Wenchuan Cai, Xiaohong Liao, and David Y. Song, Indirect Robust Adaptive Fault - Tolerant Control for Attitude Tracking of Spacecraft, Journal of Guidance, Control, and Dynamics, Vol. 31, No. 5 (2008), pp. 1456-1463.

42. B. Wie and C. T. Plescia, Attitude stabilization of flexible spacecraft during stationkeeping maneuvers, Journal of Guidance, Control, and Dynamics, Vol. 7, No. 4 (1984), pp. 430-436.

43. Edward Wong, William Breckenridge, An attitude control design for the Cassini spacecraft, American Institute of Aeronautics and Astronautics, AIAA-95-3274-CP

44. Advances in Spacecraft Technologies (Collection of articles), Edited by Jason Hall, InTech (2011), 596 p.